Steam Cracking in Dual Fluidized Beds

One Step Towards Complete Recyclability of Plastic Waste Using Thermochemical Conversion

CHAHAT MANDVIWALA
Department of Space, Earth and Environment
Division of Energy Technology
Chalmers University of Technology

Abstract

Circular use of plastic materials is crucial for reducing dependence on fossil resources and mitigating the environmental pollution from plastic waste. Thermochemical recycling offers a way to produce new plastics from plastic waste. This approach faces numerous challenges that impede its development to an industrial scale. The main challenges include reactor robustness, feedstock sensitivity, and the selective production of monomers. This thesis presents steam cracking in a dual fluidized bed (DFB) reactor as a solution to the challenges in thermochemical recycling. An ideal operating window for the selective production of light olefins and monoaromatics is determined, and these operational parameters are applied to various plastic waste streams. The bed materials tested include silica sand, olivine, bauxite, and feldspar. The development of catalytic activity in the bed materials within DFB steam crackers is also experimentally demonstrated.

The results show that the cracking severity achieved in a DFB steam cracker at temperatures between 700 and 825°C is suitable for the selective production of light olefins and monoaromatics. Within this operating window, pure polyolefin feedstocks yield up to 50% C2–C4 olefins and 20% BTXS. The yield of light olefins remains proportional to the polyolefin content of unsorted plastic wastes, regardless of the presence of other polymers. The non-polyolefin materials in plastic waste, such as PET and cellulose, are selectively converted into aromatics and syngas. Although PET and cellulose contents also lead to significant coke formation, an uninterrupted steam cracking operation without intermittent decoking procedures is demonstrated. Silica sand, olivine, feldspar, and bauxite exhibit no significant catalytic activity in their natural state. In certain situations, olivine and bauxite develop catalytic activity. The accumulation of biomass ash in olivine enhances syngas production through the steam reforming of aromatic precursors. The accumulation of transition metal oxides within the bed material negatively impacts light olefin production. Using bauxite in a reduced oxidation state promotes hydrogenation reaction, thereby enhancing the production of light olefins.

The outcomes of this thesis demonstrate that a DFB steam cracker enables direct production of light olefins from plastic waste without the need for presorting procedures or catalysts. Most of the data presented in this work are obtained from experiments conducted at a scale relevant to the petrochemical industry, showcasing the scalability and technology readiness of the DFB steam cracking process.

Keywords: Plastic waste, Thermochemical recycling, Steam cracking, Dual fluidized bed, Polyolefins, Olefins

List of publications included in this thesis

This thesis is based on the following eight appended papers, which are referred to in the text according to their Roman numerals:

Paper I

Mandviwala. C., Berdugo Vilches. T., Seemann. M., Faust. R., Thunman. H.

Thermochemical conversion of polyethylene in a fluidized bed: Impact of transition metal-induced oxygen transport on product distribution

Journal of Analytical and Applied Pyrolysis, 163 (2022) 105476

Paper II

Mandviwala. C., Berdugo Vilches. T., Seemann. M., González-Arias. J., Thunman. H.

Unraveling the hydrocracking capabilities of fluidized bed systems operated with natural ores as bed materials

Journal of Analytical and Applied Pyrolysis, 166 (2022) 105603

Paper III

Mandviwala. C., González-Arias. J., Seemann. M., Berdugo Vilches. T., Thunman. H.

Fluidized bed steam cracking of rapeseed oil: exploring the direct production of the molecular building blocks for the plastics industry

Biomass Conversion and Biorefinery, 13 (2022) 14511 – 14522

Paper IV

Mandviwala. C., González-Arias. J., Berdugo Vilches. T., Seemann. M., Thunman. H.

Comparing Bed Materials for Fluidized Bed Steam Cracking of High-Density Polyethylene: Olivine, Bauxite, Silica-Sand, and Feldspar

Journal of Analytical and Applied Pyrolysis, 173 (2023) 106049

Paper V

Mandviwala. C., Forero Franco. R., Gogolev. I., González-Arias. J., Berdugo Vilches. T., Cañete Vela. I., Thunman. H., Seemann. M.

Method development and evaluation of product gas mixture from a semi-industrial scale fluidized bed steam cracker with GC-VUV

Fuel Processing Technology, 253 (2023) 108030

Paper VI

González-Arias. J., Berdugo Vilches. T., Mandviwala. C., Cañete Vela. I., Seemann. M., Thunman. H.

Effect of biomass ash on preventing aromatization of olefinic cracking products in dual fluidized bed systems

Fuel, 338 (2023) 127256

Paper VII

González-Arias. J., Forero Franco. R., Mandviwala. C., Seemann. M.

Steam gasification as a viable solution for converting single-use medical items into chemical building blocks with high yields for the plastic industry

Resources, Conservation and Recycling, 201 (2024) 107342

Paper VIII

Mandviwala. C., Forero Franco. R., Berdugo Vilches. T., Gogolev. I., González-Arias. J., Cañete Vela. I., Thunman. H., Seemann. M.

Steam cracking in a semi-industrial dual fluidized bed reactor: Tackling the challenges in thermochemical recycling of polyolefins

Submitted for publication

Contribution report

Paper I	Principal author with main responsibility for conceptualization, methodology, investigation, data curation, and writing.
Paper II	Principal author with main responsibility for conceptualization, methodology, investigation, data curation, and writing.
Paper III	Principal author with main responsibility for conceptualization, methodology, investigation, data curation, and writing.
Paper IV	Principal author with main responsibility for conceptualization, methodology, investigation, data curation, and writing.
Paper V	Principal author with main responsibility for conceptualization, methodology, investigation, data curation, and writing.
Paper VI	Co-author with main responsibility for methodology, investigation, and writing.
Paper VII	Co-author with main responsibility for methodology, visualization, and writing.
Paper VIII	Principal author with main responsibility for conceptualization, methodology, investigation, data curation, and writing.

This thesis is also based on parts of the licentiate thesis published by the author, as part of the evaluation of his doctoral studies:

C. Mandviwala, Steam Cracking of Polyolefins in Fluidized Bed Systems: Influences of the Bed Materials on the Hydrogen Transfer Reactions, 2022

Related peer-reviewed publication not included in this thesis

Forero Franco. R., Berdugo Vilches. T., Mandviwala. C., Seemann. M., Thunman. H.

Developing a parametric system model to describe the product distribution of steam pyrolysis in a Dual Fluidized bed

Fuel, 348 (2023) 128518

ACKNOWLEDGMENTS

I would not be writing this if it weren't for some people in my life. My PhD journey has been made enjoyable by many individuals who have guided and accompanied me. Beginning with my supervisor, Martin Seemann, I would like to express my deep gratitude for his guidance and support since my first day at Chalmers. Martin taught me how to cherish every moment of my time as a doctoral student. His enthusiasm and witty jokes made my life as a PhD student much easier and more enjoyable. Without him, this journey would have been much more difficult.

I would also like to thank my co-supervisors, Henrik Thunman and Teresa Berdugo Vilches, for their invaluable guidance and support. Henrik has been an exceptional leader, always a door-knock away whenever I felt I had reached a dead-end in my research. Teresa has been an excellent teacher and mentor, and I am particularly thankful for her dedication to creating a fantastic work environment at Chalmers Kraftcentralen. I hope we can continue creating outstanding research with the steam cracker for many more years.

I have had the privilege of spending the cold winter days in one of the warmest places in Sweden: Kraftcentralen (KC). It was made possible by our 'unsung heroes' – the research engineers Jessica Bohwalli, Johannes Öhlin, and Rustan Hvitt – who created this world-class experimental infrastructure. I would also like to thank the operating staff at Akademiska Hus, Jelena, Isabel, Petrus, Richard, and Mikael for their diligent boiler operation. Your patience and dedication in ensuring the success of all the experiments have been invaluable.

I am also grateful to the rest of my research team, Isabel, Judith, Ivan, Nidia, Rene, Tharun, Judit, Johanna, and Iacopo, for making this research group exceptional. I especially thank Judith, Ivan, Rene, and Nidia for making the experiments in KC and the lab enjoyable. Ivan, I've enjoyed your company during work trips and conferences. It was so fun and memorable.

Apart from the gasification group, I would like to thank Marie, Katarina, Anna, all the seniors, and all the PhD students at Energy Technology for fostering a friendly and collaborative atmosphere.

Finally, I thank Iulia, my parents, and my sister for their unwavering love and support. Without them, I would never have been able to enjoy and complete this journey.

Chahat Mandviwala, Gothenburg 2024

ahimsā paramo dharma

Contents

This page intentionally left blank

CHAPTER 1

1 – Introduction

1.1 Motivation

Plastics are advanced materials crucial in providing society with indispensable goods and services. Their low cost of production has facilitated their wide-ranging utilization in sectors such as healthcare, food packaging, transportation, and various other industries. The extensive adoption of plastics has resulted in a continuous rise in their production over recent decades, reaching a global output of 400 million metric tonnes (MMT) in 2022.[1]

Plastics are produced from molecular building blocks, or monomers, through various polymerization methods. These molecular building blocks, such as ethylene, propylene, butadiene, benzene, and xylenes, are mainly produced through steam cracking of petroleum-derived feedstocks like naphtha, ethane, or liquefied petroleum gas (LPG). These processes account for 4%–6% of global fossil resource consumption.[2]

Additionally, due to the cost-effectiveness of plastic production, plastics quickly become waste materials. Management of commonly generated plastic waste poses significant challenges due to its resistance to degradation. In 2019, an estimated 353 MMT of plastic waste had been generated. Of this, approximately 72% was disposed of in landfills or the natural environment, 19% was incinerated, and only 9% was recycled.[3] If current trends in plastic production and waste management persist, it is projected that around 12 billion tonnes of plastic waste will accumulate in the natural environment or landfills by 2050.[4] Consequently, fossil-based plastic production and the management of resulting plastic waste present serious sustainability concerns.

The waste hierarchy prioritizes prevention as the most crucial action for reducing and managing waste.[5] However, envisioning a world without plastics appears implausible. That is due to the significant amount of alternative materials, such as paper and metals, that are needed to substitute for plastics. Despite efforts, reusing most plastics, especially those in the medical and food industries, poses significant challenges. Moreover, even the most efficient reutilization

methods can only satisfy a fraction of the plastic demand. In response to these challenges, recycling and energy recovery are two viable options for managing the copious amounts of plastic waste. Although energy recovery offers a practical solution, it falls short of the need for sustainable plastic production. Thus, recycling plastic waste into new plastics becomes the only suitable option for fostering a sustainable economy using plastics.

As of today, plastic recycling primarily relies on mechanical methods, which pose challenges when dealing with heterogeneous waste streams containing paper, cardboard, and metals.[2,4,6] Despite advancements, mechanical recycling remains limited in producing high-quality recycled materials for specific applications.[7] Moreover, the process is complex, requiring numerous steps, up to 17 for well-sorted PET bottles.[8] Additionally, the inherent properties of plastics impose constraints on the number of times they can be mechanically recycled.[2,9] Consequently, while mechanical recycling has made strides, it still struggles to fully address the diverse challenges posed by plastic waste management.[2,9,10]

In the progression towards a sustainable plastic-using economy, the imperative lies in adopting circular practices where plastic materials are used in a closed loop.[6,9] Achieving this goal necessitates recycling methods capable of producing new plastics of equivalent quality to the original, irrespective of the type of plastic waste – whether sorted or unsorted.[2,9] Thermochemical recycling, which focuses on producing the monomers of plastics from plastic waste, emerges as a preferable solution.[10–12]

By converting plastic waste into its monomers, thermochemical recycling offers the potential for unlimited recycling of any plastic material.[10–12] This method circumvents the need for advanced sorting systems, as it applies to all types of plastic waste. Additionally, thermochemical recycling provides flexibility in feedstock selection and product distribution, making the recycling system adaptable to changes in consumption and production patterns.[9] Hence, thermochemical recycling will be a crucial bridge between waste management and plastic production.

Anthropogenic waste streams, the new feedstock for the plastic industry, are more intricate than the fossil-based feedstocks conventionally utilized. These waste streams contain biogenic and inorganic materials, including paper, cardboard, and metals.[9] Moreover, the contaminants in the waste pose challenges during thermochemical conversion, potentially leading to the formation of pollutants and corrosive substances.[10,11,13] Given these complexities, there is a need for a thermochemical reactor capable of overcoming these hurdles and effectively transforming heterogeneous waste streams into valuable products.

In this context, a dual fluidized bed (DFB) has characteristics that make it suitable for the thermochemical recycling of plastic waste. A DFB reactor is well-suited for thermochemical conversion due to its efficient heat transfer properties and capability to handle heterogeneous feedstocks.[14,15] Furthermore, by using steam as the exclusive fluidization medium, a DFB reactor can operate as a steam cracker, producing a nitrogen-free product gas like that obtained from the steam cracking of fossil feedstocks.[2] To illustrate this concept further, Figure 1 provides schematics comparing a conventional steam cracker with a DFB steam cracker, offering a visual representation of their respective operational principles.

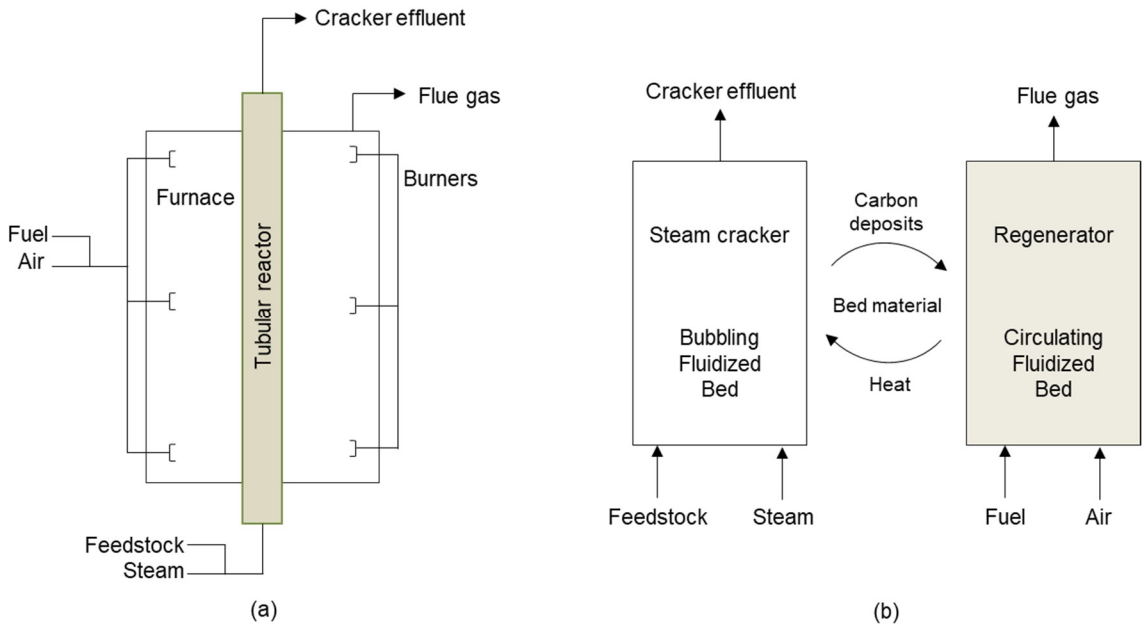

Figure 1. Schematics of a tube from a conventional steam cracker (a) and a DFB steam cracker (b).

In a DFB steam cracker, hot bed material circulates between two interconnected fluidized beds: a steam cracker and a regenerator, as shown in Figure 1. The steam cracker reactor operates in a bubbling regime, while the regenerator operates in a circulating fluidized bed (CFB) configuration. The heat required for steam cracking is transferred from the regenerator to the cracker through the bed material. This mechanism is similar to that observed in a conventional steam cracker, where heat is supplied externally through a burner. Moreover, as carbon deposits form on the surface of the bed material during steam cracking, they are continuously removed through oxidation within the regenerator. This type of configuration, if sealed thoroughly, allows the production of two separate gas streams: flue gas from the regenerator and nitrogen-free product gas from the steam cracker, referred to as the cracker effluent.

Despite its promising characteristics, commercial-scale implementation of DFB steam cracking for plastic waste has not yet been achieved. One reason is the necessity for a steam cracker to integrate with existing petrochemical clusters.[2] This makes steam cracking in DFB a centralized solution for plastic recycling. As a centralized solution, commercial DFB steam crackers must possess a feedstock processing capacity comparable to existing steam crackers, allowing them to benefit from economies of scale. However, research experience regarding DFB steam crackers at such a scale remains limited.[2,14] Therefore, there is a need for investigations into large-scale DFB steam crackers and their operation. Additionally, it is imperative to evaluate the availability of suitable plastic waste streams capable of fulfilling the current production capacity of new plastics. This evaluation is crucial for ensuring the viability and sustainability of DFB steam cracking as a recycling solution.

The cost-effectiveness of a steam cracker relates to its conversion efficiencies and the yields of economically valuable products, such as ethylene and propylene.[16] Research over the last decade on biomass gasification in DFB systems has revealed that the DFB configuration offers flexibility in carbon conversion and product distribution.[17,18] In a DFB, the product distribution can be tailored by the properties of the bed material, reactor temperature, fluidization regimes, and residence time. Steam cracking proceeds through a free radical-type reaction mechanism

in which the final product distribution is governed by the C−C and C−H bond breaking reactions.[19,20] The influences of operational conditions observed in a DFB configuration on these cracking reactions remain largely unknown. Therefore, there is a need to explore how the typical operational conditions in a DFB system affect the steam cracking reactions.

1.2 Aim and scope of this thesis

This work summarizes the results of investigations performed on a semi-industrial DFB steam cracker and a laboratory-scale DFB steam cracker. The investigations aim to strengthen the position of the DFB steam cracking technology among different thermochemical recycling methods. The primary goal of this thesis is to establish a comprehensive database comprising operating conditions and product distributions intended to serve as a foundation for developing large-scale DFB steam crackers. Furthermore, the thesis evaluates the suitability of existing plastic waste streams in society for the DFB steam cracking process. A specific focus of this research is also to shed light on the impacts of operational conditions typical to the DFB system on the reactions occurring during the steam cracking of plastics.

At the inception of this work, two seminal publications emerged as foundational works on the thermochemical conversion of plastic waste in DFB systems. Wilk and Hofbauer's pioneering study marked the first successful demonstration of thermochemical conversion of mixed plastics in a DFB unit.[14] Similarly, Thunman et al. conducted a groundbreaking analysis focusing on steam cracking in DFB systems, emphasizing its potential for circular utilization of plastics.[2] The research conducted in this thesis is influenced by these foundational works and aims to build upon them by pursuing the following research goals:

1. Develop a sampling and analysis strategy suitable for determining product distribution derived from the steam cracking of plastic waste.
2. Create a comprehensive database detailing the operating conditions of a large-scale DFB steam cracker and the resulting product distributions.
3. Identify the challenges associated with thermochemical recycling of plastic waste and address them with DFB steam crackers.
4. Evaluate the suitability of the currently available plastic waste streams for steam cracking in DFB.
5. Explore how the typical operating conditions observed in a DFB system affect the catalytic properties of the bed material and the reactions governing the steam cracking of plastics.
6. Establish appropriate operational procedures concerning the catalytic properties of the bed material to maintain or improve the quality of steam cracking products.

1.3 Contribution to this thesis

Paper I of this thesis reveals the influence of the accumulation of transition metal oxide in the bed material on its catalytic activity. This paper presents experimental results showing the exclusive impact of transition metal oxide-induced oxygen transfer on the reaction mechanism governing the steam cracking of polyolefins. **Paper II** highlights the significance of the oxidation state of bed materials in the context of steam cracking in DFB systems. This paper shows the possibility of hydrogenating unsaturated intermediate species by water molecules in a fluidized bed. **Paper III** describes the importance of biogenic resources in the context of the circular utilization of plastics. This paper provides experimental data that shows waste cooking oil is suitable for producing ethylene and propylene through steam cracking in DFB. **Paper IV** highlights the importance of natural ore bed materials in DFB steam crackers. This paper also explores the potential catalytic activity of natural ores in a hydrocarbon-steam environment. **Paper V** focuses on the sampling and analytical procedures for large-scale DFB steam crackers. This paper presents the first dataset derived from steam cracking of polyethylene in a semi-industrial DFB steam cracker. **Paper VI** shows the evolution of catalytic properties in olivine when subjected to biomass combustion in the regenerator of a DFB steam cracker. **Paper VII** presents the steam cracking of single-use medical materials in a laboratory-scale DFB steam cracker. **Paper VIII** focuses on an operational window for large-scale DFB steam crackers, illustrating product distributions across a spectrum of operating conditions and feedstocks. Additionally, this paper addresses the common challenges faced in thermochemical recycling.

1.4 Outline of this thesis

This thesis is based on the eight appended papers **(Papers I–VIII)** and this introductory essay. *Chapter 2* of the thesis introduces the principles of thermochemical recycling and provides the theoretical framework for the DFB steam cracking process. *Chapter 3* outlines the experimental setups, the materials used, and the evaluation of the experimental data presented in **Papers I–VIII**. *Chapters 4 to 8* summarize and discuss a set of experimental findings. *Chapter 9* presents the concluding remarks alongside recommendations for further research on steam cracking in DFB systems.

CHAPTER 2

2 – The Landscape

2.1 Thermochemical recycling of plastic waste

Thermochemical recycling encompasses a set of processes aimed at producing the molecular building blocks of the feedstock.[2,10] These processes theoretically enable unlimited recycling of any plastic material. Thermochemical recycling of plastic waste involves the production of molecular building blocks, such as ethylene and propylene, as shown in Figure 2.[2]

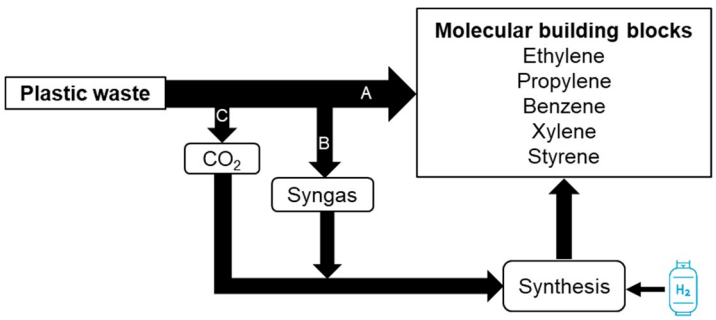

Figure 2. The thermochemical recycling principle applied to plastic waste for the production of different molecular building blocks.

In the thermochemical recycling scheme described in Figure 2, three distinct routes outline the production of molecular building blocks from plastic waste. Route A involves the direct production of these molecules. On the other hand, Routes B and C represent indirect pathways, where the molecular building blocks are produced through intermediate products.

Route B entails converting plastic waste to syngas through partial oxidation or steam gasification. Similarly, Route C involves producing pure CO_2 through the combustion of plastic waste. These intermediate products can be utilized in various synthesis processes such as Methanol-to-Olefins (MTO) or Fischer–Tropsch processes for producing a wide range of molecular building blocks.[21–24] From a thermodynamic perspective, Routes B and C are less

favorable than Route A because the synthesis processes require additional hydrogen to generate the molecular building blocks.[23]

Table 1 outlines common thermochemical processes in plastics recycling, which yield products such as olefins, liquid hydrocarbons, and syngas, depending on the process type and conditions.

Table 1. Different processes for thermochemical recycling of plastic waste.

Thermochemical process	Products	Temperature range (°C)	Suitable feedstocks
Pyrolysis	Mixture of hydrocarbons in the range of C1 – C30	400 – 1000	Polyolefin [25–34]
Catalytic cracking	Mixture of specific paraffin or olefin hydrocarbons	300 – 750	Polyolefin [26,35–45]
Gasification	CO, CO_2, H_2	800 - 1500	Suitable for all plastics [46–52]

Pyrolysis has gained significant attention in thermochemical recycling due to its simplicity and potential for generating a wide range of products. This process primarily produces liquid hydrocarbons from plastic waste through various means such as different heating rates, environments (hydrogen, steam, oxidative, and inert), and reactor systems like fluidized beds, fixed beds, and rotary kilns, among others.[11,28,33]

The liquid hydrocarbons obtained from the pyrolysis of plastic waste, commonly known as pyrolysis oils, serve as valuable feedstocks in the petrochemical industry. The pyrolysis oils are further processed into the molecular building blocks. Common methods include steam cracking of pyrolysis oils in conventional steam crackers.[11,13,33,34]

This two-step approach presents a significant advantage: it allows the pyrolysis process to function independently of petrochemical clusters. Essentially, this means that the recycling process can be decentralized and developed at different scales based on the availability of plastic waste. In this model, pyrolysis plants can operate autonomously, processing locally sourced plastic waste into pyrolysis oils. These oils can then be collectively transported to petrochemical clusters for further processing into new plastic materials.

Despite the potential of pyrolysis for thermochemical recycling of plastic waste, several challenges hinder its industrial-scale development. The pyrolysis oils obtained from plastic waste are rich in olefins, which pose difficulties for conventional steam crackers. Another challenge in the utilization of pyrolysis oils from plastic waste arises from the presence of heteroatoms such as oxygen (O), nitrogen (N), sulfur (S), and chlorine (Cl), which conventional steam crackers cannot handle.[10,13,33,34,53] The olefins and heteroatoms in pyrolysis oils exacerbate coking issues within the steam cracker tubes, necessitating more frequent decoking, ultimately reducing production capacity.[13] Pyrolysis oils from plastic waste must undergo hydrotreating to convert the olefins into paraffins.[13,28,34] Additionally, the non-polyolefin content of the plastic waste needs to be removed to obtain a pyrolysis oil with low heteroatom

content.[28,33,34] However, the high cost associated with presorting and hydrotreating increases the overall cost of the pyrolysis process.

From the standpoint of achieving circular utilization of plastics, the pyrolysis process presents additional limitations in delivering complete recyclability of plastic waste. As pyrolysis plants are typically decentralized, they often lack advanced gas separation units. Consequently, plant operators may burn off-gases generated during pyrolysis, such as methane.[19,28,32] This practice, however, reduces the recovery rate of carbon atoms present in the plastic waste. Furthermore, the feedstock sensitivity of the pyrolysis process results in the rejection of unsuitable fractions of plastic waste streams. These rejected fractions would need to be incinerated if not recycled using alternative methods, further complicating the goal of complete recyclability.

Achieving complete recyclability of plastic waste can be realized through the selective production of the molecular building blocks from plastic waste.[10,26,54] A recycling process focused on generating paraffinic liquid hydrocarbons from plastic waste could also be an attractive solution for closed-loop thermochemical recycling. These recycling processes typically involve catalytic cracking methods, such as fluid catalytic cracking (FCC) or hydrocracking processes.[37,44,55,56]

FCC is a well-established process for cracking heavy hydrocarbons into lighter products using solid acid catalysts.[56,57] Numerous studies have explored the potential of FCC processes for the thermochemical recycling of plastic waste. By employing zeolite-based catalysts, the selectivity of the FCC process can be finely tuned towards light olefins (C2 – C4) within the temperature range of 550 – 750 °C. Using a catalyst offers several benefits. Firstly, it enables a decrease in the reaction temperature compared to the pyrolysis process. Additionally, the presence of a catalyst allows for better control over product selectivity, resulting in a more precise and narrow distribution of products.[35,36,44,45,56]

The hydrocracking process, primarily utilized for diesel and jet fuel production from heavy crude feeds, operates catalytically at temperatures typically between 300 – 450°C and under high hydrogen pressures of 20 – 150 bar. Due to its ability to handle heavy hydrocarbon feedstocks, hydrocracking has gained significant attention in research efforts aimed at the thermochemical recycling of plastic waste. The hydrocracking of plastic waste yields a naphtha-like product with high paraffin content, making it suitable for further processing in conventional steam crackers. One of the advantages of hydrocracking lies in its robustness, facilitated by hydrogen, which effectively removes heteroatoms such as nitrogen, sulfur, oxygen, and halogens.[37,55,58]

The primary drawback of catalytic processes for thermochemical recycling of plastic waste is the deactivation of catalysts. This deactivation occurs due to the numerous impurities in the plastic waste, including nitrogen, sulfur, and alkali metals, which poison the catalysts.[36,58–60] Consequently, ensuring thorough pretreatment and purification of the plastic waste becomes essential to prolong the catalyst's lifetime. In the case of FCC, catalyst deactivation is inevitable due to the coking or poisoning of acidic aluminosilicates.[59] Continuous or frequent catalyst regeneration becomes crucial for maintaining conversion efficiency. Furthermore, hydrocracking necessitates the use of a significant amount of expensive hydrogen and yields less valuable products compared to the light olefins obtained in FCC.[55]

Thermochemical recycling through gasification involves partial oxidation of plastic waste for syngas production. Typically conducted at relatively high temperatures ranging from 700 to 1000°C, this process decomposes the molecular structure of polymers into CO, CO_2, H_2, and CH_4. Gasification of plastic waste is commonly a non-catalytic process performed in the presence of pure oxygen, steam, or air.[48,50,51] The high temperatures in this thermochemical process can essentially convert all plastic wastes without presorting or pretreatment.[9]

Gasification shows the potential to achieve complete recyclability of plastic waste. However, despite its promise, several factors make it economically unattractive. One primary concern is the energy required to convert plastic waste into syngas. This energy requirement increases operational costs, thus negatively impacting the economic viability of the recycling process. Another concern is the need for additional hydrogen in downstream synthesis processes to convert the CO_2 produced during gasification into the molecular building blocks.[23]

The challenges associated with the thermochemical recycling of plastic waste encompass several aspects, impeding the development of such recycling processes at an industrial scale. These challenges also hinder the complete recyclability of the plastic waste prevailing in society. Primarily, these challenges center around the selective production of monomers, the robustness of reactor configurations and catalysts, and the availability of suitable plastic wastes. This work focuses on utilizing a DFB steam cracker to address the challenges faced in the thermochemical recycling of plastic waste. By leveraging the DFB reactor design, the aim is to overcome the limitations posed by conventional reactor systems and catalysts while also achieving the selective production of desired molecular building blocks from plastic waste.

2.2 Steam cracking of plastic waste in DFB reactor configuration

Steam cracking is a fundamental process within the petrochemical industry, essential for producing molecular building blocks from fossil-based feedstocks like naphtha, LPG, or ethane.[41,57] In this method, the feedstock undergoes dilution with steam and rapid heating within a tubular reactor, as depicted in Figure 1 (a), in the absence of oxygen, at temperatures ranging from 750 to 900°C. This process yields a product stream, commonly known as cracker effluent, and primarily consists of gaseous hydrocarbons such as ethylene and propylene. A steam cracker typically has an intensive gas separation unit to separate individual components from the cracker effluent.[57]

The conditions inherent in a steam cracking process make it well-suited for the thermochemical recycling of plastic waste. Notably, these conditions encompass the process's capacity to convert feedstock without a catalyst, all within a moderate temperature range of 750 to 900°C. Furthermore, the steam environment and short residence times facilitate the selective production of ethylene and propylene by minimizing secondary reactions like aromatization.

The conditions typically found in a tubular steam cracker, such as fast heating rates, short residence time, and a steam-rich environment, can be replicated within the DFB reactor configuration. As outlined in Chapter 1, the fluidized bed design enables mixing of the feedstock, rapid heating rates, and short residence times within the reaction zone. Furthermore, by utilizing steam as the sole fluidization agent, a steam environment similar to a conventional

steam cracker results in a cracker effluent devoid of nitrogen. This approach ensures efficient conversion of heterogeneous plastic waste into a gaseous product stream, overcoming the limitations of conventional steam crackers.

Given that the cracker effluent from the steam cracking of plastic waste consists of numerous species, it becomes imperative to equip the recycling process with an intensive gas separation unit capable of isolating individual components. Consequently, such a thermochemical recycling plant must integrate with petrochemical clusters equipped with dedicated gas separation units. This integration effectively transforms DFB steam cracking into a centralized recycling process. Furthermore, these DFB steam crackers should be large-scale to adequately meet the demands of petrochemical clusters and capitalize on the economy of scale.

With DFB steam crackers operating as large-scale units within a centralized recycling solution, ensuring feedstock security becomes paramount to providing reliability to the petrochemical cluster. It is imperative to identify plastic waste streams suitable for such a recycling process and ensure that the quantity of plastic waste is adequate to sustain the operations of a given petrochemical cluster. Additionally, the waste streams should not necessitate additional pretreatment or presorting. Such preprocessing steps could diminish the economic viability and the recycling rate.

2.3 Feedstocks for a DFB steam cracking process

The similarities in molecular structures between petroleum naphtha and polyolefins lead to comparable product distribution obtained from steam cracking of both materials.[2,14] Consequently, waste streams abundant in polyolefins emerge as the most suitable feedstock for DFB steam crackers. Moreover, polyolefins, including low-density polyethylene (LDPE), high-density polyethylene (HDPE), linear low-density polyethylene (LLDPE), and polypropylene (PP), collectively represent a substantial portion, accounting for 60% of the plastic waste generated worldwide.[4] Utilizing these waste streams abundant in polyolefins addresses the need for the substantial volume of plastic waste for a thermochemical recycling process employing DFB steam crackers.

It is challenging to find a waste stream composed entirely of polyolefins despite the prevalence of polyolefins among plastic materials. Plastic waste streams in society, while rich in polyolefins, also contain other constituents such as polyethylene terephthalate (PET), polyvinyl chloride (PVC), cellulose, and several other polymers.[9] These additional constituents originate from various sources, including the production process, utilization of the plastic material, or the collection and handling of the waste stream. The composition of non-polyolefin constituents in the waste stream varies due to these factors.

The nature of the available plastic waste in society restricts the viability of mechanical recycling.[9] Furthermore, thermochemical recycling processes like pyrolysis necessitate the removal of non-polyolefin content from the waste stream to obtain a suitable quality of pyrolysis oil.[28,33] Consequently, these recycling methods best apply to a limited amount of plastic waste that is inherently composed entirely of polyolefins, such as pre-consumer plastic waste originating at the production level. This work demonstrates how the available plastic wastes

can be effectively recycled using a DFB steam cracker despite containing a significant fraction of non-polyolefin constituents.

In this work, plastic waste streams are selected considering their current availability in society, including existing waste collection systems. This consideration also factors in the available quantity of the waste stream, ensuring that it meets the requirements of a centralized recycling process. These considerations result in feedstocks with a diverse range of polyolefin content, thereby strengthening the suitability of a DFB steam cracking process for recycling a blend of polymers without the necessity of presorting.

This work also investigates the potential of products derived from other recycling processes, which may require further processing or may not meet quality standards, for recycling through DFB steam cracking. These feedstocks encompass products derived from mechanical recycling and pyrolysis of polyolefins. Additionally, a blend of polyolefin and cellulose, obtained as a reject fraction from cardboard recycling, is included as one of the feedstocks under investigation.

In a scenario where all plastic materials are derived from plastic waste and the use of fossil resources is phased out, biogenic feedstocks are needed to meet the growing demand for plastic materials. Additional feedstock may also be required to compensate for unrecoverable losses of plastic materials from the recycling system, such as losses to the environment due to mishandling of plastic waste. This work proposes waste cooking oil (WCO) as a suitable biogenic feedstock for the DFB steam cracking process.

WCOs have naphtha-like aliphatic chains in the form of fatty acids within their molecular structure, making them suitable for producing molecular building blocks through the steam cracking process.[61,62] Beyond their suitability for steam cracking, WCOs constitute a substantial portion of the available biogenic carbon resources. As of 2020, global vegetable oil production reached 210 MMT,[63] with approximately 17 MMT ending up as waste in the form of WCO.[64,65] This global production level of WCO presents a valuable feedstock for the DFB steam cracking process, particularly in light of the projected annual increase in demand for plastic materials, estimated at 11.2 MMT per year.[1]

In addition to the diverse feedstock sources previously discussed, this study incorporates clean materials such as a pre-consumer polyolefin stream and petroleum naphtha. These materials serve in developing a reference for product distributions obtained from large-scale DFB crackers. This reference database will help contribute significantly to understanding the outcomes of the steam cracking process across a wide range of parameters.

2.4 Reactions governing the steam cracking of polyolefins

The products obtained from the steam cracking of polyolefins can be categorized into three different groups according to their physical state under normal conditions:

1. Gas: H_2, CO, CO_2, C_1 – C_4 hydrocarbons.
2. Liquid: C_5 – C_{18} hydrocarbons.
3. Solid: Waxes (C_{18+} hydrocarbons), polycyclic aromatic hydrocarbons (PAHs), solid carbon.

The distribution of products among these groups depends on the reaction conditions, known as the "cracking severity." Cracking severity reflects the degree to which C−C bonds break down during the process. Lower severity cracking yields hydrocarbons in the C5 – C30 range, while higher severity produces gaseous olefins in the C2 – C4 range, mono-aromatic (BTXS), and methane. As severity increases, steam reforming of the hydrocarbon species also occurs.[14] In industrial cracking processes, severity is correlated with reaction temperature: higher temperatures result in higher severity cracking.[57] Figure 3 illustrates the evolution of steam cracking products from polyolefins with respect to the cracking severity.

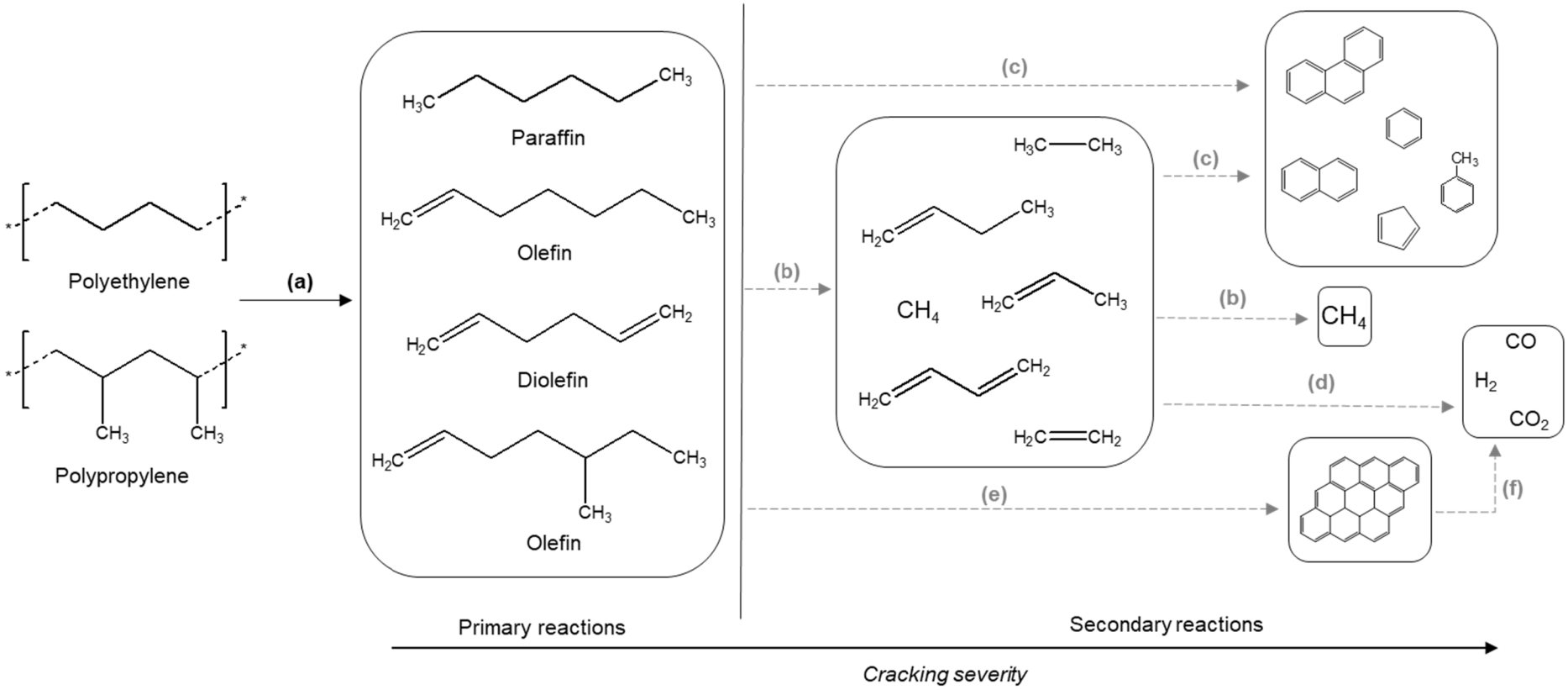

Figure 3. Evolution of the steam cracking products with respect to cracking severity. The solid arrow line represents (a) primary cracking reaction. The dotted arrow lines represent (b) secondary cracking reaction, (c) cyclization and aromatization reactions, (d) steam reforming reaction, (e) coke formation reaction, and (f) steam gasification reaction.

As shown in Figure 3, polyolefin molecules undergo primary cracking reactions to yield short-chain aliphatic hydrocarbons. These primary reactions predominantly involve random C−C bond scission, resulting in a wide range of aliphatic species spanning from C5 to C30.[19,20,66] Despite the diverse range of carbon-number species formed during primary cracking, the intermediate products are mainly paraffins, 1-olefins, and α – ω diolefins. Furthermore, branched polyolefins like PP produce iso-paraffins and iso-olefins as intermediate species.[20]

The products of primary cracking reactions undergo secondary reactions as the cracking severity increases. These secondary reactions primarily involve further C−C bond scission reactions, such as chain-end and β-scission. As a result of these reactions, the formation of the lightest hydrocarbon species, methane, occurs alongside the production of light olefins like ethylene, propylene, and butenes.[19,67,68] Consequently, as the cracking severity increases to a certain level, the product distribution becomes enriched with hydrocarbons within the range of C1 to C4. Additionally, cyclization and aromatization reactions occur, leading to the generation of cyclic olefins and aromatic hydrocarbons.[19,20,66] The steam environment facilitates steam reforming reactions, converting unstable hydrocarbons into syngas. Coke formation and steam gasification reactions become relevant at higher cracking severities.

In addition to the C−C bond scission reaction, the product distribution is also influenced by the C−H bond scission reaction, which aids in stabilizing radical species generated from C−C bond breaking reactions. This reaction involves the transfer of hydrogen atoms among different radical species, known as intermolecular hydrogen transfer.[19,20,66] The transfer of hydrogen atoms also occurs within free radicals, known as intramolecular hydrogen transfer. New free radicals and hydrocarbons with different H/C ratios emerge as the C−C and C−H bond scissions propagate. The mechanisms of intermolecular and intramolecular hydrogen transfer reactions, elucidating the C−H bond scission reaction, are shown in Figure 4.

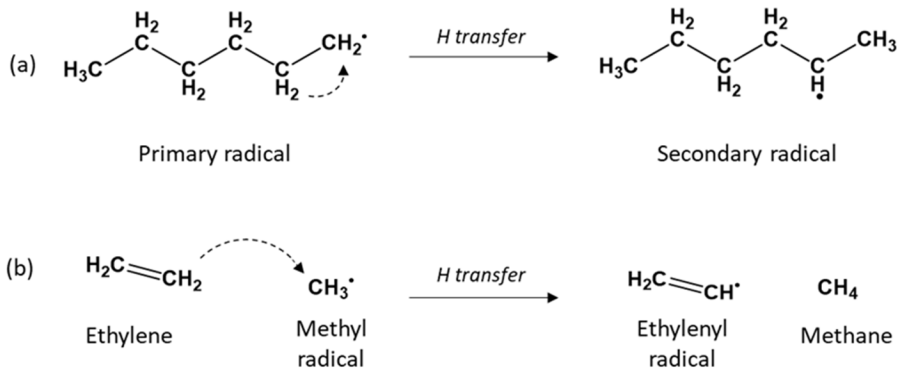

Figure 4. (a) Intramolecular hydrogen transfer; (b) Intermolecular hydrogen transfer.

The products obtained from the steam cracking of polyolefins can be further divided into three groups based on their hydrogen-to-carbon (H/C) ratios:

1. H/C < 2: di-olefins, tri-olefins, aromatics, carbon oxides, solid carbon.
2. H/C = 2: mono-olefins.
3. H/C > 2: paraffins.

Irrespective of the cracking severity, the products of steam cracking will always fall into the abovementioned three groups. The C–H bond scission reaction governs the distribution of products among these groups. The extent to which C−H bond scission propagates is the hydrogen transfer severity, which describes the deviation of the H/C ratio of the steam cracking products from the H/C ratio of the feedstock. Figure 5 illustrates the evolution of steam cracking products with respect to hydrogen transfer severity.

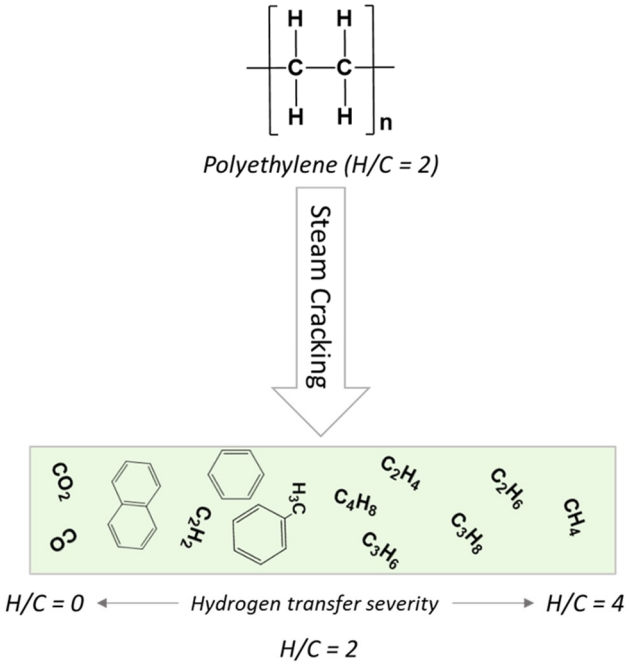

Figure 5. Evolution of the steam cracking products of polyethylene as a function of hydrogen transfer severity for a certain cracking severity.

In the absence of C−H bond scission, cracking a hydrocarbon molecule would give products with the same H/C ratio as the original molecule. For example, cracking of polymethyl methacrylate (PMMA) and PS yields 97 wt.% and 72 wt.% of their monomers, methyl methacrylate and styrene, respectively.[25,69] The steric hindrance caused by the bulky functional groups, such as -$COOCH_3$ and -C_6H_5, along the polymeric chains of PMMA and PS, respectively, hinders the intermolecular and intramolecular hydrogen transfer reactions. The cracking of PMMA is described by Equation 1.

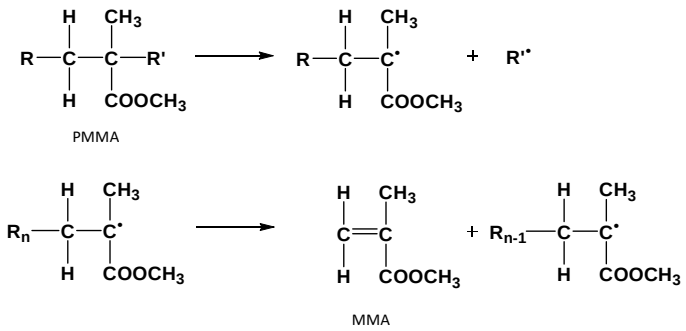

Equation 1

Unlike PS and PMMA, polyolefins such as PE and PP do not contain bulky functional groups along their polymer chains. The lack of steric hindrance along the polymeric chains of polyolefins promotes the hydrogen transfer reactions among the free radicals during steam cracking. Therefore, the C−C and C−H bond breaking reactions govern the product distribution obtained from the steam cracking of polyolefins.

In a steam cracker, the C−C and C−H bond scission persists as long as the necessary energy for these bond-breaking reactions is available in the system. The ultimate product distribution unfolds once all radical species are quenched or recombined. No additional energy is introduced at this stage to sustain further bond-breaking reactions.

In a DFB steam cracker, parameters like bed material temperature, fluidization regime, bed material circulation, and residence time determine the cracking and hydrogen transfer severities, influencing the final product distribution. The interdependence of these parameters makes it challenging to isolate a single factor defining cracking and hydrogen transfer severity. Since methane is the lightest hydrocarbon and has the highest H/C ratio, it can serve as an indicator for both cracking and hydrogen transfer severities. Van Geem et al. were the first to demonstrate the robustness of methane yield as a cracking severity index for the conventional steam cracking process.[84]

2.5 Role of bed material in DFB steam cracking

As outlined in Chapter 1, the bed material within a DFB steam cracker facilitates the mixing of heterogeneous plastic waste. It is also an efficient medium for transferring the heat required for the steam cracking reactions. Additionally, the bed material aids in the continuous removal of solid carbon deposits formed during steam cracking. This process involves combusting the carbon deposits in the regenerator of the DFB unit.

The bed material within a DFB steam cracker may also possess catalytic properties crucial for driving the cracking reactions toward a desired product distribution. FCC is the most prevalent industrial cracking process employing the DFB reactor configuration with a catalytically active bed material. Catalysts used as bed materials in the FCC process enhance cracking severity by lowering the activation energy required for C−C bond breakage.[44,56] However, the susceptibility of FCC catalysts to feedstock impurities renders them unsuitable for a DFB steam cracker dedicated to the thermochemical recycling of plastic waste.

Alternatively, a DFB reactor dedicated to the steam cracking of plastic waste can utilize natural ores as bed materials, which are resistant to feedstock impurities. Thunman et al., in the 2–4 MW_{th} DFB system at Chalmers University of Technology, showed that the products derived from steam cracking of PE are comparable to those from a conventional naphtha cracker.[2] Similarly, Wilk and Hofbauer investigated the production of olefins and aromatic hydrocarbons through thermochemical conversion of various polyolefins in a 100-kW DFB system.[14] Thunman et al. and Wilk et al. employed natural ores silica sand and olivine as bed materials in their respective DFB processes.

The cracking mechanisms outlined earlier do not consider a bed material near the cracking reactions. The suitability of a bed material for the DFB steam cracking process depends on its impact on the C−C and C−H bond breaking reactions. Consequently, in addition to the bed material's resistance to feedstock impurities, its influence on the steam cracking reactions becomes a pivotal factor in selecting the bed material for a DFB steam cracker.

Silica sand is the most extensively studied bed material for the thermochemical conversion of plastic materials in fluidized beds due to its composition primarily comprising SiO_2 (> 90 wt.%), which makes it catalytically inactive toward cracking reactions.[25,41,70] In contrast, certain natural ores like bauxite, olivine, and feldspar exhibit catalytic properties in a hydrocarbon steam environment.[14,70–73] For instance, olivine, when activated with biomass ash, has shown the ability to catalyze steam reforming reactions, thereby enhancing syngas production.[70,72] Similarly, feldspar has demonstrated catalytic activity in steam reforming reactions of hydrocarbons in fluidized beds.[71] Additionally, hydrotreated bauxite has proven effective as a hydrocracking catalyst.[73] However, their specific influences on the C−H and C−C bond breaking reactions during steam cracking of polyolefins remain unclear. **Paper IV** compares the effects of these natural ores on steam cracking reactions, providing insights into their suitability as bed materials in an industrial DFB steam cracking process.

Bed material used in a DFB system undergoes continuous transformations in both its physical properties and chemical composition.[17,18,70] The alterations in physical properties primarily result from the harsh thermal and mechanical stresses experienced in the fluidized bed environment. While these changes typically do not directly impact the cracking reactions, they can result in operational challenges such as agglomeration and loss of fluidization.[17] The changes in chemical composition arise from the presence of external species in the system, often in the form of inorganic compounds. These species may originate from the plastic waste feedstock or the fuel utilized in the regenerator section. Consequently, they accumulate within the bed material, contributing to variations in its chemical composition over time.[17]

In DFB units operated with biomass as a fuel, the bed material gradually accumulates an ash layer over time due to exposure to biomass ash. This phenomenon is particularly notable in bed materials with a limited SiO_2 content, such as olivine, bauxite, and feldspar. Interestingly, these biomass ash-exposed bed materials have exhibited catalytic properties within DFB systems, attributed to their ability to promote steam reforming reactions during the steam gasification of biomass.[70,71] Consequently, in DFB steam crackers utilizing biomass as fuel in the regenerator section, the bed material becomes exposed to biomass ash. While studies have shown that ash-exposed olivine can inhibit the formation of aromatics from biomass gasification, its impact on the steam cracking of polyolefins remains uncertain. It prompts further investigation into the influence of ash-exposed bed materials on the steam cracking reactions, a topic that was examined in detail in **Paper VI**.

The accumulation of transition metal oxides in the bed material represents another relevant change in bed material composition with notable implications. These transition metal oxides may originate from various sources, including the plastic waste or the fuel used in the regenerator section. Pissot et al. conducted a study demonstrating the accumulation of transition metal oxides in the bed material of the Chalmers DFB gasifier, originating primarily from metal-rich automotive shredder residue.[74] This accumulation triggers a phenomenon

known as oxygen transport within the DFB reactor, creating an oxidizing environment that partially or completely oxidizes the feedstock.[75] Given that an oxidizing environment is detrimental to steam cracking, it is crucial to examine the impact of bed materials containing transition metal oxides on the steam cracking reactions. **Paper I** highlights the influence of an oxidizing environment induced by the bed material on the steam cracking reactions of polyolefins.

The inherent chemical composition of the bed material also influences the oxygen transport phenomenon.[70] Natural ores typically contain some transition metal oxides alongside other species.[25,70] As these bed materials circulate between the regenerator and the steam cracker units, they change their oxidation state. It has been observed that the redox potential of transition metal oxides increases the H/C ratio of the products compared to the feedstock through the hydrogenation reaction in a hydrocarbon steam environment.[76–79] **Paper II** investigates the influence of the oxidation state of bed materials on the steam cracking reactions. Furthermore, **Paper II** is the first study to explore the possibility of hydrogenation by water molecules in a fluidized bed reactor.

CHAPTER 3

3 – The Dual Fluidized Bed reactor configuration

This chapter provides a comprehensive overview of the Chalmers DFB steam cracker and its associated gas sampling and measurement system. Additionally, it outlines the methods employed for establishing the carbon balance within the system. The laboratory-scale DFB steam cracker, which utilizes a gas sampling and measurement system similar to the Chalmers steam cracker, is also detailed in this chapter. The experimental results presented in *Chapters 4 through 8* originate from the conducted experiments in both facilities. The chapter also details the composition of bed materials and feedstocks utilized in various experiments constituting this thesis.

3.1 Description of the Chalmers DFB steam cracker

The Chalmers DFB steam cracker is a 12 MW_{th} CFB boiler retrofitted with a bubbling fluidized bed (BFB) steam cracker. The steam cracker has a capacity of up to 4 MW_{th} of feedstock, equivalent to 350 kg/h of pure PE. The boiler is fueled by wood chips and pellets and supplies heat to the Chalmers University campus from November to April each year. The surplus heat from the boiler redirects to the steam cracking reactor.

It is crucial to emphasize that the Chalmers DFB steam cracker operates on a semi-industrial scale and relies on the availability of sufficient personnel for operation. The CFB boiler operates continuously but is manned for two six-hour shifts daily by three operators who oversee operations from the control room. Additionally, three research engineers are responsible for engineering oversight, maintenance, and technical support during experiments. During each experimental campaign, a team of three researchers is present to conduct experiments, collaborating closely with operators and collecting samples from the steam cracker. Each operational point achieved with the Chalmers DFB steam cracker represents

approximately 30 man-hours of effort, excluding time allocated for sample analysis and data processing.

Figure 6 provides a simplified illustration of the system. A detailed description of the DFB system can be found in the work conducted by Larsson et al.[80]

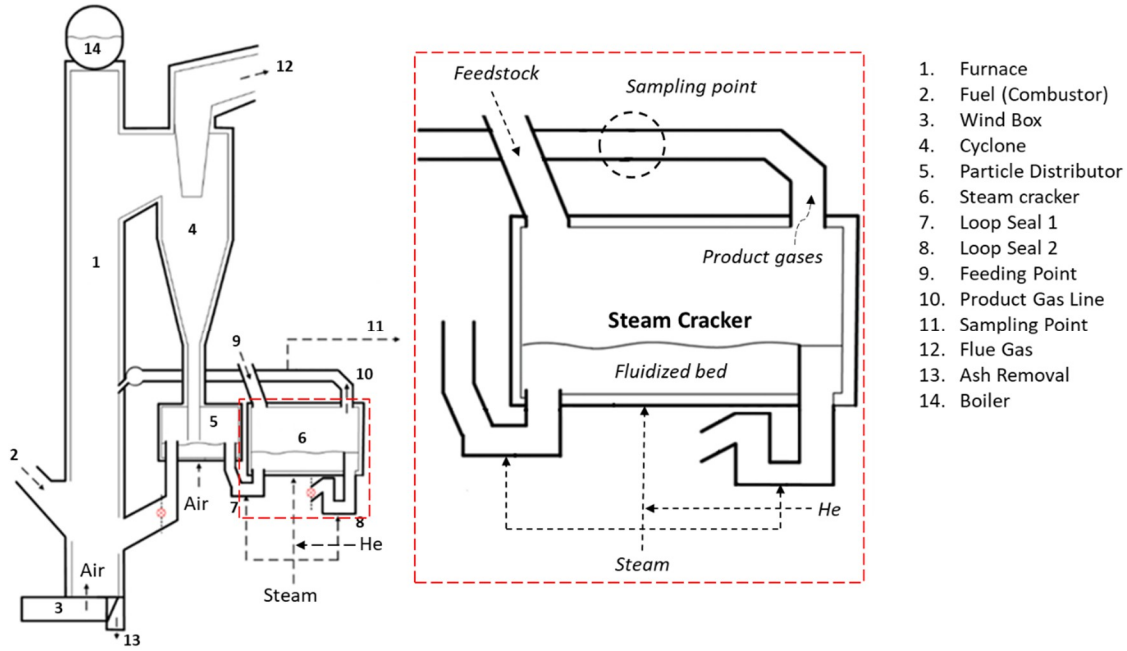

Figure 6. Schematic of the DFB steam cracker at Chalmers University of Technology. The DFB system consists of a circulating fluidized bed boiler (1) and a bubbling fluidized bed steam cracker (6). Adapted from the work performed by Larsson et al.[80]

In this system, the CFB boiler comprises a furnace (refer to (#1) in Figure 6), also referred to as 'the regenerator', and the primary cyclone (#2). When the unit operates solely in CFB mode, the primary cyclone (#2) recirculates the bed to the regenerator via the particle distributor (#5). However, in DFB mode, the bed material follows a distinct path circulating from the particle distributor (#5) to the steam cracker (#6) through the first loop seal (#7). Subsequently, the bed material returns to the regenerator via a second loop seal (#8), linked to the return leg of the regenerator, visually depicted by the two red symbols in Figure 6. The loop seals and the steam cracker undergo fluidization with steam, effectively preventing gas exchange between the regenerator and the steam cracker. The steam cracker and loop seals receive steam supplies of 150 kg/h and 35 kg/h, respectively, meeting the minimum requirements to avoid defluidization. The steam cracker is fluidized with flue gases from the boiler during periods without feedstock input. The regenerator is fluidized with either air or a combination of air and flue gases.

The feedstock is introduced near loop seal 1, as depicted in Figure 6. There are three distinct methods for delivering the feedstock into the steam cracker. The first approach involves introducing a molten feedstock stream through an extruder. This method, utilized in **Papers V** and **VIII**, offers the advantage of isolating the steam cracker from atmospheric air, thereby maintaining a controlled environment. The extruder also facilitates precise control over the feeding rate, ensuring accurate and consistent feedstock delivery onto the top of the bubbling fluidized bed. The experiments described in **Paper VI** employ another system involving the

feeding of pelletized feedstock through a rotary valve. Meanwhile, **Paper VIII** also uses a liquid feeding system, utilizing a centrifugal pump for injecting liquid hydrocarbon feedstock into the steam cracker. Regardless of the chosen feeding system, the feedstock is introduced onto the top of the fluidized bed.

The cracker effluent is directed to the regenerator through the product gas line, as illustrated in Figure 6. As this facility primarily serves as a research site, the cracker effluent undergoes combustion on the regenerator side. In contrast, in a commercial unit, additional steps involving gas cleaning processes would precede the redirection of cracker effluent toward their final application. The solid carbon deposits, commonly known as coke, formed on the surface of the bed material within the steam cracker are combusted in the regenerator. This process facilitates the reintroduction of coke-free bed material back into the steam cracker.

A crucial point to underscore is that when the regenerator operates with biomass, a portion of the ashes generated during biomass combustion accumulates on the surface and within the particles of the bed material. A daily bed material regeneration of 500 kg is implemented to manage the amount of biomass ash accumulation. It is particularly significant in the context of catalytic activity development in the bed material enriched with biomass ash. **Paper VI** investigates this phenomenon, and *Chapter 8* of this thesis outlines the key findings.

3.2 Description of the laboratory-scale DFB steam cracker

The laboratory-scale steam cracker is a standalone tubular reactor that operates as a BFB. The BFB reactor can replicate the operational dynamics of the Chalmers DFB steam cracker through a defined set of operational procedures. It is accomplished by operating the reactor in batch mode and systematically alternating the fluidization gases between steam and air. The operational concept is visually represented in Figure 7, illustrating the transition between the steam cracking and regeneration mode to mimic the behavior of the larger-scale Chalmers DFB steam cracker.

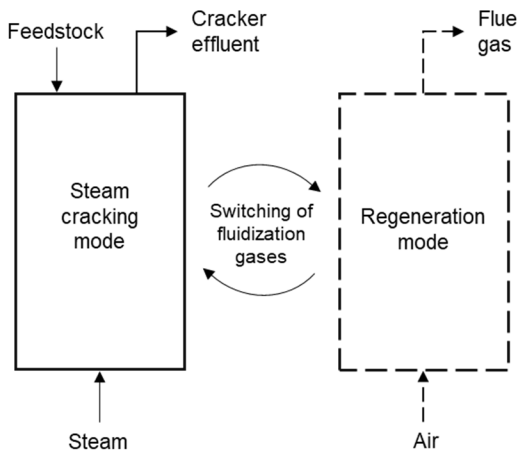

Figure 7. Diagram illustrating a laboratory-scale BFB reactor, operated in batch mode to emulate the dynamics of a large-scale DFB steam cracker.

In the laboratory setup, the fluidized bed functions as a steam cracker when fluidized with steam. During this operation, a batch of feedstock is introduced from the top of the reactor, which is open to the atmosphere. The resulting cracker effluent exits the reactor from the top, along with the fluidization steam. Fluidization gas can then be switched to air, transforming the reactor into a regenerator. This phase facilitates the combustion of carbon deposits formed during the steam cracking stage. This step ensures the introduction of carbon deposit-free bed material into the steam cracking stage, aligning with the observed practice in the Chalmers DFB steam cracker. Additionally, the bed material to feedstock ratio (on a mass basis) can be matched with the Chalmers DFB steam cracker, maintaining equivalence to the large-scale process.

The laboratory setup is a tubular reactor of stainless steel with an internal diameter of 88.9 mm and a height of 1305 mm. The reactor is placed inside an electrically heated oven. Three thermocouples within the reactor monitor the temperature during the experiments. One of these thermocouples is submerged in the fluidized bed, while the other two are in the freeboard area. The temperature in the freeboard region is regulated to match that of the bed material. The bed materials are loaded from the top of the reactor before heating the reactor. After each experiment, the reactor is cooled down and cleaned with a vacuum cleaner before loading a different batch of bed material.

The fluidization gases are introduced from the bottom of the reactor and can change between nitrogen, air, helium, steam, or a combination of these. The fluidization gases are mixed homogeneously in a mixer before entering the reactor. An evaporator with a liquid flow controller (LFC) produces the fluidization steam. Mass flow controllers (MFC) provide the required air and nitrogen. The nitrogen flow (2 ln/min) maintains a stable steam flow and prevents the back-mixing of atmospheric air from the top of the reactor.

3.3 Sampling and analysis of the cracker effluent

Sampling the cracker effluent from the Chalmers DFB and the laboratory reactor involves extracting a slipstream at the reactor outlet. The following sections provide an overview of the sampling and analytical strategies for the two reactor systems.

3.3.1 The method applied to the Chalmers DFB steam cracker

Two parallel slipstreams of the cracker effluent, approximately 10 l_n/min each, are continuously extracted for sampling from the product gas line (see 11, Figure 6). Figure 8 illustrates the gas sampling system encompassing the two slipstreams and the corresponding analytical methods applied at each slipstream.

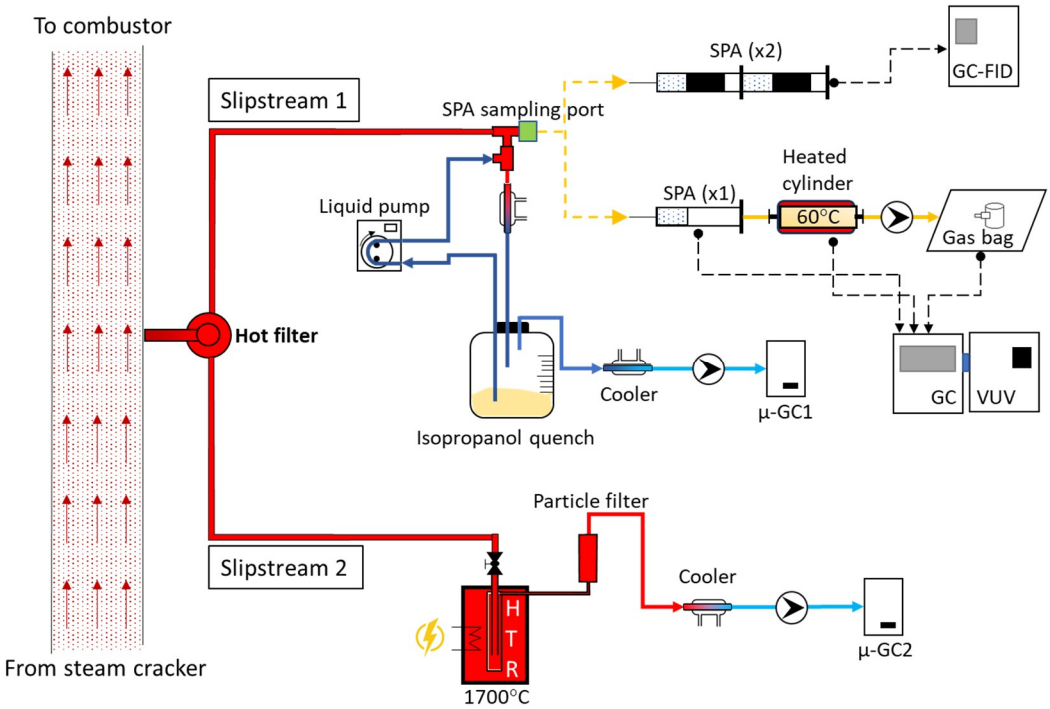

Figure 8. Schematic of the gas sampling system installed at the Chalmers DFB steam cracker, including the two parallel slipstreams. The hot filter is positioned at 'point 11' (see Figure 6). Red lines are the heat-traced lines at 350°C. The remainder of the piping corresponds to the unheated side of the slipstreams. The dotted line represents offline characterization of the individual samples, while the continuous line represents online GC measurements.

Slipstream 1 is dedicated to the sampling and analysis of individual species within the cracker effluent. Four distinct techniques are employed at Slipstream 1: (1) SPA (Solid phase adsorption), (2) hot gas sampling, (3) gas bag sampling, and (4) permanent gas analysis. Subsequently, the collected samples undergo analysis using GC-FID, GC-VUV, or GC-TCD. This comprehensive approach, developed as part of the investigation outlined in **Paper V**, enables the detection and quantification of species ranging from C1 to C18.

The second slipstream is directed towards a high-temperature reactor (HTR) to quantify the total amounts of carbon (C), hydrogen (H), and oxygen (O) in the cracker effluent. Within the HTR, the cracker effluent reacts at a temperature of 1700 °C, leading to the decomposition of all hydrocarbons into CO_2, CO, and H_2. Online monitoring of these decomposition products is conducted with a micro-GC system to calculate the elemental flows of C, H, and O exiting the steam cracker. Simultaneous sampling from both slipstreams serves to validate the carbon balance closure achieved during a stable operation. This HTR method, developed for the verification of carbon balance over the Chalmers DFB system by Israelsson et al., is a robust approach for assessing and confirming the carbon balance.[81]

The GC analyses conducted at the two slipstreams provide the share of individual species in the cracker effluent. A tracer gas is used to determine the absolute yields relative to the feedstock and establish the carbon balance over the system. Helium (He) gas is introduced into the steam cracker with steam at a known volumetric flow. Regulated by a Bronkhorst® model F-202AV MFC, the volumetric flow of He serves as the tracer across the system. The He balance converts the concentrations obtained from the GC analyses into yields, expressing their quantities in moles or mass of the product species per unit mass of the feedstock.

3.3.2 The method applied to the laboratory steam cracker

In the laboratory setup, the sampling system includes extracting two parallel slipstreams of cracker effluent through a sampling probe inserted into the reactor. The sampling probe is inserted into the freeboard approximately 10 cm above the fluidized bed. The probe is maintained at 350°C with an electrical heating band to prevent condensation of steam and hydrocarbons. Figure 9 illustrates the two slipstreams, S1 and S2, and the corresponding sampling methods applied.

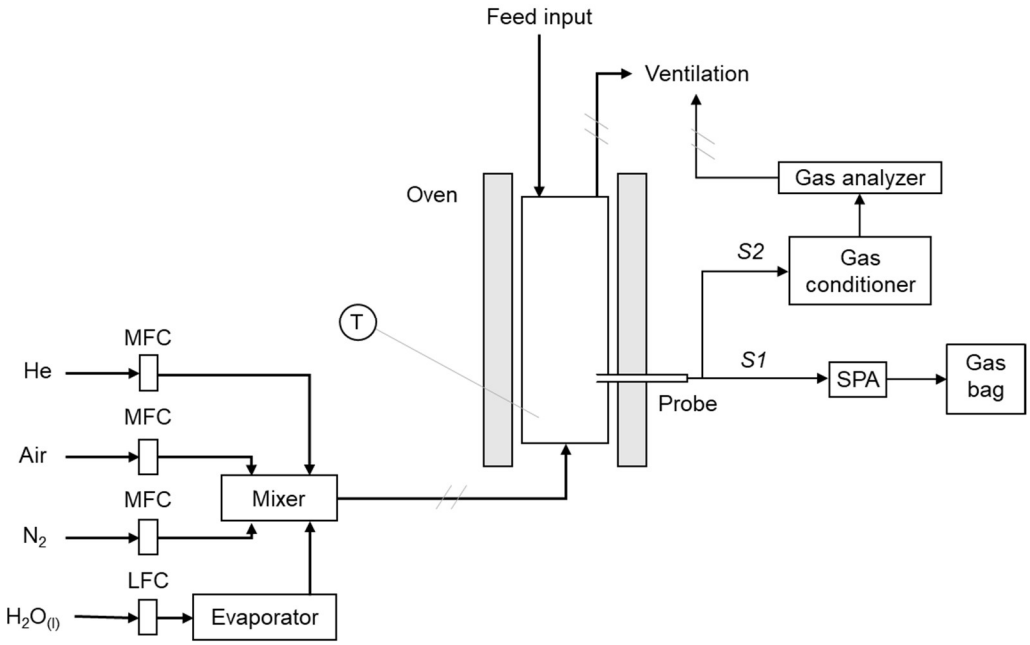

Figure 9. Schematic of the laboratory-scale fluidized bed steam cracker and the installed sampling and analysis system.

Slipstream S1 is used to sample SPA columns and gas bags, which are subsequently subjected to analysis using GC-FID and GC-TCD, respectively. The GC-TCD analysis of gas bags quantifies C1 to C4 species, and the GC-FID analysis of SPA samples quantifies specific aromatic species within the C6 to C18 range. The SPA method applied in both the Chalmers DFB steam cracker and the laboratory reactor is based on the approach developed by Israelsson et al.[82] The laboratory setup also incorporates the use of helium (He) as a tracer gas, facilitating the determination of absolute yield of cracker effluent and establishing a carbon balance over the system.

Slipstream 2 is used for the continuous monitoring of permanent gases H_2, O_2, CO, CO_2, and CH_4 in the cracker effluent. The continuous monitoring is performed using a SICK GMS 820 permanent gas analyzer (manufactured by SICK AG). The cracker effluent is dried and cooled by scrubbing with isopropanol in a gas conditioning system (see Figure 9) before it is acquired by the gas analyzer. The cracker effluent is continuously measured to determine the total reaction time and ensure no leakage of atmospheric oxygen into the reactor system during the experiments. The sampling and analysis method associated with the laboratory setup is applied through **Papers I-IV** and **Paper VII.**

For both reactor setups, the quantification of individual species in the cracker effluent revolves around GC measurement. Table 2 enlists the different GC equipment, the corresponding sample, and the species analyzed using each equipment.

Table 2. Analytical equipment applied in this work, the corresponding type of samples, and the quantified species.

Equipment	Type	Reactor system	Sample type	Species quantified
μGC1	Micro-GC Varian CP4900, with Poraplot Q and MS5A columns	Chalmers DFB steam cracker	Cracker effluent scrubbed with isopropanol at -17°C	H_2, O_2, N_2, CO, CO_2, CH_4, C_2H_2, C_2H_4, C_2H_6, C_3H_6, C_3H_8, H_2S
μGC2	Micro-GC Varian CP4900. MS5A and Poraplot U columns	Chalmers DFB steam cracker (HTR)	Outlet of HTR: cracker effluent reacted at 1700°C	H_2, O_2, N_2, CO, CO_2, CH_4, C_2H_2, C_2H_4, C_2H_6, C_3H_x
μGC3	Agilent 490 micro-GC with Poraplot U, CP-COX and CP-Sil5 columns	Laboratory steam cracker	Gas bags	H_2, Air, CO, CO_2, CH_4, C_2H_2, C_2H_4, C_2H_6, C_3H_x, C_4H_x
GC-FID	Bruker GC-430 with midpolar BR-17 ms columns	Chalmers DFB steam cracker, laboratory steam cracker	SPA	Benzene, Toluene, Xylenes, Styrene, Naphthalene, etc.
GC-VUV	Thermo Scientific TRACE 1310 with ZB1-HT and CP-Sil5 CB columns	Chalmers DFB steam cracker	Gas bags, hot gas, SPA	All hydrocarbons in the range of C3 to C18

3.4 Data evaluation

The experimental results presented in *Chapter 4* through *Chapter 8* are derived from the same analysis and evaluation methods described in this section. As a result, the systematic errors for all the data points are similar, rendering the observed trends statistically significant.

The molar yields of the species measured with the micro-GCs are calculated based on the He-tracing method. Equation 2 converts the concentration of individual species into their corresponding molar yield.

$$n_i = \frac{c_i}{m_f} \cdot \left(\frac{V_{He}}{c_{He}}\right) \cdot \frac{1}{V_m}$$

Equation 2

In Equation 2, n_i denotes the molar yield (mol/kg), and c_i is the concentration (%vol.) of species i. The terms V_{He} and c_{He} represent the volumetric flow rate (l/h) and concentration (%vol.) of

the tracer helium gas, respectively. m_f is the mass flow of the feedstock (kg/h), and V_m is the volume of one mole of an ideal gas at 0°C and 1 atm (22.4 l/mol). The molar yield of each species is transformed into the corresponding carbon and hydrogen yields based on the total carbon and hydrogen content of the feedstock.

The mass concentrations of the species measured by GC-VUV in the gas samples are converted into their corresponding molar yield using Equation 3. This equation considers the mass concentration of species *i* ($\%m_i$) and C_3H_6 ($\%m_{C3H6}$) in the gas sample, which is obtained by processing the GC-VUV chromatograph using the VUV Analyze software (developed by VUV Analytics, Inc.).[83] The variable MW_i represents the molecular weight of species *i*. The term n_{C3H6} denotes the molar yield of C_3H_6 and is obtained using Equation 2. In Equation 3, C_3H_6 serves as the reference species because it is a common component that can be measured using μGC1 and GC-VUV techniques.

$$n_{i\,VUV} = \left(\frac{\%m_i}{\%m_{C_3H_6}}\right)_{VUV} \times \left(\frac{MW_{C_3H_6}}{MW_i}\right) \times n_{C_3H_6}$$

Equation 3

The quantification of species sampled through the SPA method follows the procedure established by Israelsson et al.[82] This method takes into consideration the total molar flow of species not captured in the SPA column and incorporates a known concentration of an internal standard, added to the sample before GC analysis. This procedure remains consistent, regardless of GC-FID or GC-VUV analysis. It is noteworthy that the entire analytical measurement can be efficiently carried out using only one GC-TCD and one GC-VUV equipment, as successfully demonstrated in **Paper V**.

The results of the measurements using μGC1 and μGC2 analysis are average values obtained from multiple measurements during a stable operation lasting at least 60 minutes for the Chalmers DFB steam cracker. Stability in this context indicates consistent flows of feedstock and steam, with temperature fluctuations maintained within ±3°C. The yield of species, as measured by the two equipment, reflects the average of 10–20 chromatographs. Typically, these chromatographs exhibit a relative standard deviation of less than 2%.

The stability of the Chalmers DFB steam cracker, maintained for over 60 minutes, also ensures a fair comparison of the extracted SPA and gas samples, even though they are collected at different times. During a stable operation, four samples of gas bags, hot gas, and SPA are collected for subsequent GC analysis. Specifically, each SPA sample undergoes analysis three times with either GC-FID or GC-VUV, and the results presented reflect the average of 12 chromatographs (4 samples x 3 GC repetitions). The results of gas samples analyzed with GC-VUV are the average of the four samples taken during the stable operation.

The laboratory steam cracker, functioning as a batch reactor, relies on the repetition conducted under the same operating conditions to ensure the repeatability of the experiments. Results obtained from the laboratory setup are an average of four data points, corresponding to the four repetitions of the same experiment. During each experiment, gas bags and SPA samples are collected and analyzed three times using μGC3 and GC-FID, respectively. Notably, each data

point represents an average of 12 chromatographs (4 batch experiments x 3 GC repetitions). An experiment repetition is invalid if the relative standard deviation for the yield of the majority of the species exceeds 10%. This criterion allows for excluding any data points with substantial variability that could compromise the validity of observed trends.

3.5 Materials

3.5.1 Bed Materials

Table 3 outlines various bed materials incorporated in this thesis and their chemical compositions. A graduation change in the bed material's properties occurs upon exposure to a DFB steam cracker. This change involves structural modifications resulting from the reductive-oxidative cycles, exposure to high temperatures, and alterations induced by thermal and mechanical stresses. Additionally, the bed materials undergo transformation through interaction with ash components originating from both the steam cracker feedstock and biomass fed into the regenerator. The interactions with biomass ash are absent in the laboratory reactor since no biomass is introduced during the combustion stage. Given the impracticality of detailing the composition of bed materials at every stage of evolution, the composition presented in Table 3 reflects the chemical composition measured or calculated before the introduction of bed material into the steam cracker.

Table 3. Chemical composition (%wt.) of the tested bed materials.

	Silica sand	Olivine	Bauxite	Feldspar	Al_2O_3	$1Fe/Al_2O_3$	$2Fe/Al_2O_3$	$5Fe/Al_2O_3$
SiO_2	90	41.7[a]	6.5	67.5	-	-	-	-
Al_2O_3	5.5	0.17	88.5	78.8	99.5	97.2[b]	94.5[b]	86.9[b]
Fe_2O_3	0.6	7.4[a]	1.1	0.11	<0.05	2.8[b]	5.5[b]	13.1[b]
TiO_2	-	-	3.0	0.01	-	-	-	-
MgO	-	49.6[a]	-	0.04	-	-	-	-
Na_2O	1.2	-	-	4.3	-	-	-	-
K_2O	1.8	-	-	8.4	-	-	-	-

[a]Assumed to be present as silicates of iron and magnesium.

[b]Synthetic material, chemical composition calculated based on the synthesis procedure.

Among the bed materials utilized in this study, silica sand, olivine, bauxite, and feldspar are natural ores used without any chemical modifications. The material Al_2O_3 is synthetic neutral alumina with a purity of 99.5%, sourced from Fischer Scientific. The materials $1Fe/Al_2O_3$, $2Fe/Al_2O_3$, and $5Fe/Al_2O_3$ were prepared through incipient wetness impregnation of Al_2O_3 with iron nitrate nonahydrate solution ($Fe(NO_3)_3.9H_2O$). The nomenclatures 1Fe, 2Fe, and 5Fe denote the %weight (atom basis) of Fe in the material, calculated based on the synthesis procedure.

Leveraging the inert characteristic of silica sand, it serves as a reference material in this thesis. Its use aims to establish an ideal operating window for DFB steam crackers, representing steam

cracking scenarios of a pure polyolefin with an inert bed material. The results falling within this ideal operating window are detailed in *Chapter 5*, based on the investigations conducted in **Papers V** and **VIII**.

Paper IV examines the impact of olivine, bauxite, and feldspar in their natural state on the steam cracking reactions, with the findings featured in *Chapter 7*. Olivine was also used in the Chalmers DFB steam cracker to assess its catalytic activity when exposed to biomass ash. This investigation, documented in **Paper VI**, is highlighted in *Chapter 8*. Bauxite and olivine were used in the laboratory reactor to explore the hydrocracking potential of fluidized bed reactors. The outcomes of this study are significant and highlighted in *Chapter 8*.

The synthetic bed materials based on Al_2O_3 were used to assess the exclusive impact of transition metal oxides on the steam cracking reactions, constituting a crucial aspect of the investigation outlined in **Paper I**. The synthesis procedure involved the impregnation of Al_2O_3 with a $Fe(NO_3)_3.9H_2O$ solution, followed by drying at 105°C and calcination at 700°C in the laboratory reactor. To characterize the synthesized bed materials, scanning electron microscopy (FEI ESEM Quanta 200) was employed, and energy-dispersive x-ray spectroscopy (SEM-EDS) was conducted to evaluate the elemental composition. The outcomes of this study, integral to understanding the influence of transition metal oxides on steam cracking reactions, are thoroughly discussed in *Chapter 8*.

3.5.2 Feedstocks

A diverse range of feedstocks was introduced into the steam crackers, operating at both the scales of the reactor system. These feedstocks ensure variability in the polymer composition while considering their availability in real-life scenarios. The variability within the polymer composition revolves around the polyolefin content of the feedstock. Simultaneously, considering the feedstock availability ensures that these waste streams are present in society, eliminating the need for pre-treatment or separation before being fed into a DFB steam cracker. Products derived from alternative polyolefin recycling processes were also tested in this study. In total, 11 distinct feedstocks were tested, and Table 4 offers an overview of these feedstocks, describing their polymer composition and relevant chemical characteristics.

Table 4. Feedstocks used in this work with their respective polymer composition and general characteristics.

Feedstock	Polymer types	Chemical characteristics	Description
Polyethylene (PE)	HDPE	- high polyolefin content - low oxygen content - low ash content	Virgin polymer pellets
Naphtha	-	- high paraffin content - low olefin content - low aromatic content - low oxygen content - low ash content	Light straight run petroleum naphtha
Rapeseed oil	-	- high aliphatic content - high oxygen content - high olefin content - low ash content	Unused edible cooking oil
Pyrolysis oil	-	- high aliphatic content - high olefin content - low oxygen content - low ash content	Polyolefin pyrolysis oil (untreated)
Mechanically recycled polyolefins (MRP)	PE, PP	- high polyolefin content - low oxygen content - low ash content	Mechanically recycled post-consumer polyolefin mixture (pelletized)
Cardboard recycling reject (CRR)	PE, PP, PET, PVC, Cellulose	- medium polyolefin content - high oxygen content - high ash content	Post-consumer shredded stream of multilayer cardboard/plastic for food packaging (pelletized)
Mixed plastic waste (MPW)	PE, PP, PET, PVC, PU, PA, PS, Cellulose	- medium polyolefin content - high oxygen content - high ash content	Post-consumer unsorted mix plastic waste (shredded)
Medical materials	PP, PE, PET, PAN, PC, PS	- high polyolefin content - high oxygen content - high nitrogen content - high ash content	Unused medical materials: face masks, syringes, non-woven gloves, nitrile gloves (shredded)

PE stands out among the feedstocks listed in Table 4 as the only virgin plastic devoid of contaminants that may accumulate in plastic materials throughout their usage lifespan. Supplied by Borealis AB (Stenungsund, Sweden), the virgin PE pellets exhibit a bulk density of 945 kg/m^3 and an average pellet size of 2.5 mm. PE was used in the Chalmers DFB steam cracker for the investigations performed in **Papers V**, **VI, and VIII**. PE was also used in the laboratory reactor to explore the influence of bed material on steam cracking reactions, as shown in **Papers I**, **II**, and **IV**. *Chapters 7 and 8* discuss the outcomes of these investigations.

The thesis also encompasses three liquid feedstocks: Naphtha, Rapeseed oil, and Pyrolysis oil. Notably, these liquid feedstocks stand out as the non-polymeric alternatives used in the work. Based on **Paper VIII**, results obtained from the steam cracking of naphtha are used to establish reference operational curves for DFB steam crackers. *Chapter 5* shows these reference operational curves. Rapeseed oil, the focus of **Paper III**, is examined for its potential as a biogenic feedstock in the DFB steam cracking process. *Chapter 6* details the outcomes of this investigation. Pyrolysis oil, derived from the thermal pyrolysis of waste polyolefins, represents another liquid feedstock explored in **Paper VIII**. While specific details regarding the origin remain confidential, the paper establishes polyolefin pyrolysis oils as suitable feedstock for steam cracking in DFB systems. Notably, steam cracking of pyrolysis oil is demonstrated without additional upgrading steps like hydrogenation.

This thesis incorporates the utilization of solid plastic wastes, namely Mechanically recycled polyolefins (MRP), Cardboard recycling reject (CRR), and Mixed plastic waste (MPW), all subjected to testing in the Chalmers DFB steam cracker through the extruder feeding system. In addition, medical materials such as single-use face masks and syringes were tested in the laboratory reactor.

MRP is a post-consumer polyolefin mixture primarily composed of PE and PP. The details regarding the origin of MRP are confidential. CRR is a byproduct from recycling cardboard packaging like milk cartons, and it is a mix of cellulose and polyolefins that resist further separation through the conventional pulping method. Notably, CRR also contains a certain amount of PET and PVC. Meanwhile, MPW, sourced from domestic waste streams, encompasses various polymers, with polyolefins being the predominant component. These three waste streams are the focus of investigation in **Paper VIII**, and the outcomes are elucidated in *Chapter 6*, shedding light on the capability of DFB steam crackers in handling heterogeneous waste streams.

Analyzing the feedstocks to determine their exact polymer composition is challenging due to their heterogeneous nature. Nevertheless, the proximate and ultimate analysis provides the elemental composition of these feedstocks. Table 5 provides the C, H, O, N, S, and Cl composition of all the feedstocks used in this study. Additionally, the table includes details on moisture and ash contents for each feedstock. It is crucial to note that the elemental composition presented in Table 5 is a dry basis composition. The same dry basis approach applies to the results reported in the subsequent chapters.

Table 5. Elemental composition of the feedstocks used in this work along with their respective moisture and ash content.

	Polyethylene	Naphtha	Rapeseed oil	Pyrolysis oil	MRP	CRR	MPW	Face masks	Syringes	Non-woven gloves	Nitrile gloves
Moisture (%wt.)	0.00	0.00	0.00	0.00	0.60	4.50	3.50	0.00	0.00	0.00	0.00
Composition (%wt. dry basis)											
Carbon (C)	85.70	84.11	79.60	85.63	85.26	60.60	66.60	81.60	84.24	84.21	76.02
Hydrogen (H)	14.20	15.88	11.40	14.35	14.12	8.80	9.50	13.70	14.34	11.56	8.26
Oxygen (O)	0.00	<0.01	8.97	<0.01	0.00	21.00	14.27	4.68	0.01	0.01	9.41
Nitrogen (N)	0.00	<0.01	0.00	<0.01	0.01	0.07	0.08	0.01	0.18	0.21	6.34
Sulfur (S)	0.00	<0.01	0.03	<0.01	0.01	0.07	0.08	-	-	-	-
Chlorine (Cl)	0.00	<0.01	0.00	<0.01	0.10	0.20	0.73	-	-	-	-
Ash	0.08	0.00	0.00	0.00	0.10	8.75	8.29	5.50	0.18	0.32	5.78

CHAPTER 4

4 – Developing a sampling and analytical strategy for steam cracking of plastic waste

Sampling the cracker effluent from steam cracking of plastic waste presents several challenges due to the large number of species in the mixture, which span a wide range of boiling points. Additionally, characterization using GC analysis requires extended analysis times because of the numerous species, reducing the overall analytical throughput. The presence of steam further complicates the analytical process, as the water content within the sample can adversely affect the quality of GC analysis.

Based on insights from **Papers V** and **VIII**, this chapter presents a sampling and analysis strategy that overcomes these challenges in quantifying and characterizing species within the cracker effluent resulting from steam cracking of plastic waste. Three distinct sampling methods are introduced to sample species ranging from C1 to C18. These sampling methods are integrated with GC-VUV analysis and other established analytical techniques, forming a comprehensive approach to quantify the sampled species. Emphasis is on the GC-VUV analysis due to its effectiveness in identifying and quantifying individual hydrocarbon species. Furthermore, the method developed in this study is validated against established sampling and analysis methodologies.

4.1 A 3-step sampling and analysis approach

The proposed sampling and analysis approach involves a structured sampling process conducted in three distinct steps, targeting specific groups of carbon species. By integrating these steps with GC-TCD and GC-VUV analysis, the strategy offers a qualitative and quantitative analysis of the cracker effluent. For a more detailed insight into this methodology, refer to Figure 10, which describes the specific sampling steps and the corresponding carbon groups they cover.

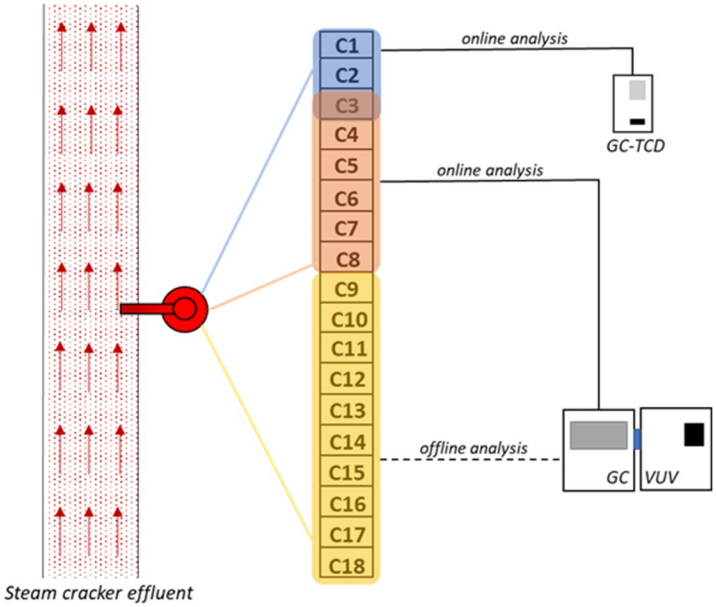

Figure 10. The sampling and analysis approach outlined in this chapter, implemented on the effluent stream of the Chalmers DFB steam cracker.

The three distinct sampling steps described in Figure 10 aim at rapid quantification of the important species obtained from the steam cracking of plastic materials. Specifically, these steps target the online identification and quantification of C1 to C8 species, which collectively constitute up to 90% of the product distribution resulting from the steam cracking of polyolefins. The C9 and higher hydrocarbon species are sampled separately and analyzed offline. This offline analysis strategy prevents interference between the analysis of the C1 – C8 species and that of the C9+ species, thereby increasing the throughput of the method.

The analytical strategy revolves around a recently developed technique called GC-VUV analysis. This method is applied to two separate sets of samples: C3 – C8 and C9 – C18, as shown in Figure 10. The utilization of GC-VUV addresses the challenge of analyzing a large number of species in the C4 to C18 range within a brief analysis timeframe. That is because the VUV detector can deconvolute up to four species that coelute from the GC column. Figure 11 visualizes this deconvolution technique that substantially reduces the analysis time while also facilitating the detection of all hydrocarbon isomers in the sample.

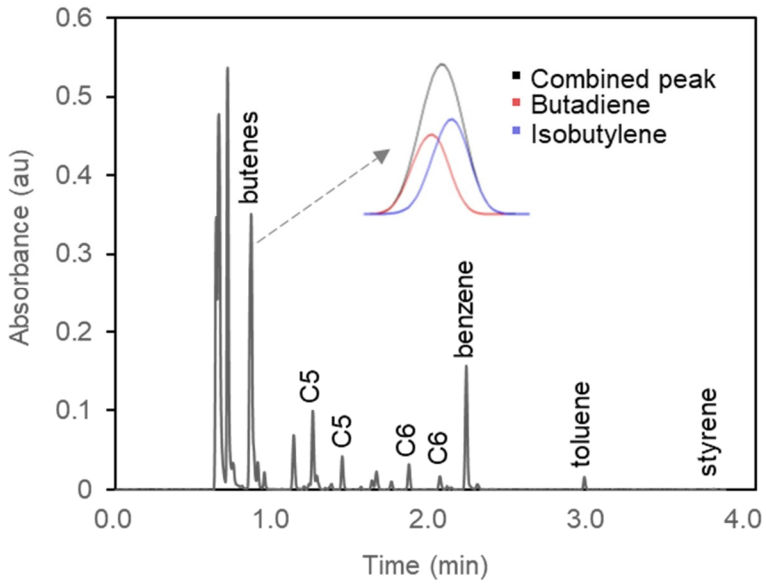

Figure 11. GC-VUV chromatograph (average 130 – 240 nm) of a cracker effluent sample. The sample was collected at the outlet of the Chalmers DFB steam cracker and quenched to 60°C before being introduced into the GC. The effectiveness of the VUV detector's deconvolution capability is demonstrated by the peak observed for butenes.

Figure 11 displays a GC-VUV chromatograph of a gas sample extracted from the Chalmers steam cracker. Before injection into the GC, the gas sample was quenched to 60°C to eliminate C9+ components. The chromatograph reveals numerous peaks corresponding to hydrocarbons ranging from C4 to C8. Some peaks overlap due to the different isomers in the gas sample that coelute from the GC column. However, the VUV detector's deconvolution capability effectively addresses this coelution issue, enabling quicker analysis of each sample. Moreover, the VUV detector quantifies each species in the chromatograph using its unique relative response factor (RRF).[83] This eliminates the necessity of calibrating the equipment with a large number of species, streamlining the analytical process. Table 6 summarizes the sampling and analysis strategy applied at the hot sampling point of the Chalmers unit (see Figure 8, *Chapter 3*).

Table 6. The sampling and analytical techniques employed at the outlet of the Chalmers steam cracker for the analysis of C1 – C18 species within the cracker effluent.

Species	Sampling method	Analytical instrument
C1 – C3	Cracker effluent scrubbed with isopropanol at -17°C	µGC1
C3 – C8	Cracker effluent quenched to 60°C, sample collected in a gas-tight sampling vessel.	GC-VUV
C9 – C18	SPA	GC-VUV

The C1 to C3 species are sampled by subjecting the cracker effluent to scrubbing with isopropanol at -17°C. The resultant gas is continuously analyzed for its volumetric composition (%vol.) using µGC1. To sample the C3 – C8 species, the cracker effluent is quenched to 60°C and collected in a sampling vessel. The collected sample is analyzed for its volumetric composition (%vol.) using GC-VUV. It's important to mention that the sample collected for

C3 – C8 analysis also encompasses C1 and C2 species. However, the analysis is exclusively conducted to quantify C3 to C8 species. The species in the range of C9 – C18 are sampled using the SPA method and analyzed using GC-VUV. **Paper V** provides detailed information about the analytical methods employed on the GC-VUV for the SPA and gas samples.

The quantification of each sampled species relies on the helium tracing method. As described in *Chapter 3*, a known flow of helium is introduced into the fluidization steam as a tracer gas. The known flow of helium is used to calculate the molar flows of C1 – C3 species based on the volumetric composition determined by μGC1 (according to Equation 2). For the quantification of C3 to C8 species using GC-VUV, the calculated molar flow of C_3H_6, based on GC-TCD analysis, serves as an internal standard. Similarly, when quantifying C9 to C18 species in the SPA method, the total molar flow of C1 to C8 species is utilized for reference. Figure 12 provides a better understanding of this process.

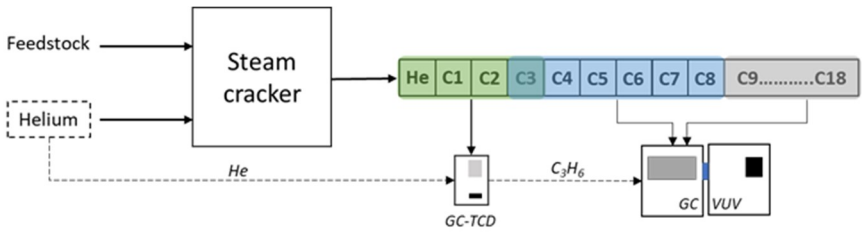

Figure 12. The quantification method developed in this work. The dotted lines represent the known amount of internal standards used for the quantification of the yield of other species.

The results are presented as carbon balances, highlighting significant insights derived from **Papers V** and **VIII**. These results are obtained from experiments conducted with the Chalmers DFB steam cracker using PE and MRP as feedstocks. Validation of the obtained results is carried out by comparing them with established methodologies developed by Israelsson et al.[81,82]

4.2 Carbon balance over the Chalmers DFB steam cracker

The GC-TCD analysis, with a runtime of 3 minutes, quantifies C1– C3 species in the cracker effluent. Figure 13 depicts the yields of these species, derived from the GC-TCD analysis of the cracker effluent scrubbed with isopropanol at -17°C. The combined yield of C1 – C3 species ranges from 60% to 70% for PE and from 50% to 60% for MRP. The wide range of yields results from distinct operating conditions used in the experiments, as described in **Papers V** and **VIII.**

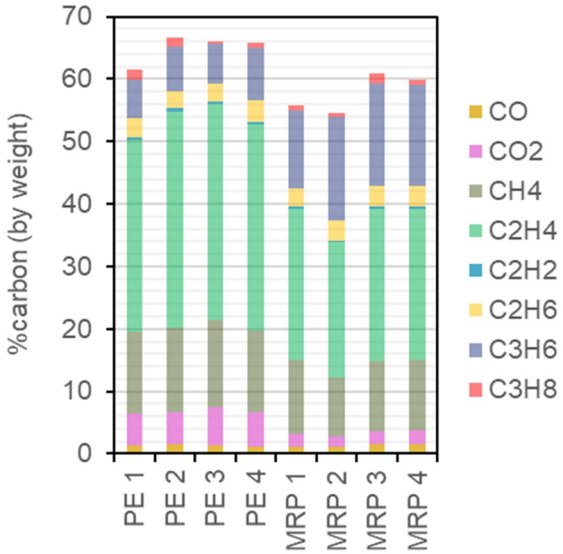

Figure 13. Yields (%carbon, by weight) of C1 to C3 species, calculated based on GC-TCD analysis of the samples obtained through scrubbing of cracker effluent with isopropanol at -17°C.

Figure 14 provides the results of GC-VUV analysis for the cracker effluent quenched to a temperature of 60°C. This figure illustrates the yields of C4 to C8 species for the three experiments. The combined yield of C4 to C8 species is in the range of 20 – 25% for PE. The total analysis time for this group is 4 minutes, as previously described in Figure 11.

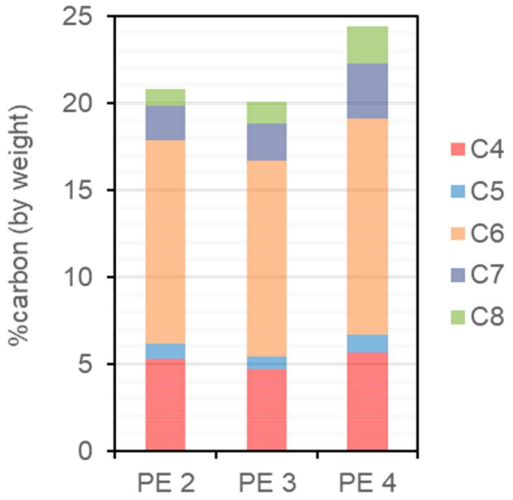

Figure 14. Yields (%carbon, by weight) of C4 to C8 species, calculated based on GC-VUV analysis of cracker effluent quenched at 60°C.

Upon a more detailed review of the GC-VUV results, insights can be drawn regarding the yield of specific C4 to C8 species. Such analysis can offer data on the average molecular weight of each carbon group and the proportion of aromatics or aliphatic species within each group. The distribution of individual species within the C4 – C8 group, as identified through GC-VUV analysis, is illustrated in Figure 15.

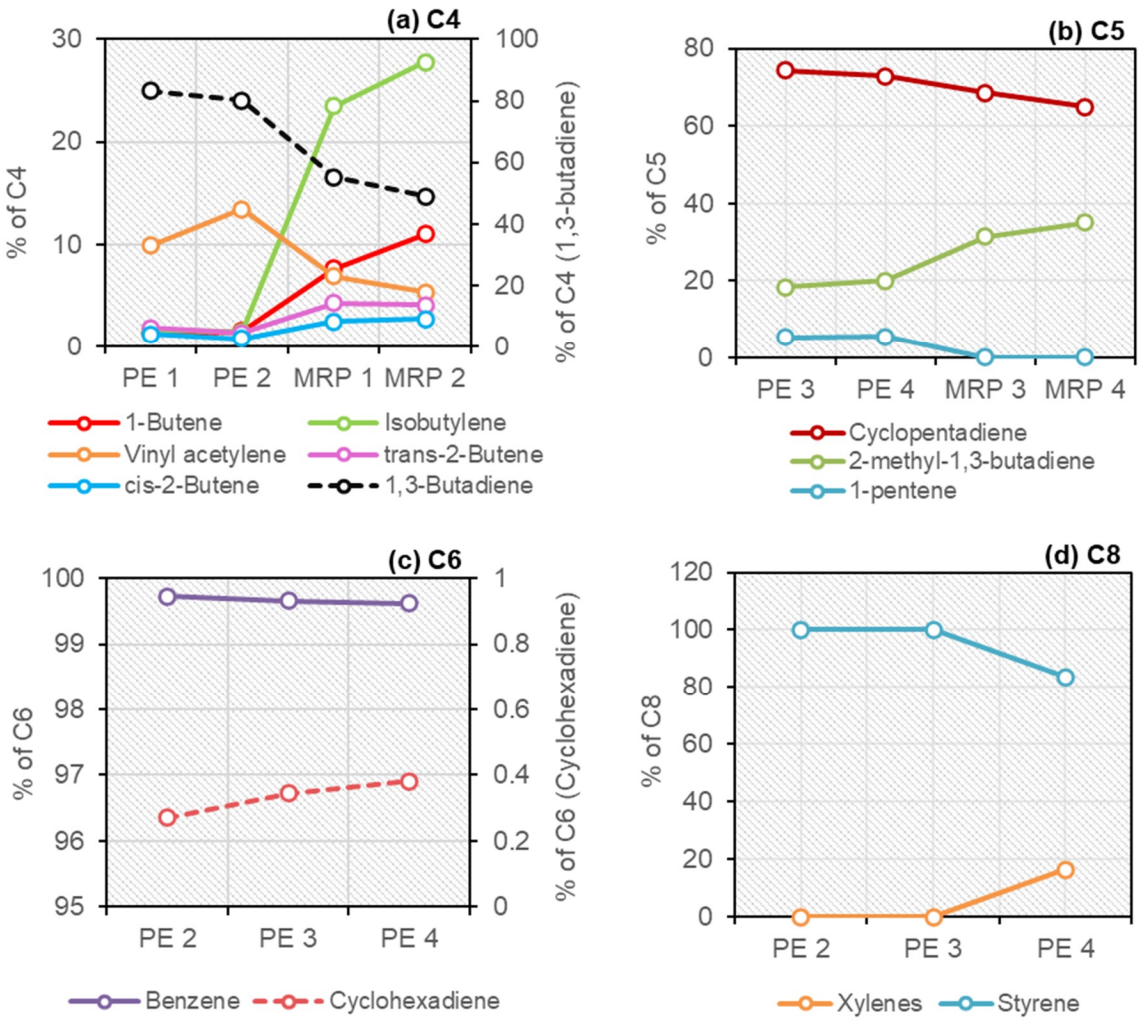

Figure 15. The share of individual species among the groups of (a) C4, (b) C5, (c) C6, and (d) C8 hydrocarbons, as determined by GC-VUV analysis of the cracker effluent quenched at 60°C. The results belonging to the secondary axis are plotted with dashed (- - - -) lines.

The C4 – C8 composition, as depicted in Figure 15, offers a clear visualization of their distribution. Within the C4 species, 1,3-butadiene emerges as the dominant species, representing 80% of the share for PE and 50% for MRP. Isobutylene appears prominently in the cracker effluent when MRP is used as the feedstock, comprising up to 28% of the C4 species. However, the share of isobutylene among the C4s is limited to less than 5% for PE. A similar trend emerges for 1-butene. The remaining C4 species, such as 2-butenes and vinylacetylene, collectively contribute less than 10% of the C4s. The contribution of butane and 1,2-butadiene is minimal, each accounting for less than 1% and therefore omitted from Figure 15.

The C5 hydrocarbon group includes three main species: cyclopentadiene, 2-methyl-1,3-butadiene, and 1-pentene. Cyclopentadiene constitutes up to 75% of C5s for PE and 65% for MRP. The share of 2-methyl-1,3-butadiene among the C5s comprises 20% for PE and nearly 40% for MRP. 1-pentene is exclusively present when PE is the feedstock. Other C5 species, not depicted in Figure 15, collectively represent less than 1% of the C5s.

The C6, C7, and C8 groups are predominantly BTXS, with traces of cyclohexadiene within the C6 group. Notably, cyclohexadiene stands out as the only non-aromatic species identified in the C6 – C8 range. The C7 group is exclusively composed of toluene, therefore not depicted in Figure 15. The C8 group consists of xylenes and styrene. Xylenes appear in only one data point, constituting approximately 20% of the C8s.

Transitioning to the last group, the C9 – C18 hydrocarbons, Figure 16 shows the yields (%carbon, by weight) of the species belonging to this group, as calculated based on the GC-VUV analysis of the SPA samples. The total time of analysis for this group of species is 22 minutes.

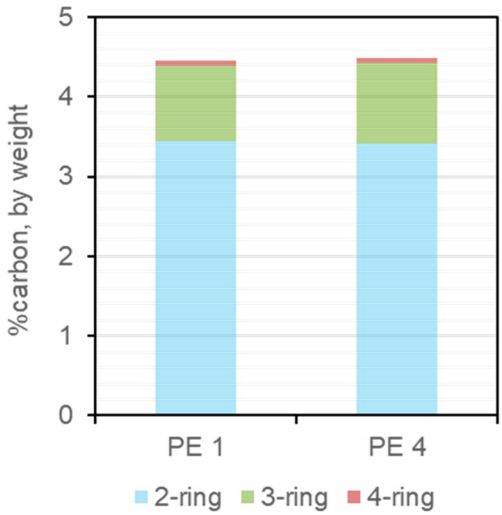

Figure 16. Yields (%carbon, by weight) of C9 to C18 species, calculated based on GC-VUV analysis of the cracker effluent sampled using the SPA method. The species are categorized as 2-ring, 3-ring, and 4-ring aromatic hydrocarbons.

Figure 16 illustrates that the C9 – C18 group is predominantly polyaromatics. The GC-VUV analysis did not detect aliphatic or naphthenic species within this range. The polyaromatic compounds account for around 4.5% (%carbon) for the data points PE1 and PE4. Analyzing the breakdown of these polyaromatics, 2-ring compounds, including naphthalene and its derivatives, hold the predominant portion. Meanwhile, the yields of 3-ring and 4-ring compounds are notably minor, constituting less than 1% of the carbon balance.

4.3 Method validation and analysis time

The carbon balance obtained with the proposed 3-step method is validated against established methods in the literature. This validation process involves taking redundant samples simultaneously and comparing the yields of important species. Figure 17 compares the yields of BTXS, derived from analyses conducted using GC-VUV and GC-FID. The GC-FID analysis is conducted on SPA samples to quantify specific aromatic species ranging from C6 to C18. This approach, developed by Israelsson et al., provides an assessment of certain aromatic compounds within the C6 to C18 range.[82]

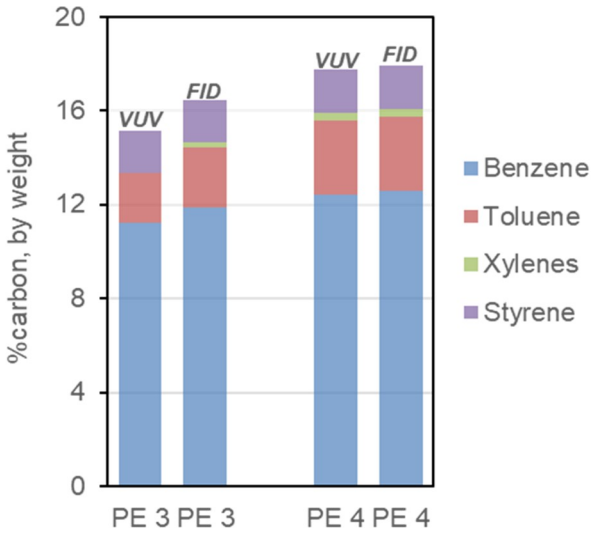

Figure 17. Comparison of the yields (%carbon) of BTXS species measured by GC-VUV and GC-FID. GC-VUV analysis was performed on cracker effluent quenched to 60°C. GC-FID analysis was performed on SPA samples.

The GC-VUV analysis of the gas samples demonstrates comparability with the corresponding GC-FID results. However, subtle differences are noticeable in the yields of xylenes and styrene, as depicted in Figure 17. Specifically, the VUV analysis shows lower quantities of xylenes and styrene than the GC-FID results. These variations relate to the relatively low concentrations of styrene and xylenes within the product mixture, as well as the influence of water vapor in the hot gas sample, which contributes to the dilution of these species. The underestimation of styrene and xylenes collectively accounts for less than 1% of the carbon balance.

Similarly, the yield of C9 – C18 species is validated by comparing the results obtained from GC-VUV and GC-FID analysis of the corresponding SPA samples. Figure 18 shows this comparison.

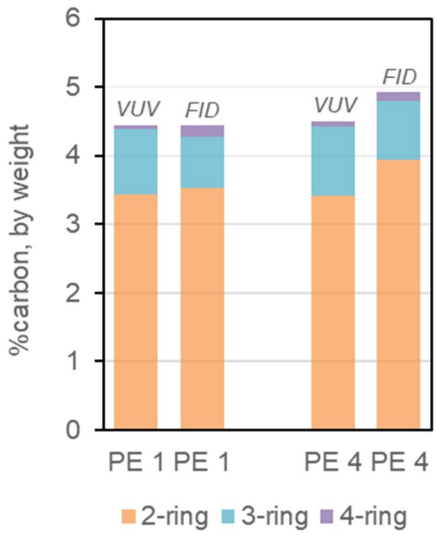

Figure 18. Comparison of the yields of C9 – C18 species measured by GC-VUV and GC-FID. Both measurements were performed on SPA samples.

The comparison of polyaromatic yields obtained from GC-VUV and GC-FID measurements of the SPA samples reveals significant similarity. Minor deviations are evident in Figure 18, where GC-VUV indicates marginally lower yields than those recorded by GC-FID. This discrepancy arises from GC-VUV underestimating 3-ring and 4-ring species compared to GC-FID. Just as with xylenes and styrene, which experience slight underestimation through VUV analysis, the underestimation of 3-ring and 4-ring polyaromatics contributes less than 1% to the carbon balance.

The validation of the overall carbon balance derived from the method introduced in this chapter is performed using the HTR method. This method, as outlined in *Chapter 3*, is used to estimate the total elemental carbon at the outlet of the Chalmers steam cracker. Essentially, it estimates the total carbon yield over the steam cracker relative to the carbon content in the feedstock. Figure 19 shows a comparison of the carbon balance closure obtained through the method developed in this chapter alongside the carbon balance derived with HTR. Additionally, the figure includes the carbon balance obtained through the reference method, where GC-FID analysis is utilized.

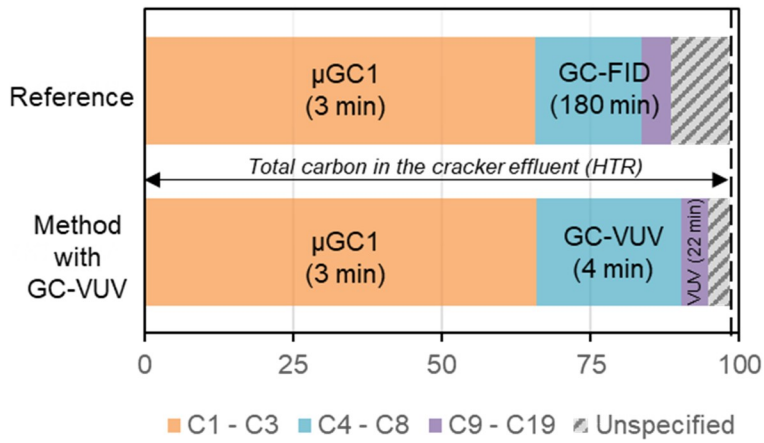

Figure 19. Carbon balance closure (for PE 4) achieved with the sampling and analysis method described in this chapter. The reference corresponds to the carbon balance obtained using the reference method with GC-FID analysis. Unspecified is the difference between the carbon balance obtained with HTR and each of the two methods. The time windows represent the time required for respective GC analysis.

Figure 19 shows that the carbon balance derived from GC-VUV analysis aligns with the carbon balance obtained through HTR. Specifically, the method developed in this work yields a carbon balance of 94.8%, approximately 3.5% lower than the total carbon estimated at the cracker outlet by HTR. In contrast, the reference method employing GC-FID analysis underestimates the carbon balance by approximately 10%. That is because the reference method fails to sample and analyze aliphatic and naphthenic species within the range of C4 – C18.

The method outlined in this chapter requires only 26 minutes for the entire analysis process. The characterization of C9 – C18 species becomes the time-determining step, accounting for a 22-minute analysis time window. In contrast, GC-FID analysis is time-consuming, requiring a substantial 180 minutes. Despite its rapid quantification capabilities, GC-VUV analysis does come with a trade-off of underestimating the yields of low-concentration species such as xylenes and polyaromatics. Nonetheless, the overall time savings and efficiency provided by

GC-VUV and its capability to detect and quantify a wide range of hydrocarbons make it a favorable choice for analyzing cracker effluent compared to the conventional GC-FID method.

The sampling strategies utilized for GC-VUV analysis predominantly rely on offline techniques, such as gas vessels and SPA samples. It's crucial to acknowledge that the manual nature of these sampling procedures introduces the potential for overall measurement errors. An online system must be implemented to address the limitations associated with offline sampling. This system would involve dehydration and quenching the cracker effluent to the dew point of C8 hydrocarbons before injecting them into the GC-VUV system. By integrating such an online system, real-time quantification of species up to C8 can be performed in just 4 minutes. Such a sampling system could also mitigate the challenges of quantifying trace species within the C7 and C8 hydrocarbon range.

Considering the time-intensive nature of characterizing C9+ hydrocarbons, it is advisable to perform this analysis offline. This approach guarantees that the C9+ hydrocarbons do not hinder the analysis of the lighter and more significant species. Implementing an offline sampling strategy for C9+ species also removes the limitation on the number of samples that can be taken during a stable operation.

The findings presented in this chapter hold significant implications for industrial processes, particularly in the context of a steam cracking process dedicated to plastic waste. Variations in the quality of collected plastic waste can result in fluctuations in the composition of the cracker effluent. This variation is evident in the composition of C4 and C5 species, as depicted in Figure 15. The increased concentrations of branched isomers, such as isobutylene and 2-methyl-1,3-butadiene, in the cracker effluent when MRP is the feedstock indicate a significant presence of branched polymer (PP) in the feedstock. The analytical strategy proposed in this chapter offers a practical solution by enabling swift detection of changes in product composition. Moreover, the utilization of VUV absorption spectra adds another layer of practicality. These spectra not only facilitate the detection of changes in hydrocarbon composition but also enable the identification of hydrocarbons containing heteroatoms. This aspect is particularly relevant as certain plastic materials may produce hydrocarbons with heteroatoms during steam cracking.

CHAPTER 5

5 – Establishing an ideal operating window for DFB steam crackers

Cracking severity is one of the primary factors influencing product distribution in a steam cracker. In a conventional steam cracker, control over the cracking severity mainly involves regulating the temperature and residence time. However, operating a DFB steam cracker presents additional complexities.

In a DFB steam cracker, numerous factors, including the temperature of the bed material, the circulation rate of the bed material, the feedstock-to-steam ratio, the fluidization regime, and the temperature in the freeboard, among others, influence the cracking severity. Due to the operational challenges inherent in managing a large-scale reactor system, investigating the influence of each parameter becomes a daunting task.

In light of these challenges, defining an operational window emerges as a pragmatic approach. This window can be characterized by various operating conditions, encompassing a spectrum of cracking severity. Such an approach provides a practical framework for optimizing the operation of a DFB steam cracker and achieving desired product distributions.

This chapter focuses on developing a reference database for large-scale DFB steam crackers, with insights drawn from **Papers V** and **VIII**. The primary goal is to identify and define an operating window for large-scale DFB steam crackers dedicated to ethylene, propylene, and BTXS production. Product distributions obtained across various cracking severities are evaluated to gain a comprehensive understanding of the product yields. The aim of this chapter is not to propose a specific optimal operating condition but rather to present an operational window favorable for the production of light olefins and monoaromatics. A clean feedstock and inert bed material, silica sand, are used to ensure minimal interference from external factors on the reactor system and steam cracking reactions.

5.1 Operational parameters

A comprehensive dataset detailing product distributions obtained from 32 unique operational points of the Chalmers DFB steam cracker is presented. These operational points encompass variations in operating conditions, including the bed material temperature, feeding rate to the steam cracker, and the bed material circulation rate. Moreover, the operational variations include two feedstocks: PE pellets and naphtha. Throughout the experimental campaign, all other parameters relevant to the steam cracking reactor of the DFB system were held constant. Table 7 provides a summary of the operational parameters.

Table 7. The range of operational parameters corresponding to the operational window encompassing 32 unique points.

Feedstock	Feeding rate (kg/h)	Bed material temperature (°C)	Bed material circulation (ton/h)	Number of operational points
PE	60 – 120	700 – 825	8 – 30	25
Naphtha	40	750 – 810	10 – 12	7

The operational points outlined in Table 7 correspond to an extensive experimental campaign spanning five years. Each data point presented in this chapter represents a stable operation of the steam cracker, lasting at least 60 minutes. Throughout the entire experimental campaign, the quality of the bed material, silica sand, was maintained by replacing 500 kg of old silica sand with fresh silica sand daily.

The results outlined in this chapter are operational curves derived by plotting the yield of various important species against cracking severity. This approach enables the evaluation of results without dependence on specific operating conditions, providing a broader understanding of the system's behavior. Additionally, these operational curves offer a clear visualization of how the product distribution evolves in response to changes in cracking severity.

This chapter additionally includes a comparison of the performance of the Chalmers DFB steam cracker when operated with PE and naphtha as feedstock. This comparison involves superimposing the data points related to naphtha onto the operational curves obtained with PE as the feedstock. This comparison aims to offer a fundamental understanding of how the cracking process of a polymeric feedstock relates to that of a conventional feedstock like petroleum naphtha. Moreover, such a comparison provides insight into the behavior of the reactor system operated with different feedstocks.

5.2 Obtained product distributions and cracking severity

As outlined in Chapter 2, methane yield serves as a crucial indicator for assessing cracking severity. The methane yield increases with rising cracking temperature due to the chain-end bond scission reaction. Figure 20 illustrates this correlation between methane yield and bed material temperature. Here, the bed material temperature represents the cracking temperature, a widely used parameter for characterizing cracking severity in the petrochemical industry.

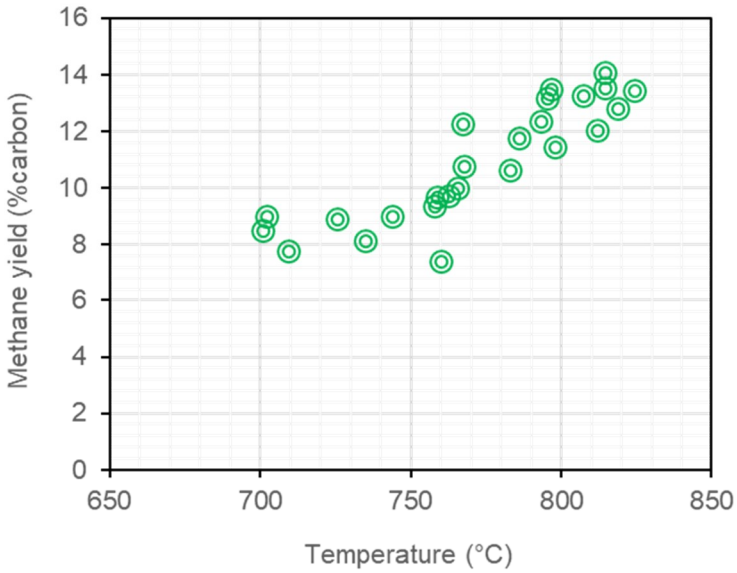

Figure 20. Relation between yield (%carbon) of methane and the cracking severity. The bed material temperature (°C) describes the cracking severity.

It is crucial to note that while Figure 20 utilizes bed material temperature to describe cracking severity, other variations in operating conditions also influence cracking severity. The points depicted in Figure 20 encompass variations in bed material circulation rate and feed flow to the steam cracker, each of which can independently impact cracking severity. However, the bed material temperature serves to simplify the visualization of the correlation between methane yield and cracking severity.

A clear trend indicating an increase in methane yield with increasing bed material temperature is evident in Figure 20. This trend aligns with the understanding that elevated temperatures or higher cracking severity favors methane formation through the chain-end scission reaction.[19,84] In the temperature range of 700 to 825°C, methane yield ranges from 8% to 15% (%carbon). The correlation between methane yield and cracking temperature suggests that methane yield can serve as a basis for describing cracking severity. The cracking severity of different cracking operations can be compared simply by evaluating methane yield. Figure 21 illustrates the correlations between the yields of different hydrocarbon species and the yield of methane.

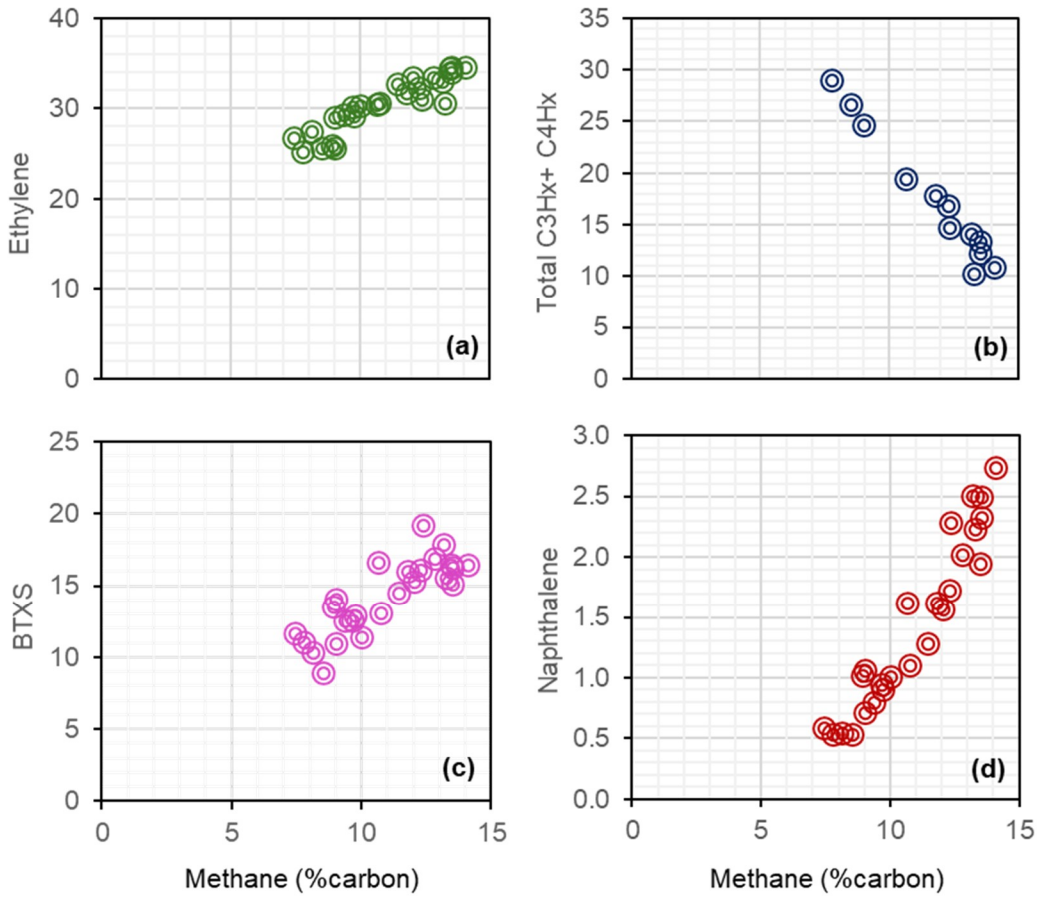

Figure 21. Relation between the yield (%carbon) of ethylene (a), C_3H_x + C_4H_x (b), BTXS (c), and naphthalene (d) and the cracking severity. Methane yield (%carbon) describes the cracking severity.

Figure 21 illustrates the yields of (%carbon) of ethylene, C_3H_x, C_4H_x, BTXS, and naphthalene as a function of methane yield. Across all tested operating conditions in the Chalmers steam cracker, trends of higher yields of ethylene, BTXS, and naphthalene with higher methane yield can be observed. Specifically, the yield of ethylene increases with the rise in methane yield, reaching a maximum yield of 35% at a methane yield of 14%. In the obtained range of methane yield, the BTXS yield falls between 9% to 18%. Notably, naphthalene exhibits the steepest increase in its yield with the increase in methane yield, with an overall range of 0.5% to 2.8%.

The total yield of C_3H_x and C_4H_x exhibits a decreasing trend with the increase in methane yield across the entire range of operating conditions. Initially, when methane yield is at its lowest, the total yield of C3 and C4 hydrocarbons is 30%. As methane yield increases, the combined yield of C3 and C4 gradually decreases, reaching its lowest point of 10% for the highest methane yield.

A part of the feedstock also converts to carbon oxides (CO and CO_2) during steam cracking, attributable to the presence of steam in the system. Figure 22 illustrates the variation in the yield (%carbon) and the composition (O/C molar ratio) of the carbon oxides with respect to the change in methane yield across all operating conditions.

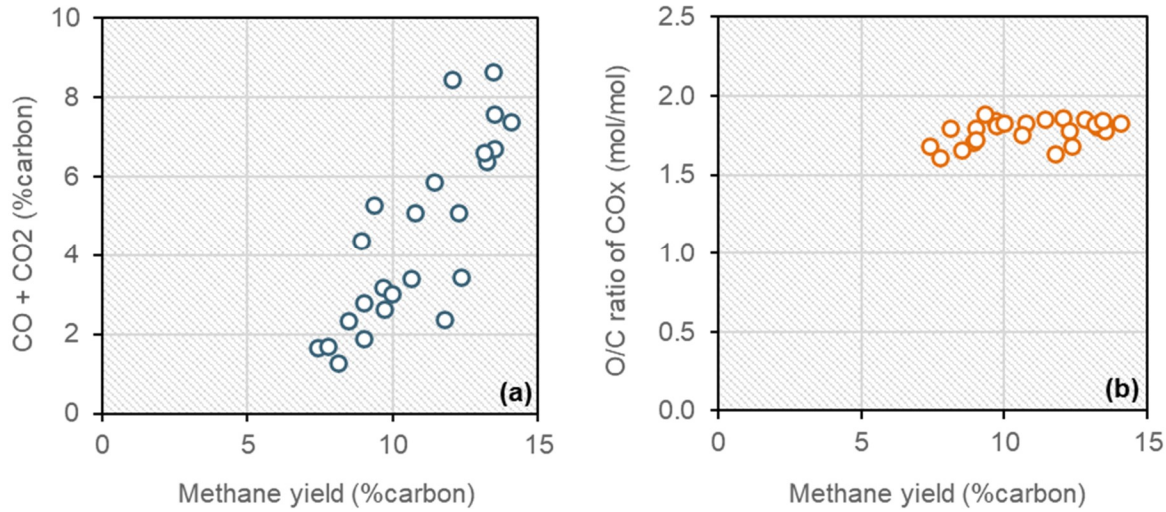

Figure 22. Correlation between (a) the combined yield of CO and CO_2 (%carbon) and the yield of methane (%carbon), (b) O/C ratio (mol/mol) of the syngas and the yield of methane.

There is a general increasing trend in the yield of CO_x with the rise in methane yield. Additionally, a consistent CO/CO_2 ratio is maintained across all operating conditions, as indicated by the stability in the O/C ratio. The yield of CO_x ranges from 1% to 8% (% carbon), while the O/C ratio of the CO_x mixture falls within a narrow range of 1.6 to 1.9.

The correlations shown in Figures 20 to 22 outline the operational window for steam cracking of PE in the Chalmers DFB steam cracker. These correlations serve as a reference for comparing the operation of different steam crackers or different operations of the same unit. They also provide a means to compare steam cracking operations with different bed materials or feedstocks to the steam cracking of PE in the presence of silica sand. The yields obtained with naphtha can be plotted onto the operational curves presented in Figures 20 to 22 to illustrate the operation of the Chalmers unit with naphtha as the feedstock. Figure 23 demonstrates the superimposition of the seven operational points with naphtha as the feedstock on the reference operational curves.

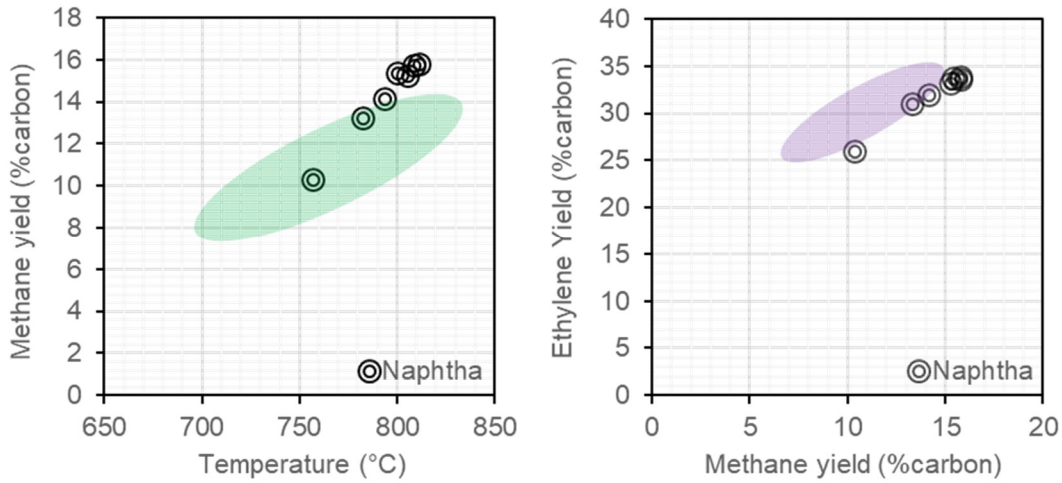

Figure 23. Operational points for steam cracking of naphtha in the Chalmers DFB steam cracker. The shaded regions in the plots show the operational curves obtained with PE as the feedstock and provide a reference for comparison.

Figure 23 compares the steam cracking of naphtha and PE within the Chalmers unit. Despite variations in operating conditions for naphtha and PE, notable similarities emerge in the methane-temperature correlation and the correlation between ethylene and methane. There is an upward trend in methane and ethylene yields with increasing cracking severity similar to that observed with PE. In addition, it is crucial to compare individual data points with the overall operational window for PE. For example, in the methane vs temperature plot, naphtha yields higher methane than PE at similar cracking temperatures. Similarly, naphtha shows a slightly lower ethylene yield than PE at equivalent cracking severities in the ethylene vs methane plot.

The deviations observed from the reference operational curve originate from the change in feedstock type within the steam cracker, with no other significant alterations made to the reactor system. Despite sharing aliphatic molecular structures, naphtha and PE differ significantly in their physical state and atomic composition. Naphtha is primarily C5 to C9 hydrocarbons and is a liquid at room temperature, whereas PE is a solid. Moreover, naphtha's smaller aliphatic chain lengths result in a lower molecular weight and a higher H/C ratio than PE (see Table 5 in *Chapter 3*).

The liquid state and lower molecular weight of naphtha make it easier to crack than PE. As a result, naphtha achieves higher cracking severity levels at given process conditions compared to PE. Consequently, slightly higher methane yields are obtained from naphtha compared to PE. Moreover, the higher H/C ratio of naphtha also plays a significant role in increasing the production of methane. Additionally, it is worth noting that all the correlations illustrated in Figures 21 and 22 also apply to naphtha, although not extensively detailed in this chapter. These correlations also indicate that the product distributions obtained from the steam cracking of naphtha in a DFB closely resemble those from a conventional steam cracker.[16,85]

This chapter establishes methane as a key factor in describing cracking severity and provides correlations for DFB steam crackers. These correlations offer a clear understanding of how product distribution evolves with changes in cracking severity. Additionally, they can serve as indicators for detecting shifts in feedstock type or potential developments in catalytic activity within the system, which may alter reaction pathways and product distribution. These correlations also provide experimental validation of the cracking mechanisms reported in the literature[19,20,66,68,84], demonstrating their applicability in the context of large-scale DFB steam crackers. They indicate that the cracking severity achieved in a DFB steam cracker operated within the range of 700–825°C is suitable for the selective production of light olefins and monoaromatics, which can constitute up to 65% of the cracker effluent.

CHAPTER 6

6 – Steam cracking of waste streams in DFB

The findings outlined in *Chapter 5* highlight the potential of steam cracking of polyolefins within a DFB system, demonstrating the ability to achieve selective production of light olefins and mono-aromatics, up to 50% and 20% (% carbon), respectively, within the identified ideal operating window. However, the ideal operating window considers pure PE as the feedstock. The broader application of this process for recycling plastic waste necessitates a thorough investigation into the product distribution derived from real-world waste streams.

This chapter explores the conversion of different waste streams within the DFB steam cracking process. The selection of waste streams, as discussed in Chapter 2, is a meticulous process that considers several factors, including their polyolefin composition, prevalence, and accessibility within society. Each selected waste stream did not undergo pretreatment or presorting before being introduced into the steam cracker. This approach ensures that the DFB steam cracking process is well-suited for recycling these wastes as they are within society.

This chapter also provides insights into integrating alternative recycling methods with DFB steam cracking to enhance overall recycling rates. Among the waste streams examined in this chapter, three originate from alternative recycling methods already established at an industrial level: cardboard recycling, mechanical recycling of polyolefins, and polyolefin pyrolysis.

The fraction rejected as waste from the cardboard recycling process (cardboard recycling reject or CRR) necessitates separating cellulose to obtain a pure polyolefin product, which becomes increasingly intensive as the cellulose content diminishes. Similarly, pyrolysis oil typically undergoes hydrotreatment to eliminate olefin and heteroatom content before integration into a tubular steam cracker.[13] These supplementary steps contribute to lower recycling rates and incur additional costs within the recycling system. Moreover, the products derived from mechanical recycling typically exhibit inferior quality compared to virgin materials, making them unsuitable for their original applications.[9] This chapter illustrates how these three products can be efficiently utilized, without pretreatment, within the DFB steam cracking process for selectively producing light olefins and mono-aromatics.

Drawing insights from **Papers III**, **VII**, and **VIII**, a comprehensive dataset of the product distributions obtained from these diverse waste streams is presented. The operating conditions within the steam cracker are selected based on the ideal operational window established in *Chapter 5*.

6.1 Investigated waste streams and their properties

The steam cracking experiments were conducted at semi-industrial and laboratory-scale DFB reactors, with a selection of operating conditions that align with the ideal operating window previously established in *Chapter 5*. The experimental framework, crucial to the analysis presented in this chapter, is outlined in Table 8.

Table 8. Experiment matrix for steam cracking of waste streams in the Chalmers DFB steam cracker and the laboratory steam cracker.

Feedstock	Temperature (°C)	Feeding rate (kg/h)	Reactor system
MRP[1]	750 – 790	50 – 100	Chalmers DFB
CRR[2]	750 – 800	50	Chalmers DFB
MPW[3]	720 – 810	50	Chalmers DFB
Pyrolysis oil	720 – 760	28	Chalmers DFB
Rapeseed oil	650 – 750	Batch feed (2 g)	Laboratory reactor
Face masks	700 – 800	Batch feed (2 g)	Laboratory reactor
Syringes	700 – 800	Batch feed (2 g)	Laboratory reactor
Nitrile gloves	700 – 800	Batch feed (2 g)	Laboratory reactor
Non-woven gloves	700 – 800	Batch feed (2 g)	Laboratory reactor

[1]MRP: mechanically recycled polyolefins; [2]CRR: cardboard recycling reject; [3]MPW: mix plastic waste

The results are presented in the form of the yields (%carbon or mol/kg) of species in the cracker effluent. The data points are compared with the reference operation, allowing for an assessment of the influence of the non-polyolefin content of the feedstock on the product distribution. Furthermore, the impact of the feedstock's olefinicity on the formation of solid carbon deposits is also investigated. Table 9 provides relevant characteristics of the feedstocks, serving as the foundation for the findings presented in this chapter.

Table 9. Properties of the feedstocks used in this work.

Feedstock	Polyolefin content (%wt.)	Oxygen content (mol O/kg)	Olefinicity (%, C = C/C – C)
MRP	100	0.00	0
CRR	47.5	13.12	0
MPW	45.8	8.92	0
Pyrolysis oil	95[a]	0.00	2.5[a]
Rapeseed oil	85[b]	5.61	10[b]
Face masks	85	2.92	0
Syringes	100	0.00	0
Nitrile gloves	70	5.88	14[c]
Non-woven gloves	100	0.00	0

[a]Calculated based on the PIONA composition of pyrolysis oil.
[b]Calculated based on the molecular structure of rapeseed oil.
[c]Calculated based on the molecular structure of nitrile butadiene rubber repeating units.

The polyolefin content of the feedstock, as outlined in Table 9, quantifies the amount of PE and PP in the feedstock. This determination of polyolefin content follows the methodology established by Forero Franco et al., which utilizes the feedstock's elemental composition and lower heating value to estimate its polymeric composition.[86] Despite rapeseed oil not being a polymer, it has been given 85% polyolefin content, calculated based on the aliphatic molecules within its molecular structure. Similarly, pyrolysis oil, composed of 95% aliphatics, is assigned a polyolefin content of 95% accordingly. The polyolefin content of nitrile gloves represents the share of nitrile butadiene rubber (NBR).

The oxygen content (mol O/kg) of the feedstock is calculated based on its elemental composition. This oxygen content primarily arises from the presence of oxygen-containing polymers like PET or cellulose within the feedstock. Although the PET and cellulose content of each feedstock can be estimated using Forero Franco et al.'s method, these details are not provided here. In the case of rapeseed oil, its oxygen content relates to the presence of oxygen atoms within its molecular structure.

The olefinicity of a given feedstock, as outlined in Table 9, is determined by the presence of carbon-to-carbon double bonds (C = C) within its molecular structure. The term "olefinicity" here should not be confused with its usage in the petrochemical industry, where it typically denotes the quantity of olefins within a hydrocarbon mixture. Olefinicity is defined as the ratio of the number of C = C bonds to the number of C – C bonds within the molecular structure of a given feedstock. For instance, in the case of NBR, each repeating unit contains one C = C bond for every five C – C bonds (as illustrated in Figure 25), resulting in an olefinicity of 20%. Consequently, if nitrile gloves are 70% NBR, their olefinicity would be 14%.

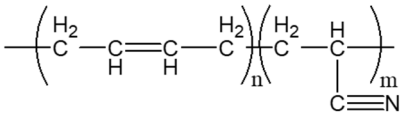

Figure 23. Molecular structure of nitrile butadiene rubber (NBR).

Materials such as MRP, CRR, MPW, face masks, syringes, and non-woven gloves are assumed to have an olefinicity of 0%. This assumption considers the absence of C = C bonds in the molecular structures of PE, PP, PET, and cellulose.

6.2 Product distributions in relation to the feedstock composition

In the steam cracking process, ethylene receives primary attention. The cracking severity plot depicted in Figure 24 provides the ethylene yield obtained from steam cracking of the different waste streams in the Chalmers DFB unit.

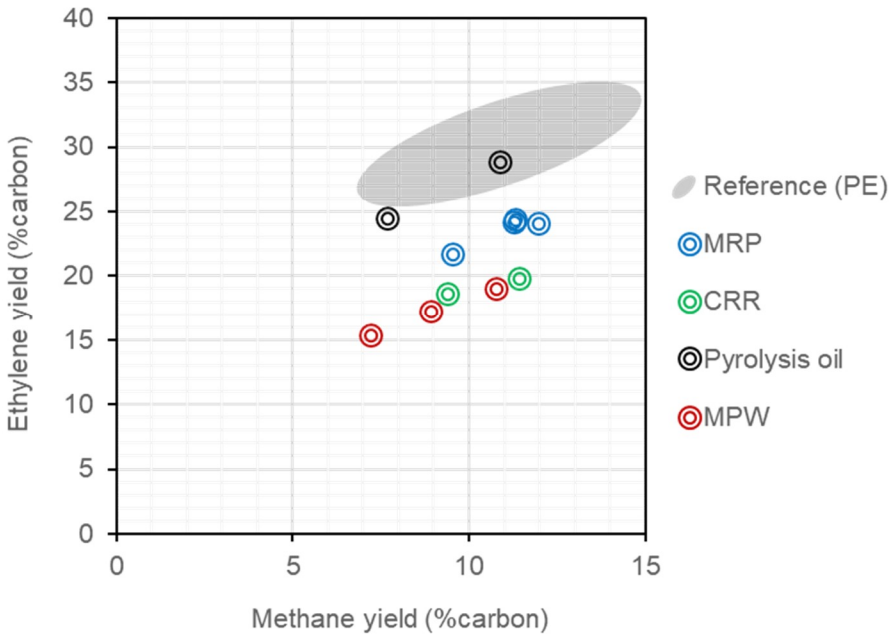

Figure 24. Operational points for steam cracking of waste streams in the Chalmers DFB steam cracker, depicted on the cracking severity plot. Cracking severity is described as the yield of methane. The reference operational curve obtained with PE as the feedstock is shown within the shaded region on the plot.

Figure 24 also illustrates the reference curve derived using PE as the feedstock, displayed within the shaded region on the plot. A consistent trend emerges across all feedstocks, showing an increase in ethylene yield with higher cracking severity, aligning closely with the observed trend in the reference curve. However, notable deviations become apparent when comparing individual ethylene yields with the reference operation.

The ethylene yield obtained with pyrolysis oil closely aligns with the reference operation, reaching a maximum of 28%. The ethylene yield for MRP, CRR, and MPW feedstocks deviates significantly from the reference. Specifically, MRP yields ethylene between 22% and 24%,

slightly below the reference curve. On the other hand, both CRR and MPW yield similar amounts of ethylene, ranging from 15% to 20%.

The yield of ethylene from steam cracking in the laboratory reactor can be depicted similarly on the cracking severity plot, as shown in Figure 25. This figure also facilitates a comparison of the ethylene yield obtained with the various feedstocks against the reference operation.

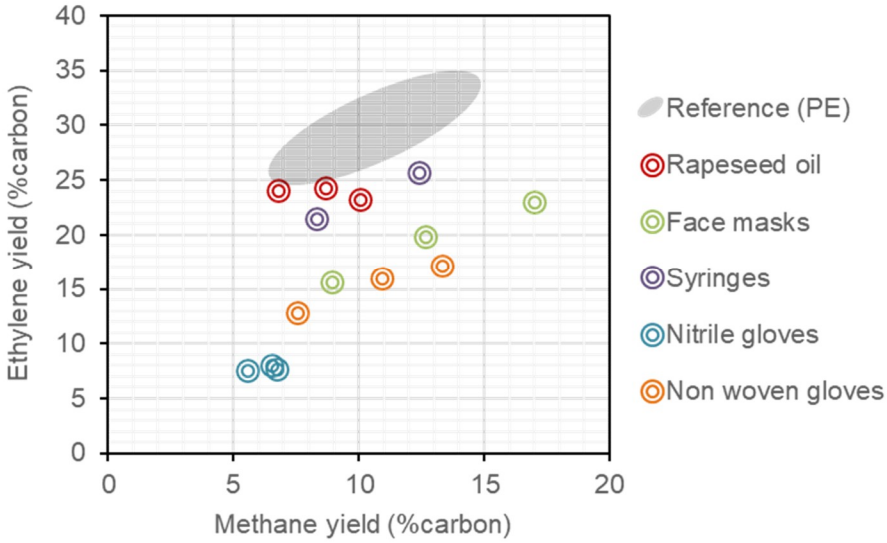

Figure 25. Operational points for steam cracking of waste streams in the laboratory reactor. The reference operational curve (PE) is shown within the shaded region.

Interestingly, a similar trend emerges, showing increasing ethylene yield with increasing cracking severity across most data points obtained from the laboratory reactor. Notably, the ethylene yield obtained from rapeseed oil closely aligns with the reference operational curve, hovering around 25%. Face masks and syringes yield ethylene comparable to the reference operation, although slightly lower, between 15% and 26%. The yield of ethylene from nitrile gloves and non-woven gloves is notably lower than the reference, at approximately 8% and 17%, respectively.

The deviations observed from the reference curve in both Figures 24 and 25 are because of the diverse compositions and molecular structures of the feedstocks. Among all the feedstocks, rapeseed oil, pyrolysis oil, and MRP exhibit the most similarity to PE. Pyrolysis oil and rapeseed oil are mostly aliphatic and share a molecular structure comparable to PE. Similarly, MRP, originating from the mechanical recycling of well-sorted polyolefins, predominantly consists of PE and PP. As a result, MRP, rapeseed oil, and pyrolysis oil yield ethylene within a range closely resembling the reference operation.

The lower ethylene yield observed in other feedstocks is primarily due to their lower polyolefin content. This lower polyolefin content is related to additional materials such as cellulose and PET in the feedstock. Furthermore, the presence of PP also contributes to deviations from the reference curve, as evidenced in the cases of MRP and MPW in Figure 24. Due to a substantial share of PP in MRP and MPW, there is an increased propylene yield and, consequently, a lower ethylene yield than the reference operation. The increased propylene production relative to ethylene is also observed for syringes, which similarly contain a significant amount of PP.

The influence of the polyolefin content of the feedstock on ethylene yield remains unclear from the data presented in Figures 24 and 25. For a fair comparison with PE, it is beneficial to plot the yields of ethylene and propylene against the polyolefin content of the feedstock. This correlation shows how polyolefins within the feedstock convert within a DFB steam cracker. Figure 26 illustrates this correlation by depicting the combined yield of ethylene and propylene in relation to the polyolefin content of the feedstock.

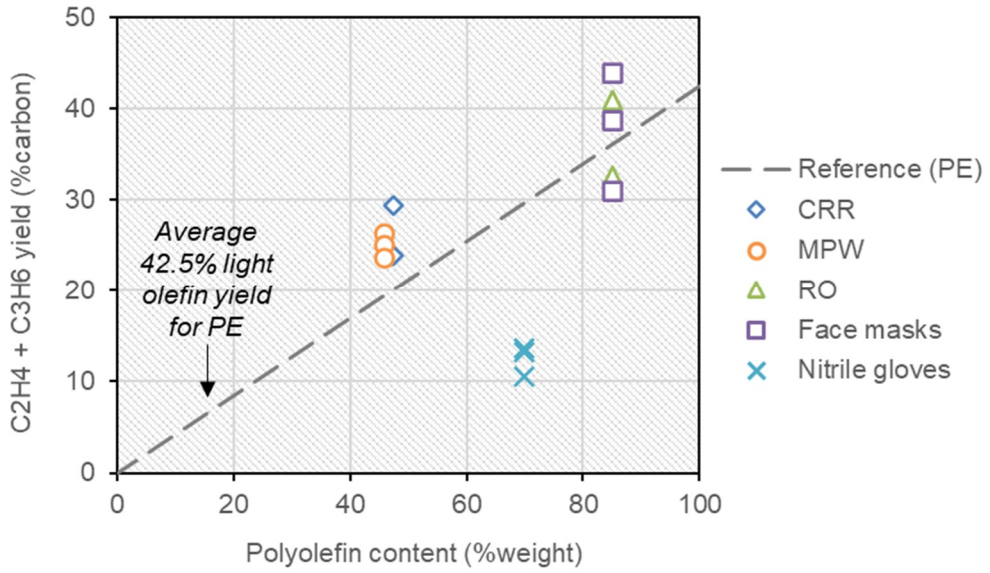

Figure 26. Correlation between the combined yield of ethylene and propylene and the polyolefin content of the feedstock. The average ethylene + propylene yield obtained with PE (100% polyolefin) is visualized with the dashed line.

Figure 26 illustrates the total yield of ethylene and propylene for feedstocks with polyolefin content lower than 100%. These feedstocks comprise CRR, MPW, RO, face masks, and nitrile gloves, with polyolefin content ranging from 42% to 85%. A dashed line is included as a reference, representing the average ethylene + propylene yield obtained with PE across the dataset presented in *Chapter 5*.

The combined yield of ethylene and propylene obtained with CRR, MPW, RO, and Face masks closely align with the reference line, suggesting that the polyolefins in these feedstocks convert to C2 – C3 olefins in a similar proportion as PE. Furthermore, data points above the reference line indicate slightly higher ethylene and propylene production than PE, potentially originating from other materials such as PET and cellulose in these feedstocks.

The yield of ethylene and propylene from Nitrile gloves notably diverges below the reference line. With a polyolefin content of 70%, the combined yield of ethylene and propylene ranges from 10 to 15%. This deviation relates to the distinctive molecular structure of NBR. Despite falling under the category of polyolefins, the presence of C = C and C ≡ N bonds within NBR hinders the generation of low molecular weight olefins during the steam cracking process.

The polymer composition and molecular structures also influence the aromatics yield in the cracker effluent. The presence of PET and PS in the feedstock results in an increase in the yield of aromatics.[52,86] Additionally, the C = C bonds within molecular structures enhance the

formation of the aromatic.[87] Figure 27 provides the yield of aromatics obtained from the different feedstocks.

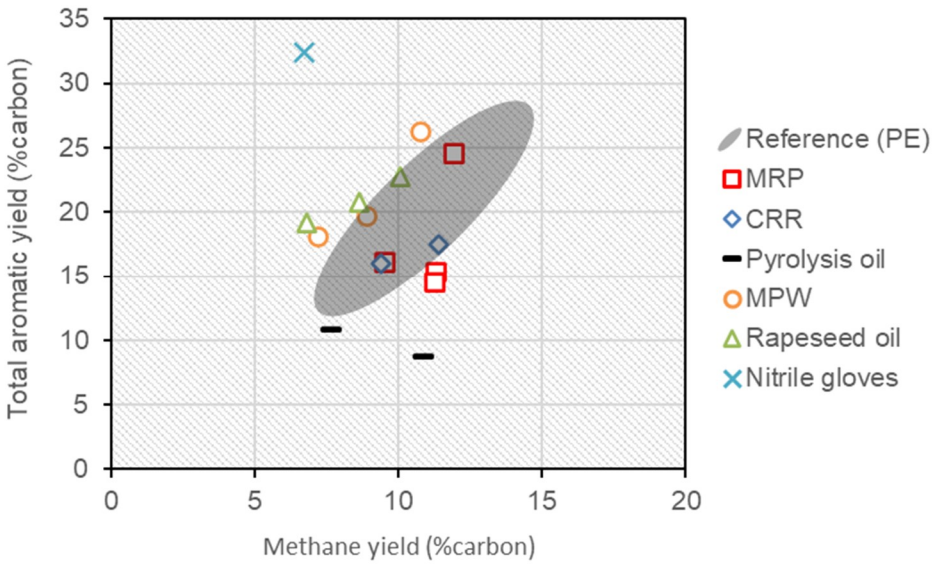

Figure 27. Correlation between the yield of aromatics and the yield of methane. The yield of methane serves as the indicator of the cracking severity. The reference curve obtained with PE is visualized with the shaded region in the plot.

Figure 27 shows the yield of aromatics from MRP, CRR, Pyrolysis oil, MPW, Rapeseed oil, and Nitrile gloves plotted against cracking severity, with methane yield as the cracking severity indicator. CRR and MPW are feedstocks with PET and PS, while Pyrolysis oil, rapeseed oil, and Nitrile gloves represent those with C = C bonds. Furthermore, the aromatic yield from MRP, devoid of PET, PS, and C = C bonds, is also shown. The shaded region on the plot shows the reference.

The aromatic yield obtained from MRP (15 – 25%) and CRR (16 – 18%) falls within the shaded region in Figure 27, indicating a similar yield to that of PE. This similarity for MRP shows its exclusive composition of PE and PP. For CRR, the resemblance to PE in aromatic yield relates to its non-polyolefin content, primarily composed of cellulose with minimal PET and PS content. In contrast, MPW, with a higher proportion of PET and PS than CRR, yields more aromatics, surpassing both CRR and the reference operation. Similarly, rapeseed oil and nitrile gloves produce higher aromatic yields because of C = C bonds. Interestingly, pyrolysis oil is the only feedstock with a significantly lower aromatic yield than PE.

The C = C bonds within the molecular structure of feedstocks also influence the formation of carbon deposits during the steam cracking process. Although the accumulation of carbon deposits on the bed material may not notably affect the operation of the DFB steam cracker, it remains an important parameter to consider. Because the carbon deposits will undergo combustion in the regenerator of the DFB unit, converting to CO_2. Figure 28 illustrates the yield of carbon deposits obtained from feedstocks containing C = C bonds, shown as a function of the olefinicity of the feedstock.

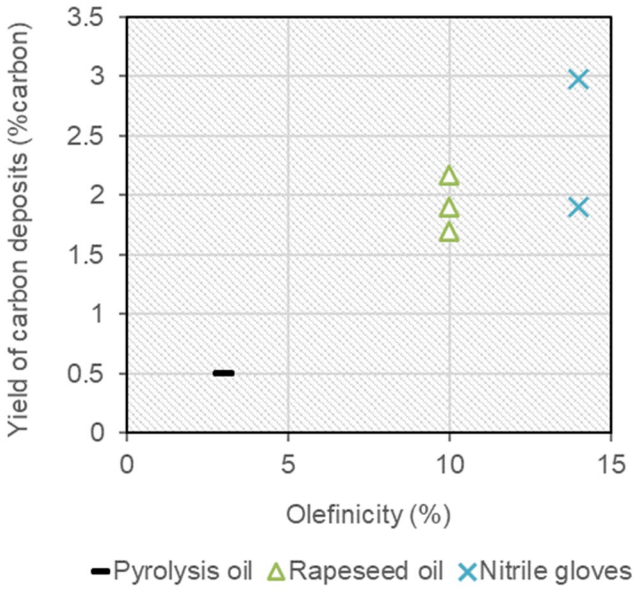

Figure 28. Correlation between the yield of solid carbon deposits and the olefinicity of the feedstock.

Figure 28 illustrates the yield of carbon deposits obtained from pyrolysis oil, rapeseed oil, and nitrile gloves—three feedstocks characterized by the C = C bonds in their molecular structures. Pyrolysis oil exhibits the lowest carbon deposit yield at 0.5%. As the olefinicity of the feedstock increases, there is a corresponding rise in the yield of carbon deposits. The yield of carbon deposits for rapeseed oil is between 1.6 and 2.2%. Nitrile gloves, which have the highest olefinicity among the three, yield carbon deposits of up to 3%.

Transitioning to the final characteristic of feedstocks, the oxygen content of the feedstock. It is imperative to address its implications on the product distribution obtained from a steam cracker. The presence of oxygen poses challenges as it can partially or fully oxidize the feedstock, resulting in the formation of carbon oxides. Despite this undesirability, it's inevitable to encounter waste streams with oxygen content due to the inherent presence of PET and cellulose. Figure 29 illustrates the correlation between the yield of oxygen atoms in the cracker effluent and the oxygen content of the feedstock.

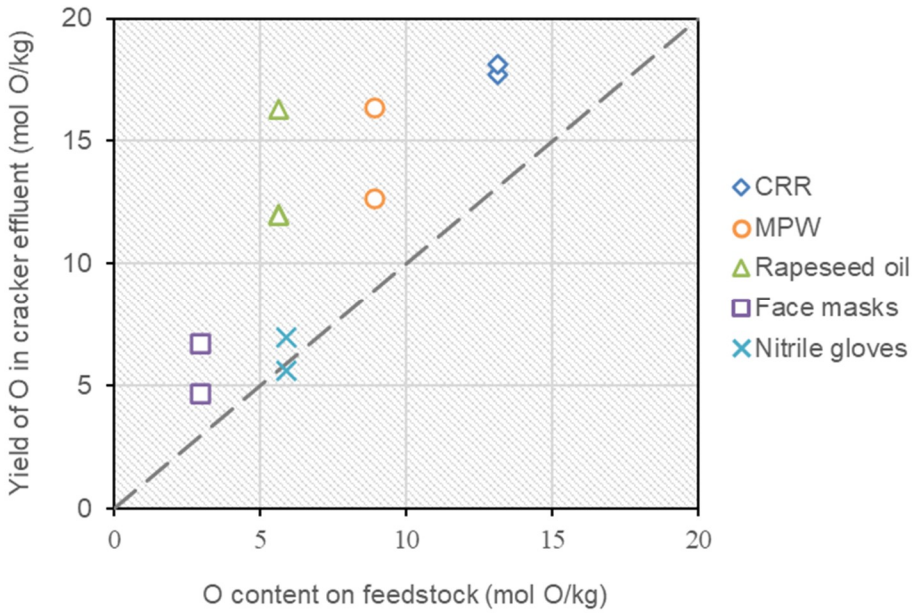

Figure 29. Correlation between the yield of oxygen in the cracker effluent and the oxygen content of the feedstock. The dashed line on the plot corresponds to an equal amount of oxygen in the cracker effluent and the feedstock.

Figure 29 provides the oxygen yield in the cracker effluent for CRR, MPW, rapeseed oil, face masks, and nitrile gloves. A dashed line on the plot indicates an equal amount of oxygen in the cracker effluent and the feedstock. It's important to note that the oxygen yield in the cracker effluent corresponds exclusively to carbon oxides. The oxygen yield in the form of hydrocarbons is negligible and disregarded in this plot.

The oxygen yield obtained for nearly all data points exceeds the reference line in Figure 29, suggesting a higher oxygen presence in the cracker effluent than in the feedstock. This excess oxygen in the effluent could stem from various sources, including the steam reforming of hydrocarbons or the water gas shift reaction. While it is plausible that oxygen could also originate from the oxidation of the feedstock by the bed material, this contribution is marginal due to the low oxidation potential of silica sand at the temperatures employed in this study.

The yield of oxygen in the cracker effluent, obtained primarily in the form of syngas, underscores the potential for converting the syngas into molecular building blocks to enhance the recycling rate of the overall process. As outlined in **Chapter 2**, the production of molecular building blocks from syngas (Route B in Figure 2) can be achieved through various synthesis processes such as MTO and FT. Optimal conversion of syngas in these synthesis processes typically requires an R ratio of 2.[23] Figure 30 provides a visualization of the R ratio of the produced syngas alongside the oxygen content of the feedstock.

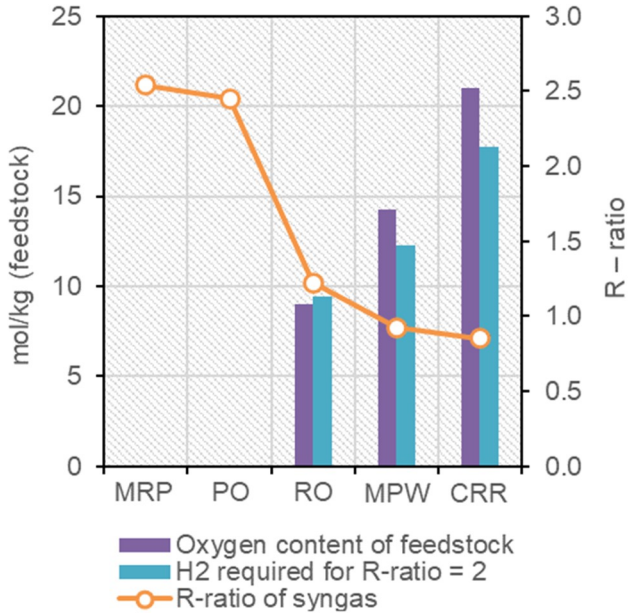

Figure 30. The R ratio of the syngas and the amount of additional H_2 required to obtain the optimal R ratio of 2 for the oxygen-containing feedstocks. MRP and Pyrolysis oil (PO), both devoid of oxygen, are used as references. The R ratio is defined as $R = (H_2 - CO_2)/(CO + CO_2)$.

Figure 30 illustrates a clear trend: as the oxygen content of the feedstock increases, the R ratio of the syngas obtained from the steam cracking process decreases. Pyrolysis and MRP, which have no oxygen content, exhibit an R ratio of syngas around 2.5. Conversely, the oxygen-containing feedstocks show R ratios of syngas significantly lower than 2, indicating an increased need for additional H_2 in downstream synthesis processes. This trend highlights the increasing requirement for additional hydrogen as the oxygen content of the feedstock increases. Furthermore, Figure 30 also highlights the amount of hydrogen needed to achieve the optimal R ratio of 2. The syngas obtained from pyrolysis oil and MRP, with R ratios exceeding 2, do not necessitate additional hydrogen for downstream synthesis processes.

6.3 On the ability of DFB steam crackers to process unsorted plastic waste

The findings outlined in this chapter underscore the potential of leveraging a DFB steam cracking process to recycle the heterogeneous plastic waste generated in society. Despite variations in polymer composition, the DFB steam cracker effectively converts the waste streams. The conversion of the polyolefin content of the feedstock into ethylene and propylene occurs in a proportion similar to that of PE, which is approximately 42.5%. Importantly, this proportion remains consistent regardless of the other materials in the feedstock, such as PET and cellulose. This finding underscores the DFB steam cracker's ability to effectively differentiate between polyolefin and non-polyolefin contents during conversion, providing an in-situ sorting mechanism.

The chapter highlights the influence of non-polyolefin materials, including PET, PS, and cellulose, on the resultant product distribution. As the non-polyolefin content in the feedstock rises, the cracker effluent sees an enrichment of syngas and aromatics. This increase in non-polyolefin content within plastic waste raises the overall energy demands of the recycling

process, primarily due to the need for additional hydrogen necessary for synthesizing molecular building blocks from the produced syngas.

The chapter also sheds light on the ability of a DFB steam cracker to process feedstocks with a high degree of unsaturation. It is noteworthy because of the tendency for increased unsaturation to lead to the formation of solid carbon deposits on the bed material surface. However, thanks to the resilient design of the DFB configuration, these carbon deposits are efficiently removed on the regenerator side without necessitating interruptions to the steam cracker operation.

Given the DFB steam cracker's ability to selectively produce molecular building blocks from feedstocks with diverse compositions, including varying polyolefin content, PET, cellulose, and levels of unsaturation, it presents a promising solution to common challenges encountered in thermochemical recycling processes. Moreover, the versatility of the DFB steam cracker extends to products obtained from alternative recycling methods, such as mechanical recycling and pyrolysis. This chapter proves that pyrolysis oils can undergo steam cracking in a DFB steam cracker without additional energy-intensive processes such as hydrotreatment.

This chapter also establishes WCO as a suitable biogenic feedstock for DFB steam cracking. Moreover, waste medical materials such as face masks, gloves, and syringes, which have their own dedicated and established waste management system, can be effectively recycled using the DFB steam cracking process. Overall, these findings provide valuable insights towards developing a comprehensive thermochemical recycling system centered around the DFB steam cracking process.

CHAPTER 7

7 – Selection of bed materials

The results presented in *Chapters 4, 5, and 6* are from investigations conducted in the Chalmers DFB cracker, with silica sand as the bed material. This choice aligns with a longstanding trend among researchers who have favored silica sand for fluidized bed processes involving the thermochemical conversion of plastic materials. The primary reasons for this preference are its cost-effectiveness and resilience under harsh process conditions. Additionally, the high SiO_2 content (>90%) makes it chemically inert in the context of hydrocarbon cracking reactions. In contrast, some natural ores have shown catalytic activity in a hydrocarbon-steam environment within fluidized beds.

This chapter is based on **Paper IV** and undertakes a comparative analysis of four different natural ores. The objective is to assess the impact of natural ores on the steam cracking of polyethylene under the operating conditions observed in a DFB steam cracker. The evaluation centers on the performance of the steam cracking process by comparing parameters such as cracking severity, conversion rates, and the distribution of products among different hydrocarbon groups. The selected operating conditions ensure comparability and minimize external influences, emphasizing that the chapter does not aim to recommend specific bed materials or operating conditions for optimizing product yields. Instead, its focus is to highlight the interaction between bed materials and cracking reactions, providing valuable insights to guide the selection of bed materials for specific applications.

7.1 Natural ores: Silica sand, Olivine, Bauxite and Feldspar

Table 10 provides the characteristics of the bed materials discussed in this chapter, including their potential catalytic activities as reported in the literature. The primary goal of this chapter is to clarify the impact of these bed materials, in their natural state, on the steam cracking reactions.

Table 10. Characteristics of the bed materials investigated in this chapter and their potential catalytic activity in a hydrocarbon-steam environment.

Bed material	Properties	Catalytic potential
Silica sand	- 90% SiO_2 - 316 mm avg. particle size - 2650 kg/m^3 particle density	Assumed inert
Olivine	- 41.7% SiO_2 - 288 mm avg. particle size - 3300 kg/m^3 particle density	Potential steam reforming catalyst when activated with biomass ash[70,75,88]
Bauxite	- 6.5% SiO_2 - 288 mm avg. particle size - 3300 kg/m^3 particle density	Potential hydrocracking catalyst because of high Al_2O_3 content (>80%)[73]
Feldspar	- 67.5% SiO_2 - 288 mm avg. particle size - 3300 kg/m^3 particle density	Potential steam reforming catalyst when activated with biomass ash[71,75]

The selection of the bed material affects the performance of the cracking process, mainly due to interactions between two cracking reactions: C−C and C−H bond breaking reactions. Interactions with C−C bond breaking impact the cracking severity, determining how extensively the hydrocarbon feedstock breaks down into smaller molecules. Interactions with C−H bond breaking can influence product distribution or secondary reaction pathways. This chapter highlights the interactions of silica sand, bauxite, olivine, and feldspar with the two primary reactions.

The C−C bond breaking interactions of the bed materials are compared based on two key parameters: the conversion rate and cracking severity. The conversion rate is the percentage of the feedstock successfully cracked into smaller molecules through cracking reactions. Specifically, the conversion rate is the total yield (%carbon, by weight) of C1 – C4 species, aromatic compounds, PAHs, and carbon deposits. Notably, aliphatic and naphthenic hydrocarbons with chain lengths of C5 and higher are not in the conversion rate calculation. These species are typically considered unconverted in a steam cracking process, often necessitating a secondary cracking step downstream, such as FCC or hydrocracking. The calculation of the conversion rate is provided by Equation 4.

$$conversion\ rate\ (\%) = \%C_{CO_x} + \%C_{CH_4} + \%C_{C_2H_x} + \%C_{C_3H_x} + \%C_{C_4H_x} + \%C_{aromatics} + \%C_{PAHs} + \%C_{carbon\ deposits}$$

Equation 4

The assessment of cracking severity involves a comparison of methane yield. A correlation between ethylene and methane yields is used for this assessment. The evaluation of C−H bond breaking interactions of the bed materials involves examining the distribution of hydrogen atoms among various species in the cracker effluent and the average H/C ratio of the cracker effluent. These assessments of the reactive interactions of the bed materials rely on the carbon and hydrogen balances derived over the steam cracker.

The results originate from the experiments conducted in the laboratory setup at a temperature of 750°C. This specific temperature of the bed material favors the production of light olefins, as seen in Chapter 5. A batch of 2g of PE pellets and a bed material-to-feedstock ratio of 250 were used in each experiment. The experiments involved fully oxidized bed materials to emulate the dynamics of a DFB steam cracker, where the bed material enters the steam cracking reactor after being fully oxidized in the regenerator.

7.2 Observed effect on C−C bond breaking

The study of bed material interaction with C−C bond breaking reactions involves assessing the extent to which the feedstock cracks into smaller molecules for a specific bed material. An alternative approach is to analyze the yield of cracker effluent resulting from the effective cracking of the feedstock. In this context, the comparison of conversion rates of the feedstock and the severity of cracking serves as a valuable metric. Figure 31 presents the conversion rate obtained from the experiments, calculated according to Equation 4, considering the overall yields of C1 – C4 species, BTXS, and PAHs.

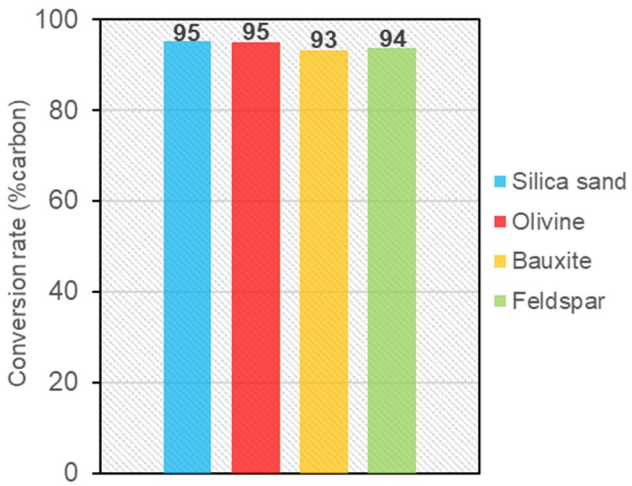

Figure 31. Conversion rates for steam cracking of PE with silica sand, olivine, bauxite, and feldspar as bed materials.

The results show that all four bed materials effectively convert PE, with conversion rates ranging from 93% to 95%. Silica sand demonstrates the highest conversion rate of 95%, while bauxite has the lowest conversion of 93%. Olivine and feldspar yield 95% and 94% conversion, respectively. The differences in conversion rates between the four bed materials are small, with a maximum difference of only 2%.

To further illustrate the interaction of the bed materials with the C−C bond breaking reaction, Figure 32 shows the variation in the cracking severity using the cracking severity plot.

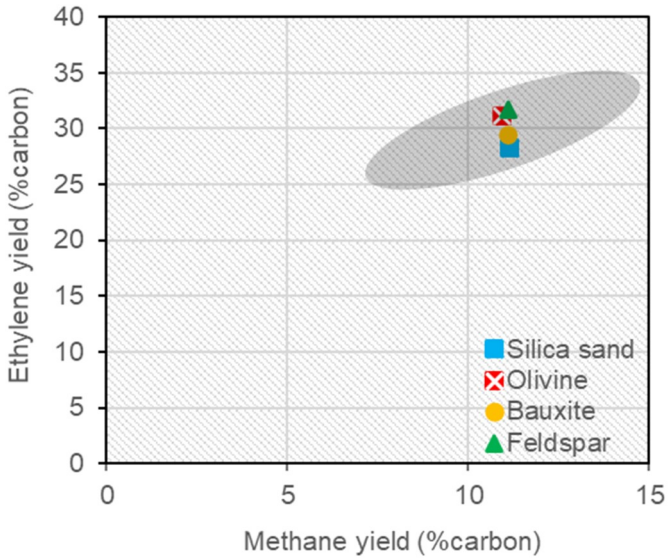

Figure 32. The yield of ethylene (%carbon, by weight) obtained with silica sand, olivine, bauxite, and feldspar as bed materials, shown on the cracking severity plot. The yield of methane serves as the indicator of the cracking severity. The reference curve obtained with the Chalmers DFB unit is visualized with the shaded region in the plot.

Figure 32 illustrates the correlation between the yield of ethylene and cracking severity, with methane yield as the indicator for cracking severity. Additionally, the figure presents the reference cracking severity curve obtained from the Chalmers DFB steam cracker. This inclusion allows for comparison, providing insights into how the studied bed materials perform relative to the reference operation.

Notable observation emerges upon comparing the operations of the lab reactor with the Chalmers DFB steam cracker. All four data points obtained from the lab reactor cluster closely within the shaded region shown in Figure 32. The cracking severities obtained with the four bed materials and the corresponding ethylene yield closely resemble the reference operation. Subtle differences become noticeable upon closer examination of the individual data points. Olivine and feldspar yield marginally lower cracking severity compared to bauxite and silica. Additionally, feldspar and olivine yield slightly higher ethylene than the other two bed materials. Nevertheless, the difference in ethylene yield among the bed materials is less than 2%.

7.3 Observed effect on C−H bond breaking

Analyzing the interaction between bed materials and the C−H bond breaking reaction requires evaluating the degree to which C−H bonds undergo cleavage in the presence of a particular bed material. As detailed in *Chapter 2*, C−H bond breaking leads to an alteration in the H/C ratio of the product species, deviating from the original H/C ratio of the feedstock. The C−H bond scission reaction results in three distinct product groups categorized based on their H/C ratio:

H/C > 2, H/C = 2, and H/C < 2. Figure 33 illustrates the distribution of the carbon atoms of the feedstock among these three product groups. Furthermore, Figure 33 shows the average H/C ratio of the entire cracker effluent, calculated by determining the weighted average of the H/C ratios of the individual species within the cracker effluent.

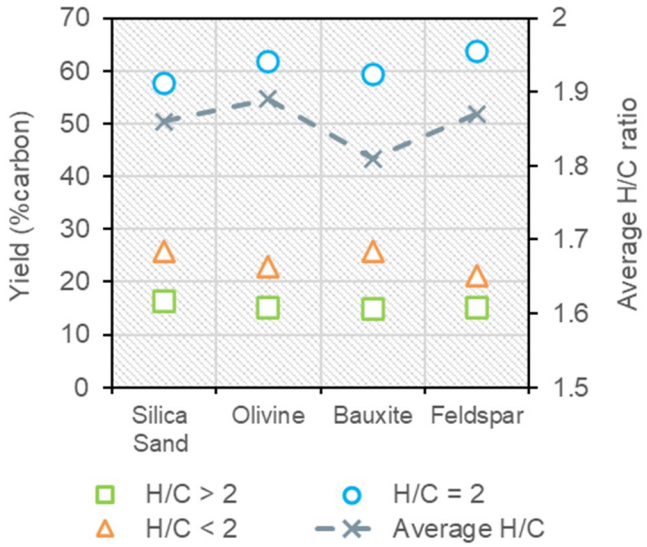

Figure 33. Distribution of the carbon atoms of the feedstock among the three product groups: H/C < 2, H/C = 2, and H/C > 2. The secondary axis corresponds to the average H/C ratio of the entire cracker effluent.

The product distribution among the three H/C groups appears consistent across all bed materials, with subtle observable differences. These subtle distinctions lead to a minor variation in the average H/C for the cracker effluent among the bed materials. Examining the right axis of the chart in Figure 33 reveals that bauxite exhibits the lowest average H/C of the products at 1.8, while olivine has the highest at 1.9.

The data in Figure 33 illustrates the hydrogen associated with the hydrocarbons within the cracker effluent. Incorporating these findings with the molecular hydrogen generated during steam cracking provides a comprehensive understanding of the total hydrogen content in the cracker effluent. This perspective also allows for examining how hydrogen atoms are distributed between the hydrocarbons and H_2, as visualized in Figure 34.

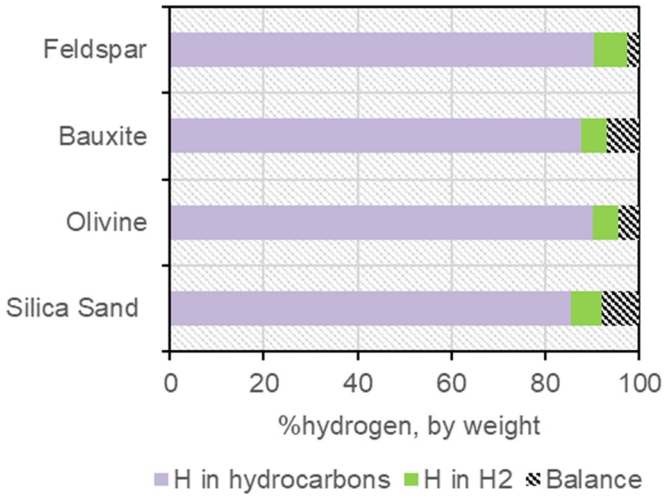

Figure 34. Total amount of hydrogen in the cracker effluent, present as hydrocarbons and molecular hydrogen. Balance represents the difference between the amount of hydrogen in the feedstock and the amount measured in the cracker effluent.

The deficit in hydrogen ('Balance' in Figure 34) observed in the cracker effluent suggests that hydrogen atoms from the feedstock undergo oxidation to form H_2O. Notably, silica-sand and bauxite demonstrate higher missing hydrogen than olivine and feldspar. It indicates a higher oxidizing nature for silica-sand and bauxite in contrast to olivine and feldspar. The increased oxidizing capability of silica-sand and bauxite is because of their higher Fe_2O_3 content, as detailed in Table 3. Despite olivine having a Fe_2O_3 content 70 times higher than feldspar, its missing hydrogen amount is lower and comparable to that of feldspar. This discrepancy relates to the accessibility of iron in olivine. Olivine, an iron-magnesium silicate, is known for having low surface availability of iron oxide.[88]

Furthermore, a correlation exists between the yield of products with $H/C < 2$ and the quantity of hydrogen oxidized by the bed material, as depicted in Figure 35. This correlation demonstrates the influence of bed materials, specifically silica sand and bauxite, on the increased production of products with $H/C < 2$. The increased production of these species observed with silica sand and bauxite can be associated with a higher level of C−H bond breaking interactions of the bed materials during steam cracking, wherein the hydrogen atoms undergo oxidation.

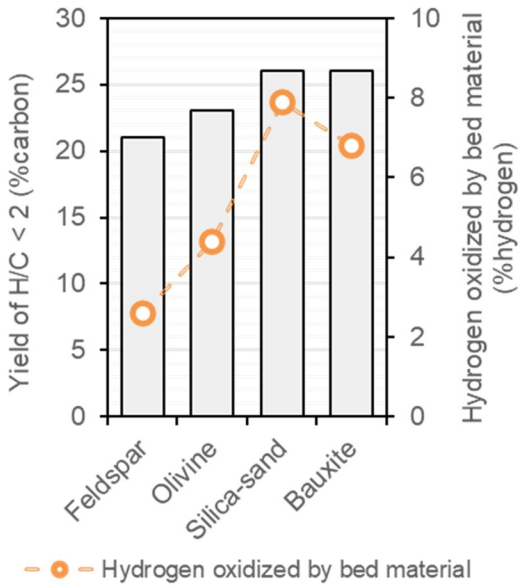

Figure 35. Yield of products with H/C < 2 (%carbon, by weight) and the amount of hydrogen oxidized by bed material. The oxidized hydrogen is the difference between the total hydrogen in the feedstock and the amount of hydrogen measured in the product mixture.

The preceding discussion highlights that, in their natural form, the bed materials bauxite, olivine, and feldspar exhibit limited catalytic activity, producing product distributions comparable to that of silica sand. Silica sand and bauxite contribute to a marginally higher cracking severity and a more oxidizing environment in the steam cracker, resulting in elevated yields of products with H/C < 2 compared to olivine and feldspar.

7.4 Selection criteria

The discussion on C−C and C−H bond breaking interactions underscores a significant finding: the catalytic behavior reported in fluidized bed conversion literature for activated olivine, bauxite, and feldspar does not manifest in their natural state. Instead, the free iron oxide content of the bed material emerges as the sole characteristic influencing the cracking reactions, leading to a shift in the H/C ratio of the cracker effluent through the oxidation of H atoms. However, despite this difference, a product distribution similar to silica sand is observed with these bed materials in their natural form. This observation suggests that these materials can be used interchangeably in fluidized bed steam crackers without compromising the quality of the cracker effluent as long as their natural state is maintained.

However, the transition to industrial-scale DFB steam crackers introduces external factors that change the bed material's natural state. Physical factors like attrition and agglomeration can alter the bed material's physical properties, while the accumulation of external species within the bed material changes its chemical composition. To address these challenges, continuous regeneration of the bed material becomes essential.

In the context of the Chalmers DFB steam cracker, a practical solution involves the daily addition of 500 kg of new silica sand to maintain the average particle size and chemical composition. For reactor systems where the accumulation of external chemical species is not a

concern, olivine and feldspar emerge as suitable alternatives to silica sand due to their superior abrasion-resistant properties. Conversely, in reactor systems where regeneration is inevitable due to the accumulation of chemical species, silica sand is a preferred choice due to its lower cost compared to olivine and feldspar. Bauxite emerges as a less favorable option because of its high amounts of free iron oxides and susceptibility to abrasive attrition.

In essence, bed material selection for a DFB steam cracker involves considering catalytic behavior, physical and chemical stability, abrasion resistance, and regeneration requirements, ensuring an optimal balance between performance and practicality.

CHAPTER 8

8 – Development of catalytic properties in bed materials in DFB steam cracker

The findings presented in *Chapter 7* highlight the absence of catalytic activity in the selected bed materials when utilized in their natural state. However, when considering the transition to a large-scale DFB steam cracker for plastic waste, maintaining the bed material's natural state becomes challenging. In this context, chemical species accumulation within the bed material poses a significant concern.

Existing research on gasification in DFB systems has highlighted the accumulation of ash species in the bed material and its potential impact on product distribution.[17,89] Additionally, certain studies have demonstrated the development of oxygen transport capacity in the bed material due to the accumulation of transition metal oxides.[74,75] In DFB steam crackers dedicated to converting plastic waste, these ash species may originate from both the regenerator fuel and the plastic waste itself.

This chapter explores the development of catalytic properties in bed materials within the context of a DFB steam cracker, drawing insights from **Papers I**, **II**, and **VI**. The primary objective is to assess the catalytic potential of bed materials under the conditions encountered in a large-scale DFB steam cracker. The evaluation uses synthetic and natural ores as bed materials to understand their impact on reactions integral to the steam cracking process, specifically the C−H bond breaking reaction. This chapter does not focus on developing catalytically active bed materials to enhance the yield of valuable species. Instead, the emphasis lies on exploring the catalytic properties inherently developed in bed materials exposed to biomass ash and transition metal oxides in a DFB steam cracker. The findings presented herein are obtained from experiments conducted at both the laboratory-scale and the semi-industrial DFB steam crackers.

8.1 Chemical modifications of the bed material observed in a DFB

Table 12 provides an overview of the bed materials discussed in this chapter, outlining various chemical modifications observed within a typical DFB reactor configuration. The main aim of this chapter is to investigate how these different states of bed materials influence the C−H bond breaking reaction and, consequently, the product distribution.

Table 12. The bed materials explored in this chapter and the corresponding types of chemical modifications investigated.

Bed material	Chemical modification	Investigation	Reactor system
Olivine	Natural	Reference	Both
	Exposed to biomass ash	Influence of biomass ash accumulation	Chalmers DFB steam cracker
	Reduced oxidation state	Reversing the influence of transition metal oxide	Laboratory steam cracker
Bauxite	Natural	Reference	Laboratory steam cracker
	Reduced oxidation state	Reversing the influence of transition metal oxide	
Al_2O_3	99.5% neutral Al_2O_3	Influence of transition metal oxide accumulation	Laboratory steam cracker
	Doped with 1% Fe		
	Doped with 2% Fe		
	Doped with 5% Fe		

Table 12 summarizes the investigations presented in **Papers I, II,** and **VI**. **Paper VI** explores the impact of biomass ash-exposed olivine on steam cracking reactions. This investigation was performed on the Chalmers DFB steam cracker, where natural olivine underwent a continuous three-day exposure to biomass combustion. Shifting attention to another vital chemical modification pertinent to DFB systems, **Paper I** focuses on the accumulation of transition metal oxides. This examination unfolded in the laboratory reactor, with synthetic Al_2O_3 bed materials doped with controlled amounts of iron oxide. Lastly, the investigation detailed in **Paper II** revolves around counteracting the effects of transition metal oxides on steam cracking reactions by reducing the bed material before exposure to the steam cracker. Reduced bauxite and olivine were used as bed materials in the laboratory reactor in this investigation. Collectively, these investigations contribute to a nuanced understanding of the effects of chemical modifications that may occur in bed materials within a DFB steam cracker.

In the investigation detailed in **Paper VI**, experiments unfolded over a 3-day campaign involving continuous exposure of olivine to biomass ash within the regenerator of the DFB steam cracker. Each day of operation (Days 1, 2, and 3) featured a distinct steam cracking test, with each test lasting several hours. Cracker effluent measurements were conducted during

selected stable periods within each test. Notably, the olivine circulated continuously throughout the three days, with no replacement or addition of new olivine—maintaining constant contact with biomass ash in the regenerator. Similar operating conditions across the three days of experiments were used to ensure a fair assessment of the impact of ash-exposed olivine on the cracking reactions. Minor deviations in operating conditions can be observed because of the challenges and limitations in fine adjustments of a large-scale plant. Table 13 outlines the key operational parameters of this investigation.

Table 13. Operational conditions used during the 3-day experimental campaign carried out in the Chalmers DFB steam cracker with olivine as the bed material.

Operational point	Steam cracker temperature (°C)	Feedstock flow to steam cracker (kg/h)	Average temperature in the regenerator (°C)
Day 1	788	132	840
Day 2	786	135	850
Day 3	782	120	858

The investigations described in **Papers I** and **II** were conducted within the laboratory reactor, focusing on the impact of transition metal oxides on steam cracking reactions. This chapter organizes these investigations into three parts, categorized by the oxidation state of the transition metal oxides in the utilized bed material. Table 14 provides crucial parameters concerning the operational conditions of these experiments.

Table 14. Operational conditions and the oxidation state of the bed materials used for the investigation on the influence of transition metal oxides on steam cracking reactions.

State of bed material	Bed material	Reactor temperature (°C)
Neutral	Al_2O_3	700
Oxidized	Fe/Al_2O_3, bauxite, olivine	700, 750[1]
Reduced	r-bauxite[2], r-olivine[2]	750

[1]Reactor temperature of 750°C was used with bauxite and olivine as bed materials in **Paper II.**
[2]r-bauxite and r-olivine are the bed materials olivine and bauxite in a reduced oxidation state.

The results outlined in this chapter originate from the carbon and hydrogen balances performed over the two reactor configurations. PE was used as the feedstock in both reactor systems.

8.2 Catalytic properties of bed material exposed to biomass ash

Figure 36 displays the yield (%carbon, by weight) of various groups of species over the three days of operation. A noticeable evolution of the cracker effluent is evident from Figure 36 from Days 1 to 3. The yield of CO and CO_2 increases by 50% from Day 1 to Day 2 and by 250% from Day 1 to Day 3. Additionally, the yield of H_2 exhibits a significant increase from Day 1 to Day 3, although Figure 36 does not depict this trend.

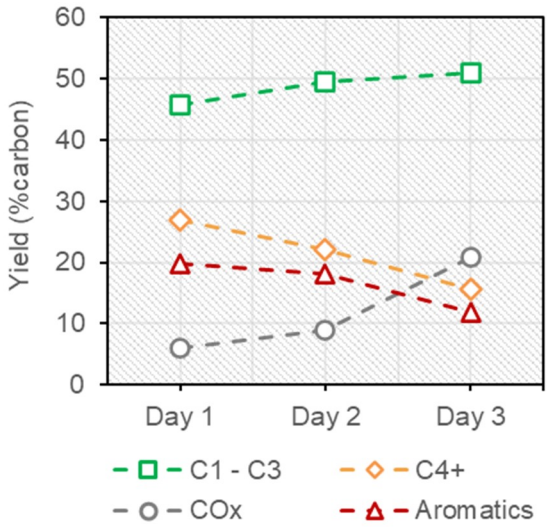

Figure 36. Evolution of the cracker effluent over the three days of the experimental campaign showing the influence of biomass ash-exposed olivine on the product distribution. Yields are in the form of %carbon (by weight).

Among the C1 – C3 hydrocarbons, CH_4 and C_2H_4 are the predominant species, with their composition showing a consistent trend of slight decrease from Day 1 to 3. Conversely, there is an increasing trend in the case of C_3H_6 as the exposure of olivine to biomass ash progresses. The increase in the yield of C_3H_6 can be manifested from the increasing trend of the C1 – C3 group shown in Figure 36.

Aromatic species, including BTXS and PAHs, exhibit a decreasing trend from Day 1 to Day 3. The total aromatic yield on Day 2 was recorded at 18% (%carbon), indicating a decrease of approximately 9% compared to Day 1. This reduction in aromatic yield increases to 41% when comparing the initial day (Day 1) with the day of maximum olivine exposure to biomass ash (Day 3). Individual analysis of aromatic species reveals a reduction in yields for almost all compounds from Day 1 to Day 3.

The C4+ group, comprising aliphatic and naphthenic species with four or more carbon atoms, demonstrates a declining trend from Day 1 to Day 3. This category also includes carbon deposits formed on the bed material surface during steam cracking. However, these carbon deposits contribute less than 1% to the carbon balance. The yield of C4+ species decreases from 27% to 22% (%carbon) over the first two days of ash exposure, further dropping to 16% by the end of the experimental campaign.

The changes in the yield of CO_x and C1 – C3 species, with the reduction in aromatic species, highlight the impact of biomass ash-exposed olivine on steam cracking reactions. Results indicate that olivine exposed to biomass ash yields higher H_2, CO, and CO_2 at the expense of the aromatic and C4+ hydrocarbons. The C4+ fragments, formed as intermediate products during steam cracking (see Figure 3, *Chapter 2*), undergo a reaction pathway leading to syngas formation rather than aromatics. Furthermore, the large share of H_2 in the cracker effluent suggests that C4+ fragments preferentially undergo steam reforming, converting into carbon oxides and H_2 as the ash exposure progresses. The simultaneous reduction in aromatic yield

also relates to steam reforming, which inhibits the subsequent aromatization of initial cracking products.

8.3 Catalytic properties in bed materials containing transition metal oxides

The influence of the transition metal oxide content of the bed material and its oxidation state on steam cracking reactions is analyzed using the average H/C ratio of the cracker effluent. Higher catalytic activity of the bed material towards the C−H bond breaking reaction results in a deviation of the H/C ratios of the cracker effluent from the H/C ratio of the feedstock. Figure 37 illustrates the average H/C ratios of the cracker effluent obtained from experiments covering the three oxidation states of the bed materials.

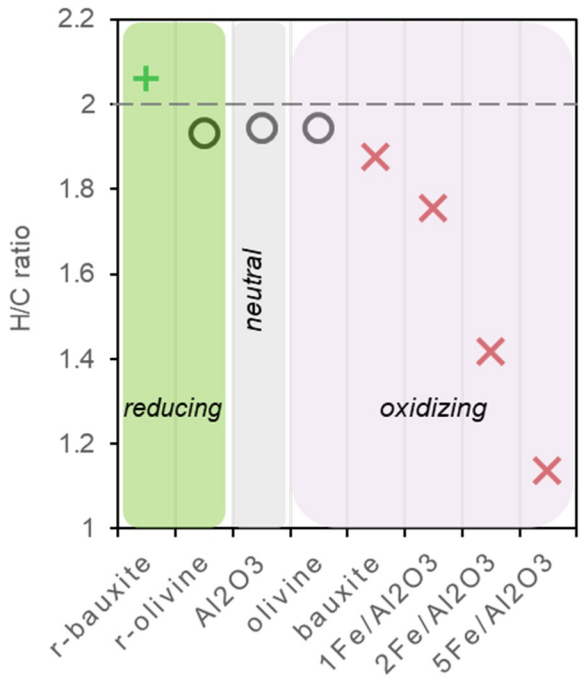

Figure 37. The average H/C ratio of the cracker effluent obtained with different bed materials used under different oxidation states. The dotted line represents the H/C ratio of the PE feedstock.

The average H/C ratios obtained with the bed materials bauxite, 1Fe/Al_2O_3, 2Fe/Al_2O_3, and 5Fe/Al_2O_3 are notably lower than 2. With an increase in the iron oxide content of the bed material, the average H/C ratios of the cracker effluent decrease. In the absence of iron oxide in the bed material, such as Al_2O_3, the average H/C ratios of the products closely resemble that of the initial PE molecule. Products derived using 5Fe/Al_2O_3, the bed material with the highest iron oxide content, exhibit the lowest H/C ratio of 1.13. This decrease in the H/C ratio primarily occurs because of the increased formation of aromatics, carbon oxides, and carbon deposits in the presence of bed materials containing iron oxide.

Lower H/C ratios of the cracker effluent, in the presence of oxidizing bed material, indicate dehydrogenation of PE, followed by oxidation of the hydrogen atoms of the feedstock to H_2O. When an oxidizing bed material is present, the initial PE molecule undergoes dehydrogenation before cracking down into smaller molecules. The product distribution resulting from the

cracking of a dehydrogenated PE molecule is well explained with the reaction mechanism depicted in Figure 38.

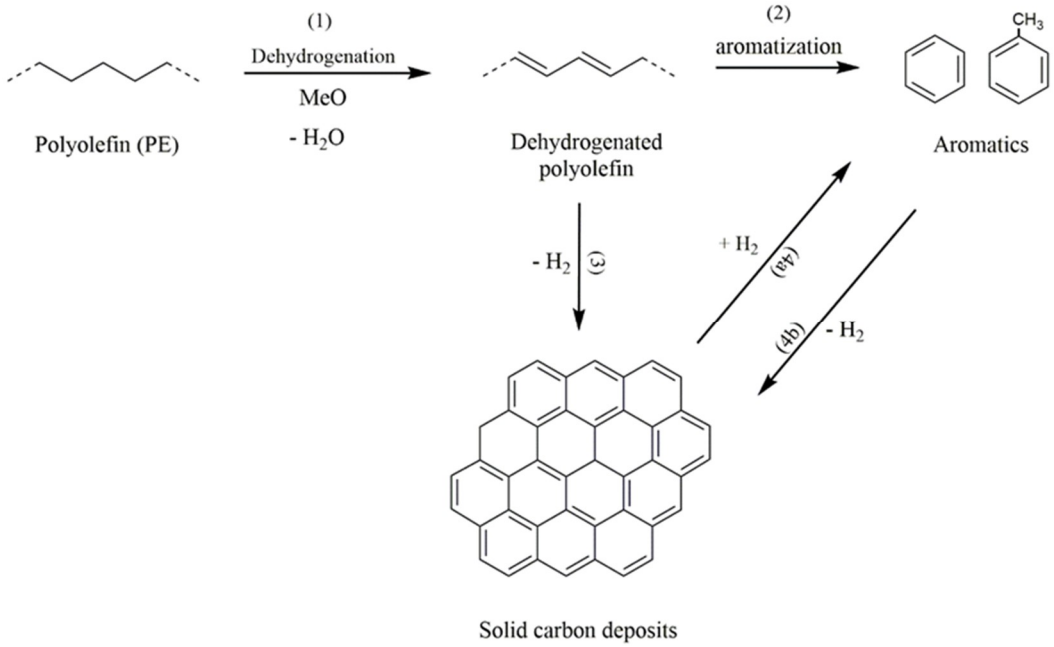

Figure 38. Reaction mechanism governing the formation of aromatics and solid carbon deposits from a dehydrogenated polyethylene molecule.

The formation of aromatic species occurs via the random cleavage of the dehydrogenated PE molecule, followed by aromatization. The formation of solid carbon deposits follows two distinct routes: (1) random chain cleavage of the dehydrogenated PE molecule with subsequent recombination into a mesh-like structure (reaction pathway (3) in Figure 38) and (2) polymerization of the produced aromatic rings (reaction pathway (4b) in Figure 38). Additionally, random cleavage within the structure of the carbon deposits also contributes to the formation of aromatic rings (reaction pathway (4a) in Figure 38).

The proposed reaction mechanism primarily influences product distribution through the interaction of bed material with the C−H bond breaking reaction. The iron oxide in the material accelerates the breaking of C−H bonds, primarily in the form of dehydrogenation. The observation that the formation of aromatics and carbon deposits because of the presence of iron oxide on the bed material surface suggests that the proposed dehydrogenation step occurs predominantly on the surface of the bed material. In a DFB steam cracking process, dehydrogenation of polyolefins will occur when the bed material accumulates transition metal oxides on its surface.

The cracker effluent obtained with Al_2O_3, olivine, and r-olivine has an average H/C ratio similar to a PE molecule, suggesting minimal interaction with the C−H bond-breaking reaction. In contrast, with r-bauxite, the product distribution shows a higher H/C ratio than PE due to the increased production of molecules with an H/C ratio of 2 or greater. The rise in the average H/C ratio of the cracker effluent when using r-bauxite as the bed material confirms the hydrogenation of intermediate unsaturated species, facilitated by hydrogen produced from the water dissociation reaction. Figure 39 illustrates this phenomenon.

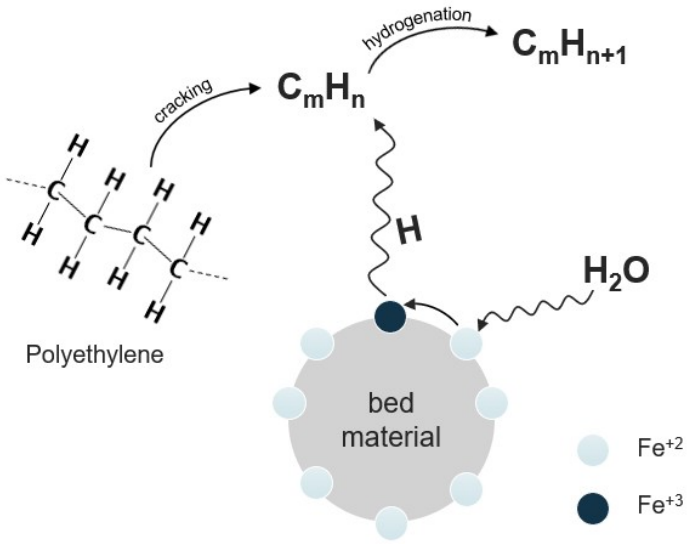

Figure 39. Hydrogenation of unsaturated species (C_mH_n) produced from steam cracking of PE in the presence of a bed material containing a transition metal oxide in a reduced oxidation state (e.g., FeO).

Both r-bauxite and r-olivine catalyze the water dissociation reaction alongside steam cracking. However, using r-olivine results in a similar H/C ratio of the cracker effluent as obtained with olivine. This discrepancy can be explained by comparing the two bed materials in terms of two parameters affecting the hydrogenation of unsaturated species during steam cracking: (1) the ability of the environment to donate hydrogen and (2) the bed material's capability to transfer the donated hydrogen to the hydrocarbon species.

The hydrogen-donation capacity of water is associated with the quantity of hydrogen produced through the water dissociation reaction. The comparable yields of molecular hydrogen (**Paper II**) confirm that the hydrogen-donation capability of water remains consistent regardless of the presence of r-bauxite or r-olivine.

The ability of the bed material to transfer the generated hydrogen to hydrocarbon species relies on its physical and chemical properties. Conventional hydrogenation or hydrocracking catalysts typically consist of amorphous silica-alumina, zeolite, or a blend of both, known for their porous nature, providing ample surface area for hydrogenation reactions.[58] In this instance, properties of bauxite, such as porosity and Al_2O_3 content, resemble those of a conventional hydrogenation or hydrocracking catalyst.[73] On the other hand, olivine has no properties corresponding to those of a hydrocracking or hydrogenation catalyst. Olivine, being a magnesium silicate, is known to contain negligible concentrations of free Al_2O_3 and SiO_2.[88,89]

The findings highlight the potential to reverse the impact of transition metal oxides on the steam cracking reaction by reducing the bed material before its introduction into the steam cracker. Figure 40 proposes a modified DFB steam cracker featuring an additional fluidized bed that enables the reduction of the bed material after the regenerator. This process allows the introduction of transition metal oxides in a reduced oxidation state into the steam cracker.

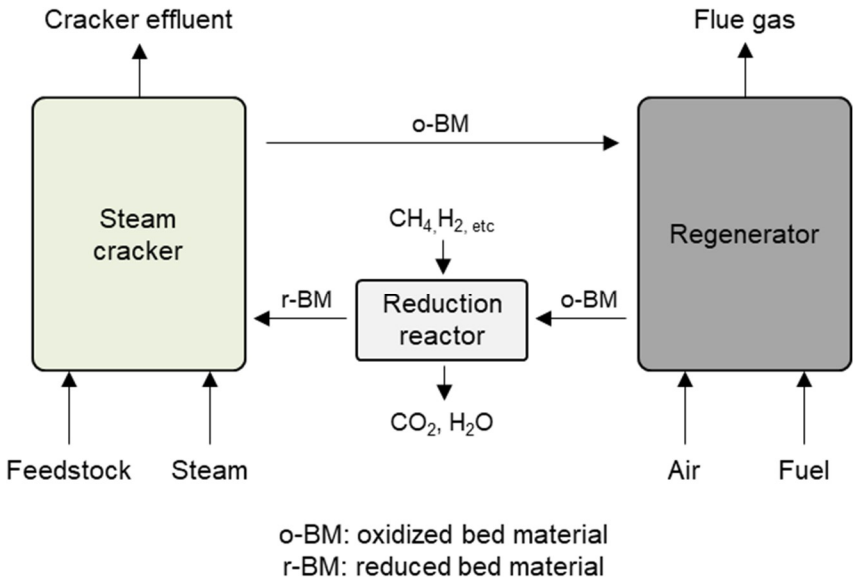

Figure 40. Schematic of a DFB steam cracker that enables continuous reduction of the bed material before entry into the steam cracker.

Introducing the reduction step before the steam cracker allows the effect of transition metals to be counteracted and leveraged to enhance the yield of product species with H/C ratios ≥ 2 through the hydrogenation of unsaturated intermediate species. However, it is essential to acknowledge that factors such as the chemical composition, porosity, and surface density of active sites of the bed material significantly influence its hydrogenation potential. While this study did not examine these bed material properties, understanding them remains crucial for further application.

The catalytic properties of bed materials that inherently develop in a DFB steam cracker can be advantageous or detrimental, depending on the circumstances. The increase in syngas production with a bed material exposed to biomass ash can be beneficial if the steam cracker has downstream synthesis processes capable of converting the syngas into more valuable hydrocarbons. However, this increase in syngas production comes at the expense of monoaromatics and ethylene. Therefore, the accumulation of biomass ash within the bed material inventory may not be advantageous if the steam cracker lacks such downstream synthesis processes.

The catalytic property of the bed material, which develops due to the accumulation of transition metal oxides, is expected to be detrimental to the process under any circumstances. This is because transition metal oxides lead to increased production of solid carbon deposits and PAHs through the dehydrogenation reaction. Therefore, large-scale DFB steam crackers prone to the accumulation of transition metal oxides in the bed material should routinely replace the bed material with fresh material. This practice will help maintain a low level of transition metal oxides and keep the intensity of the dehydrogenation reaction low.

Alternatively, the detrimental effect of transition metal oxides can be mitigated by reducing the bed material before it enters the steam cracker. Furthermore, when using bauxite as the bed material, the effect of reduced transition metal oxides can be leveraged to drive the hydrogenation reaction in the steam cracker.

CHAPTER 9

9 – Summary and Conclusions

Steam cracking in a DFB reactor configuration is an alternative to the conventional steam cracking process. This work aims to demonstrate the effectiveness of the DFB steam cracking process in the thermochemical recycling of plastic waste. The experimental work, forming the foundation of this thesis, spans from laboratory to semi-industrial reactors, aiming to establish a robust understanding of DFB steam cracking operations and product distributions.

The thesis extends its investigation by using actual waste streams from society in the DFB steam cracking process for the selective production of light olefins and monoaromatics. This investigation is complemented by a proposed integration strategy, aiming to elevate overall recycling rates by combining alternative processes like polyolefin pyrolysis with DFB steam cracking.

In addition, the thesis explores the role of bed material within a DFB steam cracker, examining its influence on steam cracking reactions and its implications on the cracker operation. Notably, the impact of the bed material on the C–C and C–H bond breaking reactions, crucial to steam cracking, is investigated. Furthermore, the study sheds light on the development of catalytic properties in the bed materials within a DFB steam cracker and its effect on steam cracking reactions.

The outcomes of this thesis, which lay the groundwork for future advancements in plastic recycling through steam cracking in DFB systems, are summarized below:

- The cracking mechanisms for polyolefins established in the literature, which indicate that at a certain cracking severity, the product distribution becomes enriched with light olefins and monoaromatics, are also applicable to large-scale DFB steam crackers.

- A DFB steam cracker within the cracking temperature range of 700 – 825°C achieves a cracking severity that results in up to 50% C2 – C4 olefins and 20% BTXS from a pure polyolefin feedstock.

- The DFB steam cracking process eliminates the need to separate polyolefins from waste streams by selectively producing ethylene and propylene in proportion to the polyolefin content of the waste stream, approximately 45%.

- A DFB steam cracker can process waste streams with varying amounts of non-polyolefins, such as PET, PS, and cellulose, by selectively converting them into aromatics and syngas. The downstream separation of the cracker effluent provides in-situ sorting of the products derived from both the polyolefin and non-polyolefin contents.

- The inherent capability of a DFB steam cracker to remove carbon deposits also eliminates the necessity for additional preprocessing steps, such as hydrotreatment, typically required for steam cracking of feedstocks prone to coke formation, such as pyrolysis oils and waste cooking oils.

- Natural ores like silica sand, olivine, feldspar, and bauxite do not show significant differences in interacting with the C−C and C−H bond-breaking reactions. These natural ores can be used interchangeably in a DFB steam cracker. However, the choice of bed material should consider factors like abrasion resistance and the potential accumulation of chemical species in the reactor.

- In a DFB steam cracker fueled with biomass, biomass ash accumulates in the bed material. Olivine, exposed to biomass ash within a DFB steam cracker, develops catalytic properties. This catalytic transformation shifts reaction pathways towards favoring the formation of syngas over aromatics, driven by the steam reforming of unsaturated intermediate species.

- The accumulation of transition metal oxides in the bed material creates an oxidizing environment in the steam cracker. The oxidizing bed material causes dehydrogenation of the feedstock, resulting in increased production of species with H/C < 2, such as carbon oxides, aromatics, and solid carbon deposits.

- Reducing the bed material before it enters the steam cracker can decrease the extent of the dehydrogenation reaction. Using bauxite as the bed material in this setup promotes hydrogenation of the feedstock, thereby increasing the overall H/C ratio of the cracker effluent.

- If the accumulation of biomass ash or transition metal oxides proves detrimental to the process, it can be mitigated by continuously replacing the bed material inventory with fresh bed material.

Recommendations for future work

The findings outlined in this thesis highlight the potential of the DFB steam cracking process for the thermochemical recycling of plastic waste. The results also pinpoint several critical areas that require further exploration to ensure the applicability and economic viability of the process.

One notable aspect highlighted is the product distribution obtained from the steam cracking of pure polyolefins, where the yield of light olefins plateaus at approximately 50%. Enhancing the yield of light olefins through improved heat transfer mechanisms would enhance the economic viability of the process. The influence of heat transfer rates on the kinetics and residence times also requires thorough investigation.

An oversight in the investigation pertains to the fate of heteroatoms (N, S, and Cl) present in plastic waste that could poison polymerization processes downstream of the steam cracker. Investigating the formation of catalyst poisons from heteroatom-containing polymers in the DFB steam cracking process is necessary. Developing sampling and analysis techniques for rapidly quantifying these species in the cracker effluent is also desirable.

Further research avenues involve investigating the development of oxygen transport in large-scale DFB steam crackers. This endeavor would necessitate an experimental campaign involving feedstocks that contribute to the oxygen transport capability of the bed material.

The results revealed the dependence of the hydrogenation of unsaturated intermediate species on the hydrogen transfer capacity of the bed material. The influence of bed material properties, such as chemical composition, porosity, and surface density of active sites, on its hydrogen transfer capability needs further research.

Pyrolysis stands out as a highly versatile thermochemical recycling process. The pyrolysis oil used in this work was obtained from the pyrolysis of well-sorted polyolefins. Future research should investigate the DFB steam cracking of pyrolysis oils obtained from unsorted plastic wastes. Additionally, efforts to minimize the production of off-gases during the pyrolysis process will be beneficial. These initiatives are crucial for improving the circularity and sustainability of the pyrolysis process.

Nomenclature

BFB	Bubbling fluidized bed
BTXS	Benzene toluene xylenes styrene
CFB	Circulating fluidized bed
CRR	Cardboard recycling reject
DFB	Dual fluidized bed
FCC	Fluid catalytic cracking
FID	Flame ionization detector
GC	Gas chromatograph
HDPE	High density polyethylene
HTR	High temperature reactor
LDPE	Low density polyethylene
LFC	Liquid flow controller
LLDPE	Linear low density polyethylene
LPG	Liquified petroleum gas
MFC	Mass flow controller
MMT	Million metric tonnes
MPW	Mixed plastic waste
MRP	Mechanically recycled polyolefins
MTO	Methanol to Olefins
NBR	Nitrile butadiene rubber
PE	Polyethylene
PET	Polyethylene terephthalate
PMMA	Poly methyl methacrylate
PO	Pyrolysis oil
PP	Polypropylene
PS	Polystyrene
PVC	Polyvinyl chloride
RRF	Relative response factor
TCD	Thermal conductivity detector
VUV	Vacuum ultraviolet
WCO	Waste cooking oil

c_{He}	Concentration of helium [%vol]
c_i	Concentration of species i [%vol]
C_i	Yield of species i [%carbon]
m_f	Mass flow rate of the feedstock [kg/h]
m_i	Mass fraction of species i [%mass]
MW_i	Molecular weight of species i [mol/kg]
n_i	Molar yield of species i [mol/kg]
V_{He}	Volumetric flow rate of helium [l/h]
V_m	Molar volume of ideal gas at 0°C and 1 atm [l/mol]

References

1. Plastics Europe (2023). Plastics – the fast Facts 2023. Annual production of plastics worldwide from 1950 to 2022 (in million metric tons). https://www.statista.com/statistics/282732/global-production-of-plastics-since-1950/.

2. Thunman, H., Berdugo Vilches, T., Seemann, M., Maric, J., Vela, I.C., Pissot, S., and Nguyen, H.N.T. (2019). Circular use of plastics-transformation of existing petrochemical clusters into thermochemical recycling plants with 100% plastics recovery. Sustainable Materials and Technologies *22*. https://doi.org/10.1016/j.susmat.2019.e00124.

3. OECD (2022). Plastic waste generation worldwide from 1980 to 2019, by application. Plastic waste generation worldwide from 1980 to 2019, by application (in million metric tons). https://www.statista.com/statistics/1339124/global-plastic-waste-generation-by-application/.

4. Geyer, R., Jambeck, J.R., and Law, K.L. (2017). Production, use, and fate of all plastics ever made. Sci Adv *3*. https://doi.org/10.1126/sciadv.1700782.

5. European Parliament and Council (2008). Directive 2008/98/EC of the European Parliament and of the Council of 19 November 2008 on waste and repealing certain directives (Waste framework https://doi.org/2008/98/EC.; 32008L0098.

6. Zhao, X., Korey, M., Li, K., Copenhaver, K., Tekinalp, H., Celik, S., Kalaitzidou, K., Ruan, R., Ragauskas, A.J., and Ozcan, S. (2022). Plastic waste upcycling toward a circular economy. Preprint, https://doi.org/10.1016/j.cej.2021.131928 https://doi.org/10.1016/j.cej.2021.131928.

7. Chen, S., and Hu, Y.H. (2024). Advancements and future directions in waste plastics recycling: From mechanical methods to innovative chemical processes. Preprint at Elsevier B.V., https://doi.org/10.1016/j.cej.2024.152727 https://doi.org/10.1016/j.cej.2024.152727.

8. Kutz, M. (2016). Applied Plastics Engineering Handbook: Processing, Materials, and Applications: Second Edition.

9. Cañete Vela, I., Berdugo Vilches, T., Berndes, G., Johnsson, F., and Thunman, H. (2022). Co-recycling of natural and synthetic carbon materials for a sustainable circular economy. J Clean Prod *365*. https://doi.org/10.1016/j.jclepro.2022.132674.

10. Abbas-Abadi, M.S., Ureel, Y., Eschenbacher, A., Vermeire, F.H., Varghese, R.J., Oenema, J., Stefanidis, G.D., and Van Geem, K.M. (2023). Challenges and opportunities of light olefin production via thermal and catalytic pyrolysis of end-of-life polyolefins: Towards full recyclability. Preprint, https://doi.org/10.1016/j.pecs.2022.101046 https://doi.org/10.1016/j.pecs.2022.101046.

11. Lopez, G., Artetxe, M., Amutio, M., Bilbao, J., and Olazar, M. (2017). Thermochemical routes for the valorization of waste polyolefinic plastics to produce fuels and chemicals. A review. Preprint, https://doi.org/10.1016/j.rser.2017.01.142 https://doi.org/10.1016/j.rser.2017.01.142.

12. Kwon, G., Cho, D.W., Park, J., Bhatnagar, A., and Song, H. (2023). A review of plastic pollution and their treatment technology: A circular economy platform by thermochemical pathway. Preprint, https://doi.org/10.1016/j.cej.2023.142771 https://doi.org/10.1016/j.cej.2023.142771.

13. Kusenberg, M., Eschenbacher, A., Djokic, M.R., Zayoud, A., Ragaert, K., De Meester, S., and Van Geem, K.M. (2022). Opportunities and challenges for the application of post-consumer plastic waste pyrolysis oils as steam cracker feedstocks: To decontaminate or not to decontaminate? Preprint, https://doi.org/10.1016/j.wasman.2021.11.009 https://doi.org/10.1016/j.wasman.2021.11.009.

14. Wilk, V., and Hofbauer, H. (2013). Conversion of mixed plastic wastes in a dual fluidized bed steam gasifier. Fuel *107*. https://doi.org/10.1016/j.fuel.2013.01.068.

15. Maric, J., Berdugo Vilches, T., Thunman, H., Gyllenhammar, M., and Seemann, M. (2018). Valorization of Automobile Shredder Residue Using Indirect Gasification. Energy and Fuels *32*. https://doi.org/10.1021/acs.energyfuels.8b02526.

16. Ren, T., Patel, M., and Blok, K. (2006). Olefins from conventional and heavy feedstocks: Energy use in steam cracking and alternative processes. Energy *31*. https://doi.org/10.1016/j.energy.2005.04.001.

17. Larsson, A., Kuba, M., Berdugo Vilches, T., Seemann, M., Hofbauer, H., and Thunman, H. (2021). Steam gasification of biomass – Typical gas quality and operational strategies derived from industrial-scale plants. Fuel Processing Technology *212*. https://doi.org/10.1016/j.fuproc.2020.106609.

18. Karl, J., and Pröll, T. (2018). Steam gasification of biomass in dual fluidized bed gasifiers: A review. Preprint, https://doi.org/10.1016/j.rser.2018.09.010 https://doi.org/10.1016/j.rser.2018.09.010.

19. Levine, S.E., and Broadbelt, L.J. (2009). Detailed mechanistic modeling of high-density polyethylene pyrolysis: Low molecular weight product evolution. Polym Degrad Stab *94*. https://doi.org/10.1016/j.polymdegradstab.2009.01.031.

20. Marongiu, A., Faravelli, T., and Ranzi, E. (2007). Detailed kinetic modeling of the thermal degradation of vinyl polymers. J Anal Appl Pyrolysis *78*. https://doi.org/10.1016/j.jaap.2006.09.008.

21. Tian, P., Wei, Y., Ye, M., and Liu, Z. (2015). Methanol to olefins (MTO): From fundamentals to commercialization. Preprint, https://doi.org/10.1021/acscatal.5b00007 https://doi.org/10.1021/acscatal.5b00007.

22. Stöcker, M. (1999). Methanol-to-hydrocarbons: Catalytic materials and their behavior. Microporous and Mesoporous Materials *29*. https://doi.org/10.1016/S1387-1811(98)00319-9.

23. Atsbha, T.A., Yoon, T., Seongho, P., and Lee, C.J. (2021). A review on the catalytic conversion of CO2using H2for synthesis of CO, methanol, and hydrocarbons. Preprint, https://doi.org/10.1016/j.jcou.2020.101413 https://doi.org/10.1016/j.jcou.2020.101413.

24. Wender, I. (1996). Reactions of synthesis gas. Fuel Processing Technology *48*. https://doi.org/10.1016/S0378-3820(96)01048-X.

25. Kaminsky, W. (2021). Chemical recycling of plastics by fluidized bed pyrolysis. Fuel Communications *8*. https://doi.org/10.1016/j.jfueco.2021.100023.

26. Eschenbacher, A., Varghese, R.J., Abbas-Abadi, M.S., and Van Geem, K.M. (2022). Maximizing light olefins and aromatics as high value base chemicals via single step catalytic conversion of plastic waste. Chemical Engineering Journal *428*. https://doi.org/10.1016/j.cej.2021.132087.

27. Supriyanto, Ylitervo, P., and Richards, T. (2021). Gaseous products from primary reactions of fast plastic pyrolysis. J Anal Appl Pyrolysis *158*. https://doi.org/10.1016/j.jaap.2021.105248.

28. Anuar Sharuddin, S.D., Abnisa, F., Wan Daud, W.M.A., and Aroua, M.K. (2016). A review on pyrolysis of plastic wastes. Preprint, https://doi.org/10.1016/j.enconman.2016.02.037 https://doi.org/10.1016/j.enconman.2016.02.037.

29. Fu, Z., Hua, F., Yang, S., Wang, H., and Cheng, Y. (2023). Evolution of light olefins during the pyrolysis of polyethylene in a two-stage process. J Anal Appl Pyrolysis *169*. https://doi.org/10.1016/j.jaap.2023.105877.

30. López, A., de Marco, I., Caballero, B.M., Laresgoiti, M.F., and Adrados, A. (2011). Influence of time and temperature on pyrolysis of plastic wastes in a semi-batch reactor. Chemical Engineering Journal *173*. https://doi.org/10.1016/j.cej.2011.07.037.

31. Kusenberg, M., De Langhe, S., Parvizi, B., Abdulrahman, A.J., Varghese, R.J., Aravindakshan, S.U., Kurkijärvi, A., Gandarillas, A.M., Jamieson, J., De Meester, S., et al. (2024). Characterization and impact of oxygenates in post-consumer plastic waste-derived pyrolysis oils on steam cracking process efficiency. J Anal Appl Pyrolysis *181*. https://doi.org/10.1016/j.jaap.2024.106571.

32. Onwudili, J.A., Insura, N., and Williams, P.T. (2009). Composition of products from the pyrolysis of polyethylene and polystyrene in a closed batch reactor: Effects of temperature and residence time. J Anal Appl Pyrolysis *86*. https://doi.org/10.1016/j.jaap.2009.07.008.

33. Kusenberg, M., Zayoud, A., Roosen, M., Thi, H.D., Abbas-Abadi, M.S., Eschenbacher, A., Kresovic, U., De Meester, S., and Van Geem, K.M. (2022). A comprehensive experimental investigation of plastic waste pyrolysis oil quality and its dependence on the plastic waste composition. Fuel Processing Technology *227*. https://doi.org/10.1016/j.fuproc.2021.107090.

34. Kusenberg, M., Roosen, M., Zayoud, A., Djokic, M.R., Dao Thi, H., De Meester, S., Ragaert, K., Kresovic, U., and Van Geem, K.M. (2022). Assessing the feasibility of chemical recycling via steam cracking of untreated plastic waste pyrolysis oils: Feedstock impurities, product yields and coke formation. Waste Management *141*. https://doi.org/10.1016/j.wasman.2022.01.033.

35. Hussein, Z.A., Shakor, Z.M., Alzuhairi, M., and Al-Sheikh, F. (2023). Thermal and catalytic cracking of plastic waste: a review. Preprint, https://doi.org/10.1080/03067319.2021.1946527 https://doi.org/10.1080/03067319.2021.1946527.

36. Vollmer, I., Jenks, M.J.F., Mayorga González, R., Meirer, F., and Weckhuysen, B.M. (2021). Plastic Waste Conversion over a Refinery Waste Catalyst. Angewandte Chemie - International Edition *60*. https://doi.org/10.1002/anie.202104110.

37. Liu, S., Kots, P.A., Vance, B.C., Danielson, A., and Vlachos, D.G. (2021). Plastic waste to fuels by hydrocracking at mild conditions. Sci Adv *7*. https://doi.org/10.1126/sciadv.abf8283.

38. Choi, I.H., Lee, H.J., Rhim, G.B., Chun, D.H., Lee, K.H., and Hwang, K.R. (2022). Catalytic hydrocracking of heavy wax from pyrolysis of plastic wastes using Pd/Hβ for naphtha-ranged hydrocarbon production. J Anal Appl Pyrolysis *161*. https://doi.org/10.1016/j.jaap.2021.105424.

39. Hasan, M.M., Batalha, N., Fraga, G., Ahmed, M.H.M., Pinard, L., Konarova, M., Pratt, S., and Laycock, B. (2022). Zeolite shape selectivity impact on LDPE and PP catalytic pyrolysis products and coke nature†. Sustain Energy Fuels *6*. https://doi.org/10.1039/d2se00146b.

40. Deng, L., Guo, W., Ngo, H.H., Zhang, X., Wei, D., Wei, Q., and Deng, S. (2023). Novel catalysts in catalytic upcycling of common polymer wastes. Preprint, https://doi.org/10.1016/j.cej.2023.144350 https://doi.org/10.1016/j.cej.2023.144350.

41. Gholami, Z., Gholami, F., Tišler, Z., Tomas, M., and Vakili, M. (2021). A review on production of light olefins via fluid catalytic cracking. Energies (Basel) *14*. https://doi.org/10.3390/en14041089.

42. Zhang, L., Wu, Q., Fan, L., Liao, R., Zhang, J., Zou, R., Cobb, K., Ruan, R., and Wang, Y. (2024). Monocyclic aromatic hydrocarbons production from NaOH pretreatment metallized food plastic packaging waste through microwave pyrolysis coupled with ex-situ catalytic reforming. Chemical Engineering Journal *484*. https://doi.org/10.1016/j.cej.2024.149777.

43. Xu, D., Lu, X., Zhang, Y., Shearing, P.R., Zhang, S., Brett, D.J.L., and Wang, S. (2022). Insights into in-situ catalytic degradation of plastic wastes over zeolite-based catalyst from perspective of three-dimensional pore structure evolution. Chemical Engineering Journal *450*. https://doi.org/10.1016/j.cej.2022.138402.

44. Elordi, G., Olazar, M., Castaño, P., Artetxe, M., and Bilbao, J. (2012). Polyethylene cracking on a spent FCC catalyst in a conical spouted bed. Ind Eng Chem Res *51*. https://doi.org/10.1021/ie3018274.

45. Palos, R., Rodríguez, E., Gutiérrez, A., Bilbao, J., and Arandes, J.M. (2022). Cracking of plastic pyrolysis oil over FCC equilibrium catalysts to produce fuels: Kinetic modeling. Fuel *316*. https://doi.org/10.1016/j.fuel.2022.123341.

46. Svadlenak, S., Rochefort, S., and Goulas, K.A. (2021). Syngas production from polyolefins in a semi-batch reactor system. AIChE Journal *67*. https://doi.org/10.1002/aic.17479.

47. Hasanzadeh, R., Mojaver, M., Azdast, T., and Park, C.B. (2021). Polyethylene waste gasification syngas analysis and multi-objective optimization using central composite design for simultaneous minimization of required heat and maximization of exergy efficiency. Energy Convers Manag *247*. https://doi.org/10.1016/j.enconman.2021.114713.

48. Weiland, F., Lundin, L., Celebi, M., van der Vlist, K., and Moradian, F. (2021). Aspects of chemical recycling of complex plastic waste via the gasification route. Waste Management *126*. https://doi.org/10.1016/j.wasman.2021.02.054.

49. Madanikashani, S., Vandewalle, L.A., De Meester, S., De Wilde, J., and Van Geem, K.M. (2022). Multi-Scale Modeling of Plastic Waste Gasification: Opportunities and Challenges. Preprint, https://doi.org/10.3390/ma15124215 https://doi.org/10.3390/ma15124215.

50. Arena, U. (2012). Process and technological aspects of municipal solid waste gasification. A review. Waste Management *32*. https://doi.org/10.1016/j.wasman.2011.09.025.

51. Lopez, G., Artetxe, M., Amutio, M., Alvarez, J., Bilbao, J., and Olazar, M. (2018). Recent advances in the gasification of waste plastics. A critical overview. Preprint, https://doi.org/10.1016/j.rser.2017.09.032 https://doi.org/10.1016/j.rser.2017.09.032.

52. Li, S., Cañete Vela, I., Järvinen, M., and Seemann, M. (2021). Polyethylene terephthalate (PET) recycling via steam gasification – The effect of operating conditions on gas and tar composition. Waste Management *130*. https://doi.org/10.1016/j.wasman.2021.05.023.

53. Kusenberg, M., Roosen, M., Doktor, A., Casado, L., Jamil Abdulrahman, A., Parvizi, B., Eschenbacher, A., Biadi, E., Laudou, N., Jänsch, D., et al. (2023). Contaminant removal from plastic waste pyrolysis oil via depth filtration and the impact on chemical recycling: A simple solution with significant impact. Chemical Engineering Journal *473*. https://doi.org/10.1016/j.cej.2023.145259.

54. Selvam, E., Kots, P.A., Hernandez, B., Malhotra, A., Chen, W., Catala-Civera, J.M., Santamaria, J., Ierapetritou, M., and Vlachos, D.G. (2023). Plastic waste upgrade to olefins via mild slurry microwave pyrolysis over solid acids. Chemical Engineering Journal *454*. https://doi.org/10.1016/j.cej.2022.140332.

55. Munir, D., Irfan, M.F., and Usman, M.R. (2018). Hydrocracking of virgin and waste plastics: A detailed review. Preprint, https://doi.org/10.1016/j.rser.2018.03.034 https://doi.org/10.1016/j.rser.2018.03.034.

56. De La Puente, G., Klocker, C., and Sedran, U. (2002). Conversion of waste plastics into fuels recycling polyethylene in FCC. Appl Catal B *36*. https://doi.org/10.1016/S0926-3373(01)00287-9.

57. Chadwick, S.S. (1988). Ullmann's Encyclopedia of Industrial Chemistry. Preprint, https://doi.org/10.1108/eb049034 https://doi.org/10.1108/eb049034.

58. Saab, R., Polychronopoulou, K., Zheng, L., Kumar, S., and Schiffer, A. (2020). Synthesis and performance evaluation of hydrocracking catalysts: A review. Preprint, https://doi.org/10.1016/j.jiec.2020.06.022 https://doi.org/10.1016/j.jiec.2020.06.022.

59. Cerqueira, H.S., Caeiro, G., Costa, L., and Ramôa Ribeiro, F. (2008). Deactivation of FCC catalysts. Preprint, https://doi.org/10.1016/j.molcata.2008.06.014 https://doi.org/10.1016/j.molcata.2008.06.014.

60. Chen, X., Cheng, L., Gu, J., Yuan, H., and Chen, Y. (2024). Chemical recycling of plastic wastes via homogeneous catalysis: A review. Preprint, https://doi.org/10.1016/j.cej.2023.147853 https://doi.org/10.1016/j.cej.2023.147853.

61. Mosher, M. (1992). Organic Chemistry. Sixth edition (Morrison, Robert Thornton; Boyd, Robert Neilson). J Chem Educ *69*. https://doi.org/10.1021/ed069pa305.2.

62. Orsavova, J., Misurcova, L., Vavra Ambrozova, J., Vicha, R., and Mlcek, J. (2015). Fatty acids composition of vegetable oils and its contribution to dietary energy intake and dependence of cardiovascular mortality on dietary intake of fatty acids. Int J Mol Sci *16*. https://doi.org/10.3390/ijms160612871.

63. USDA - United States Department of Agriculture (2023). Oilseeds: World markets and trade. Foreign Agricultural Service *23*.

64. Loizides, M.I., Loizidou, X.I., Orthodoxou, D.L., and Petsa, D. (2019). Circular bioeconomy in action: Collection and recycling of domestic used cooking oil through a social, reverse logistics system. Recycling *4*. https://doi.org/10.3390/recycling4020016.

65. Gui, M.M., Lee, K.T., and Bhatia, S. (2008). Feasibility of edible oil vs. non-edible oil vs. waste edible oil as biodiesel feedstock. Preprint, https://doi.org/10.1016/j.energy.2008.06.002 https://doi.org/10.1016/j.energy.2008.06.002.

66. Mastral, J.F., Berrueco, C., and Ceamanos, J. (2007). Modelling of the pyrolysis of high density polyethylene. Product distribution in a fluidized bed reactor. J Anal Appl Pyrolysis *79*. https://doi.org/10.1016/j.jaap.2006.10.018.

67. Abbas-Abadi, M.S., Zayoud, A., Kusenberg, M., Roosen, M., Vermeire, F., Yazdani, P., Van Waeyenberg, J., Eschenbacher, A., Hernandez, F.J.A., Kuzmanović, M., et al. (2022). Thermochemical recycling of end-of-life and virgin HDPE: A pilot-scale study. J Anal Appl Pyrolysis *166*. https://doi.org/10.1016/j.jaap.2022.105614.

68. Ueno, T., Nakashima, E., and Takeda, K. (2010). Quantitative analysis of random scission and chain-end scission in the thermal degradation of polyethylene. Polym Degrad Stab *95*. https://doi.org/10.1016/j.polymdegradstab.2010.04.020.

69. Maafa, I.M. (2021). Pyrolysis of polystyrene waste: A review. Preprint, https://doi.org/10.3390/polym13020225 https://doi.org/10.3390/polym13020225.

70. Berdugo Vilches, T., Marinkovic, J., Seemann, M., and Thunman, H. (2016). Comparing Active Bed Materials in a Dual Fluidized Bed Biomass Gasifier: Olivine, Bauxite, Quartz-Sand, and Ilmenite. Energy and Fuels *30*. https://doi.org/10.1021/acs.energyfuels.6b00327.

71. Berguerand, N., and Berdugo Vilches, T. (2017). Alkali-Feldspar as a Catalyst for Biomass Gasification in a 2-MW Indirect Gasifier. Energy and Fuels *31*. https://doi.org/10.1021/acs.energyfuels.6b02312.

72. Pfeifer, C., Koppatz, S., and Hofbauer, H. (2011). Steam gasification of various feedstocks at a dual fluidised bed gasifier: Impacts of operation conditions and bed materials. Biomass Convers Biorefin *1*. https://doi.org/10.1007/s13399-011-0007-1.

73. Yue, Y., Li, J., Dong, P., Wang, T., Jiang, L., Yuan, P., Zhu, H., Bai, Z., and Bao, X. (2018). From cheap natural bauxite to high-efficient slurry-phase hydrocracking catalyst for high temperature coal tar: A simple hydrothermal modification. Fuel Processing Technology *175*. https://doi.org/10.1016/j.fuproc.2018.03.006.

74. Pissot, S., Berdugo Vilches, T., Maric, J., Cañete Vela, I., Thunman, H., and Seemann, M. (2019). Thermochemical Recycling of Automotive Shredder Residue by Chemical-Looping Gasification Using the Generated Ash as Oxygen Carrier. Energy and Fuels *33*. https://doi.org/10.1021/acs.energyfuels.9b02607.

75. Pissot, S., Faust, R., Aonsamang, P., Berdugo Vilches, T., Maric, J., Thunman, H., Knutsson, P., and Seemann, M. (2021). Development of Oxygen Transport Properties by Olivine and Feldspar in Industrial-Scale Dual Fluidized Bed Gasification of Woody Biomass. Energy and Fuels *35*. https://doi.org/10.1021/acs.energyfuels.1c00586.

76. Sato, T., Sumita, T., and Itoh, N. (2015). Effect of CO addition on upgrading bitumen in supercritical water. Journal of Supercritical Fluids *104*. https://doi.org/10.1016/j.supflu.2015.06.004.

77. Fedyaeva, O.N., and Vostrikov, A.A. (2012). Hydrogenation of bitumen in situ in supercritical water flow with and without addition of zinc and aluminum. Journal of Supercritical Fluids *72*. https://doi.org/10.1016/j.supflu.2012.08.018.

78. Hosseinpour, M., Ahmadi, S.J., and Fatemi, S. (2016). Deuterium tracing study of unsaturated aliphatics hydrogenation by supercritical water in upgrading heavy oil. Part I: Non-catalytic cracking. Journal of Supercritical Fluids *107*. https://doi.org/10.1016/j.supflu.2015.08.004.

79. Hosseinpour, M., Fatemi, S., and Ahmadi, S.J. (2015). Catalytic cracking of petroleum vacuum residue in supercritical water media: Impact of α-Fe2O3 in the form of free nanoparticles and silica-supported granules. Fuel *159*. https://doi.org/10.1016/j.fuel.2015.06.086.

80. Larsson, A., Seemann, M., Neves, D., and Thunman, H. (2013). Evaluation of performance of industrial-scale dual fluidized bed gasifiers using the chalmers 2-4-MWth gasifier. Energy and Fuels *27*. https://doi.org/10.1021/ef400981j.

81. Israelsson, M., Larsson, A., and Thunman, H. (2014). Online measurement of elemental yields, oxygen transport, condensable compounds, and heating values in gasification systems. Energy and Fuels *28*. https://doi.org/10.1021/ef501433n.

82. Israelsson, M., Seemann, M., and Thunman, H. (2013). Assessment of the solid-phase adsorption method for sampling biomass-derived tar in industrial environments. Energy and Fuels *27*. https://doi.org/10.1021/ef401893j.

83. Schug, K.A., Sawicki, I., Carlton, D.D., Fan, H., McNair, H.M., Nimmo, J.P., Kroll, P., Smuts, J., Walsh, P., and Harrison, D. (2014). Vacuum ultraviolet detector for gas chromatography. Anal Chem *86*. https://doi.org/10.1021/ac5018343.

84. Van Geem, K.M., Reyniers, M.F., and Marin, G.B. (2005). Two severity indices for scale-up of steam cracking coils. Ind Eng Chem Res *44*. https://doi.org/10.1021/ie048988j.

85. Gholami, Z., Gholami, F., Tišler, Z., and Vakili, M. (2021). A review on the production of light olefins using steam cracking of hydrocarbons. Energies (Basel) *14*. https://doi.org/10.3390/en14238190.

86. Forero-Franco, R., Cañete-Vela, I., Berdugo-Vilches, T., González-Arias, J., Maric, J., Thunman, H., and Seemann, M. (2023). Correlations between product distribution and feedstock composition in thermal cracking processes for mixed plastic waste. Fuel *341*. https://doi.org/10.1016/j.fuel.2023.127660.

87. Zámostný, P., Bělohlav, Z., Starkbaumová, L., and Patera, J. (2010). Experimental study of hydrocarbon structure effects on the composition of its pyrolysis products. J Anal Appl Pyrolysis *87*. https://doi.org/10.1016/j.jaap.2009.12.006.

88. Devi, L., Craje, M., Thüne, P., Ptasinski, K.J., and Janssen, F.J.J.G. (2005). Olivine as tar removal catalyst for biomass gasifiers: Catalyst characterization. Appl Catal A Gen *294*. https://doi.org/10.1016/j.apcata.2005.07.044.

89. Faust, R., Berdugo Vilches, T., Malmberg, P., Seemann, M., and Knutsson, P. (2020). Comparison of Ash Layer Formation Mechanisms on Si-Containing Bed Material during Dual Fluidized Bed Gasification of Woody Biomass. Energy and Fuels *34*. https://doi.org/10.1021/acs.energyfuels.0c00509.